FIELD EVALUATION OF CORROSION IN REINFORCED CONCRETE STRUCTURES IN MARINE ENVIRONMENT

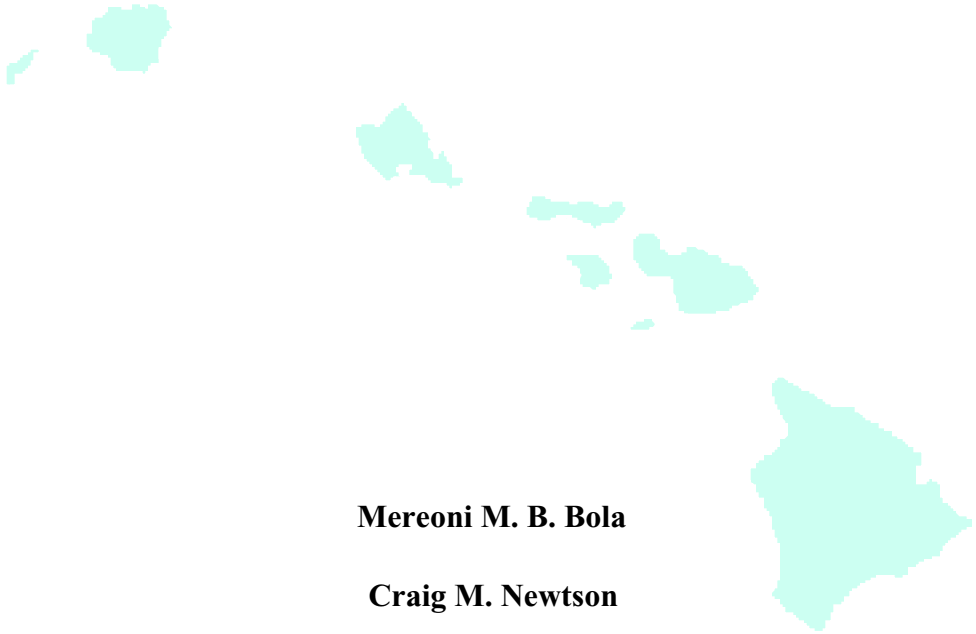

Mereoni M. B. Bola

Craig M. Newtson

Prepared in cooperation with the State of Hawaii Department of Transportation, Highways Division and U.S. Department of Transportation, Federal Highway Administration

UNIVERSITY OF HAWAII
COLLEGE OF ENGINEERING

DEPARTMENT OF CIVIL AND ENVIRONMENTAL ENGINEERING

Research Report UHM/CE/00-01

June 2000

ABSTRACT

Eight sites were selected for field evaluation in cooperation with the Harbors Division of the Hawaii Department of Transportation. Seven of the sites used a calcium nitrite based admixture as a corrosion inhibitor. The eighth site used epoxy coated reinforcing steel to combat corrosion. Each site was tested for permeability, chloride ion concentration, half-cell potential, polarization resistance, resistivity, and pH. Corrosion activity identified by the half-cell potential measurements, polarization resistance measurements, and visual inspection of bars taken from cores indicated that high dosages of calcium nitrite (4.0 to 4.5 gal/yd^3) provided the steel with significantly greater protection than lower dosages (2.5 gal/yd^3). Visual inspection of epoxy coated bars taken from cores also demonstrated that the epoxy coating effectively protected the steel. Resistivity measurements often contradicted the results from the half-cell potential and polarization resistance tests. However, visual inspections supported the half-cell and polarization resistance tests, indicating that the resistivity measurements were erroneous.

TABLE OF CONTENTS

LIST OF TABLES

LIST OF FIGURES

CHAPTER 1
INTRODUCTION

1.1 Introduction

Reinforced concrete is one of the most widely used construction materials worldwide. Over the years, concrete structures have been promoted as having indefinitely long service lives requiring negligible maintenance. Even though some deterioration of reinforced concrete had been noted in the past, the good experiences had always outweighed the problems. This began to change in the United States around the late 1960's when severe deterioration of many reinforced concrete decks that had been exposed to deicing salts was noted (Slater 1983). Large sums of money were used to rehabilitate these structures and investigate possible measures to solve the problem.

In general, good quality concrete provides both physical and chemical protection for the embedded steel against corrosion. The physical protection is provided by the concrete acting as a barrier, preventing aggressive chemicals, such as chloride ions, from reaching the steel. The chemical protection is provided by the concrete's high alkalinity, which forms a thin passive layer on the steel, and shields it from corrosion (Liam et. al. 1992).

Regardless of exposure conditions, corrosion of reinforcing steel occurs when the protective passive layer is disrupted. Chloride ions may enter the concrete from the environment, through the seawater and salt spray, or from deicing salts in bridge decks and parking structures. Chlorides may also be added through accelerating admixtures, chloride-contaminated aggregates, and brackish mixing water. Steel passivity is broken

down when a sufficient amount of chlorides is present in the pore solution (Hussain et. al. 1996).

Corrosion can also occur without the presence of chloride ions. For example, carbonation reduces the alkalinity of concrete, allowing corrosion of reinforcing steel to occur. Because carbonation is a relatively slow process, this is not as common as corrosion induced by chloride ions.

In marine environments, structures such as jetties, piers and wharves are exposed to excessive chloride attack. For these structures, a higher level of corrosion protection has to be incorporated to delay the onset of corrosion. Much research has been performed to investigate corrosion protection methods that could be used to extend the life of these reinforced concrete structures. Some of the remedial measures that have been studied include the use of corrosion-inhibiting admixtures, epoxy-coated reinforcing steel, waterproofing membranes, penetrants and sealers, galvanized reinforcing steel, electrochemical removal of chlorides, and cathodic protection (Gu et. al. 1997). The common function of these corrosion-protection systems is to prevent aggressive agents, mainly chloride ions, from attacking the surface of the reinforcing steel.

In the past decade, the use of corrosion inhibitors has emerged as a promising method for delaying the onset of corrosion. It offers a cost-effective solution due to its convenient and economical application to both new structures and repair of existing buildings. Inhibitors raise the chloride concentration necessary for the initiation of corrosion. Once corrosion is initiated, the inhibitor may also reduce the rate of corrosion.

Other methods of corrosion protection include low permeability concrete, made by adding pozzolanic materials or latex to the mixture. The amount of chloride that penetrates to the reinforcing steel is greatly influenced by the permeability of the concrete; lowering the permeability of concrete reduces the number chloride ions that will reach the steel surface.

One other way to protect the steel from corrosion is to coat the reinforcing steel with an inert sealer such as epoxy. The epoxy coating provides an impermeable barrier between the steel and the concrete, inhibiting aggressive chloride ions from contacting the steel.

1.2 Objective

The objective of this research was to evaluate the effectiveness of corrosion-inhibiting measures that were adopted for some of the piers along Hawaii's shorelines. The sites tested used either a corrosion-inhibiting admixture or epoxy-coated reinforcing steel as their method of combating corrosion. All sites were exposed to a marine environment that promoted the corrosion of reinforcing steel. Field evaluation methods performed on site included non-destructive test methods, such as the half-cell potential test, polarization resistance test, resistivity test, permeability test, chloride concentration analysis and pH tests. Cores were also taken from the piers for strength testing and further analysis of the chloride concentrations.

1.3 Scope

This report discusses the findings from the field evaluations that were performed on eight test sites. Chapter 2 presents a literature review for corrosion of reinforcing steel, and several methods of evaluating corrosion. The mechanisms of corrosion are explained, and the non-destructive tests used in this study are described. Chapter 3 describes the test sites, and presents the experimental procedures that were performed. Results obtained from the field tests and a detailed discussion of these results are provided in Chapter 4. Finally, Chapter 5 provides a summary of the project and conclusions drawn from the study.

CHAPTER 2
BACKGROUND AND LITERATURE REVIEW

2.1 Introduction

Corrosion of reinforcing steel in concrete is a common cause of structural deterioration. Maintenance, rehabilitation, or replacement of concrete structures damaged by corrosion are not only labor intensive tasks, but are also expensive processes that generally provide only limited success in restoring the structure. The incidence of corrosion of reinforcing steel is greatest in structures such as piers, jetties and wharves. These structures are built in marine environments, and exposed to high concentrations of chlorides. This chapter discusses the mechanisms of the corrosion process in reinforcing steel, the problems it causes, and some of the corrosion monitoring techniques that are in use today.

2.2 Mechanisms of corrosion of steel in concrete

Corrosion, by definition, is the deterioration or destruction of a metal caused by either a chemical or electrochemical reaction with the environment (Cornet et. al. 1968). Corrosion of steel that results from burning (direct oxidation) or acid attack, are forms of chemical corrosion (Verbeck 1975). Since chemical corrosion is of little concern in concrete, the most common form of corrosion of reinforcing steel is electrochemical.

In order for corrosion to occur, electrons must flow between the cathodic and anodic regions of the reinforcing steel. Both the anodic and cathodic regions develop on the steel based on differences in electrical potential at various points on the reinforcing

bar. These differences in potential arise from various causes. Differences in oxygen concentration, temperature differences, and differences in stress between the two electrodes are examples of some of the causes (Cornet et. al. 1968). The reinforcing steel acts as an electrical conductor, transporting electrons between the anode and the cathode, whereas the moist concrete provides the aqueous medium, which transports the ions between the electrodes (ACI 222R-96 1996).

The basic electrochemical cycle involves oxidation and reduction reactions occurring at the anodic and the cathodic areas, respectively. Figure 2.1 illustrates the complete corrosion cell showing the processes that occur at both the anode and the cathode. Oxidation occurs at the anode when the iron in the steel is oxidized to ferrous-oxide, and electrons are released (Hime and Erlin 1987). Therefore, corrosion occurs at the anode.

$$\text{Anodic reation:} \quad \underset{\text{Iron}}{Fe} \longleftrightarrow \underset{\text{Iron ion}}{Fe^{++}} + \underset{\text{2 electrons}}{2e^{-}} \tag{2.1}$$

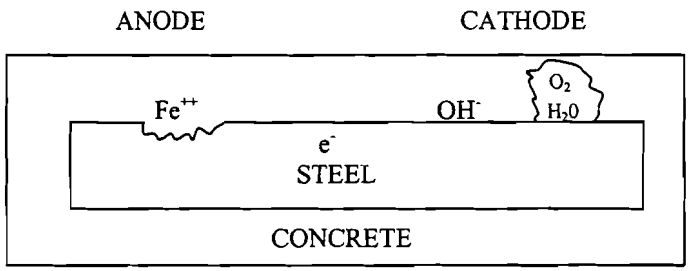

Figure 2.1. Corrosion cell in reinforced concrete (Hime and Erlin 1987)

At the cathode, oxygen is the direct acceptor of electrons released by the anode (Hausmann 1967). The flow of current from an anodic to a cathodic area, in the presence of oxygen and water, produces hydroxyl ions (OH^-) at the cathode. Then the hydroxyl ions migrate to the anode, and react with ferrous ion to form hydrous iron oxides (Erlin and Verbeck 1975).

$$\text{Cathodic reaction:} \quad \underset{\text{oxygen}}{\tfrac{1}{2}O_2} + \underset{\text{water}}{H_2O} + \underset{\text{2 electrons}}{2e^-} \longleftrightarrow \underset{\text{2 hydroxyl ions}}{2OH^-} \qquad (2.2)$$

Although concrete is relatively impermeable, an aggressive environment will either lower the pH of the concrete, or transport chloride ions to the steel surface. Then, the passive layer becomes less stable and is easily breached. When the normally passive steel corrodes, the corrosion products occupy more volume than that of the original steel (Loto 1992). This expansion exerts stresses that crack the concrete and weakens the bond between the concrete and steel, and eventually the anchorage of the steel in the concrete. The loss of bond and anchorage decrease the load carrying capacity of the reinforced concrete, and also influences the behavior of the structure (Cabrera 1996).

2.3 Factors influencing corrosion

The properties of concrete that affect the reinforcing steel environment are discussed in this section.

2.3.1 Concrete permeability

Although concrete is a hard, dense material, it does contain pores that are interconnected throughout the material. These pores provide some permeability in the concrete (Slater 1983). Permeability of concrete is very important to the corrosion process. For chloride to act as a catalyst for corrosion, both chloride ions and oxygen must be present at the steel. The permeability of concrete determines the rate at which aggressive species penetrate the concrete to reach the steel. For a given concrete cover, chloride ions will penetrate the concrete relatively quickly at areas of high permeability (Lewis and Copenhagen 1959).

High water-cement ratios generally lead to either a greater number of pores, or larger pores, both of which lead to a relatively permeable concrete (Stratfull 1957). Some other factors that influence the permeability of concrete are the type, size and gradation of the aggregates, consolidation methods, curing conditions and temperature (Kitowski and Wheat 1997).

2.3.2 Alkalinity

As previously mentioned, the natural alkalinity of concrete (pH > 12) inhibits corrosion (Erlin and Verbeck 1975), by forming a passive film on the surface of the steel. The protective quality of the film depends largely on the pH of the concrete, which appears to be governed by the free calcium hydroxide within the concrete (Slater 1983). As the pH of the concrete is reduced, the steel becomes more susceptible to corrosion.

Values of pH for concrete generally range between 12 and 13 (Gonzalez et. al. 1993).

2.3.3 Chloride concentrations

Chlorides may infiltrate concrete from several different sources. Certain environments will provide an external source of chloride ions. For example, chlorides in seawater are common in marine structures and deicing salts are a common source of chloride for bridge decks (ACI 222R-96 1996). Soluble chlorides may also be introduced into the concrete by the use of aggregates, admixtures and accelerators that contain chlorides. When the chloride ion concentration in the vicinity of the embedded steel reaches a critical value, corrosion commences (Berke and Hicks 1994).

2.3.4 Corrosion inhibiting admixtures

Corrosion inhibiting admixtures may be classified as either organic, inorganic or both. An ideal corrosion inhibitor is a chemical compound that when added in sufficient amounts to concrete, can prevent corrosion of reinforcing steel without decreasing concrete strength (Hope and Ip 1989).

According to Berke (1991), there are several inhibitors that have been tested by many researchers, but only one (calcium nitrite) has been used commercially on a wide scale in the United States, Japan, and Europe. In general, calcium nitrite improves the properties of hardened concrete. Many other inhibitors have resulted in a decrease in compressive strength of concrete (Loto 1992). Even though corrosion inhibitors have been widely used over the years, there is considerable debate about their long-term

benefits and abilities to prolong the service lives of structures.

2.4 Electrical techniques

Corrosion is an electrochemical process. Therefore, both electrical and chemical tests are performed to evaluate corrosion of reinforcing steel in concrete. These tests focus on evaluating the rate at which the corrosion is occurring, and the potential for corrosion to occur in the future. The electrical techniques that are primarily used today will be discussed in this section.

2.4.1 Half-cell potential

The half-cell potential test is the most common technique used to assess corrosion of reinforcing steel. It measures the electrical potential of steel in concrete against a reference half-cell placed on the concrete surface. Saturated calomel and copper/copper-sulfate cells are commonly used as reference cells (Dhir et. al. 1991). Since the potential of the standard electrode is constant, the measured potentials result from variation in the potential of the steel and concrete. As shown in Figure 2.2, the test equipment is simple. The half-cell potential test involves making an electrical connection to the embedded steel at a convenient position. This allows electrode potentials to be measured at any location by moving the half-cell over the concrete.

Results from the half-cell potential test indicate the likelihood that corrosion is occurring within the concrete. Once the potential measurements are obtained, an

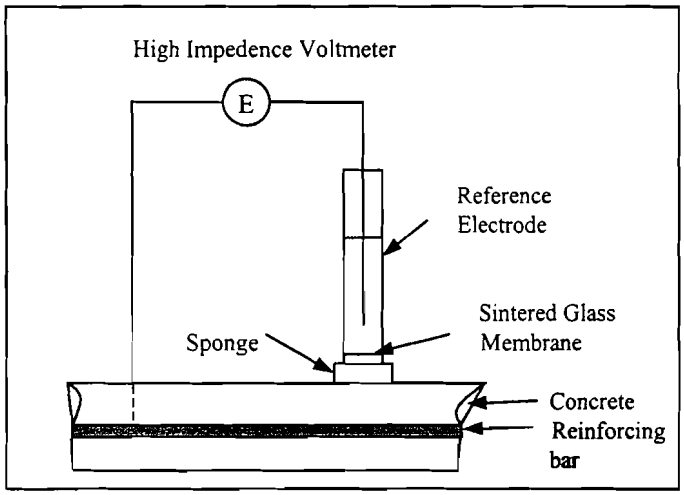

Figure 2.2. Setup for half-cell potential test (Suryavanshi and Nayak 1990).

equipotential contour map for the tested area can be drawn, and the corrosion activity in different regions of the structure between marked areas may be interpreted using Table 2.1.

Because the equipment used to conduct the half-cell test is simple, the test is inexpensive and simple to perform. This allows large structures to be surveyed fairly quickly. The data gained from the half-cell tests are also easy to interpret with the use of Table 2.1.

A major limitation of the half-cell test is that it is a qualitative method of assessing corrosion. The half-cell potential test does not provide any information on the

Table 2.1: Interpretation of Half-cell potential results (Suryavanshi and Nayak 1990).

Measured potential (mV)	Statistical risk of corrosion occurring (%)
< -350	90
Between –350 and –250	Uncertain
-200	10

corrosion rates of the actively corroding steel. It only provides an estimate of the probability that corrosion is occurring at the location tested. Another limitation of the half-cell test is that results are often inconclusive. The large range of potentials (-200 mV to –350 mV) that correspond to uncertain probabilities in Table 2.1 illustrate this limitation. The statistical risk of corrosion for a potential measurement in the range of –200 mV to –350 mV is not clearly defined.

2.4.2 Polarization resistance

Polarization resistance, R_p, is defined as the electrical resistance across the metal-concrete interface of a system. The polarization resistance technique uses the principle that a linear relationship exists between potential and applied current, for potentials that are only slightly different from the corrosion potentials (Srinivasan et al. 1994).

A three-electrode system is adopted for the polarization resistance test, as shown in Figure 2.3. The system consists of a reference electrode, which is located on the concrete surface, a working electrode (the steel bar being tested), and a counter electrode located either on the concrete surface or within the concrete. The polarizing current is applied to the specimen by the counter electrode (Dhir et. al. 1991).

Polarization resistance measurements may be performed using one of three techniques: the potentiostatic method, the galvanostatic method, or the potentiodynamic method (Srinivasan et. al. 1994). The most common test is the potentiostatic method, which involves applying a constant potential to the rest potential of the working electrode (Gower et. al. 1994). The induced current flow declines exponentially with time, and is

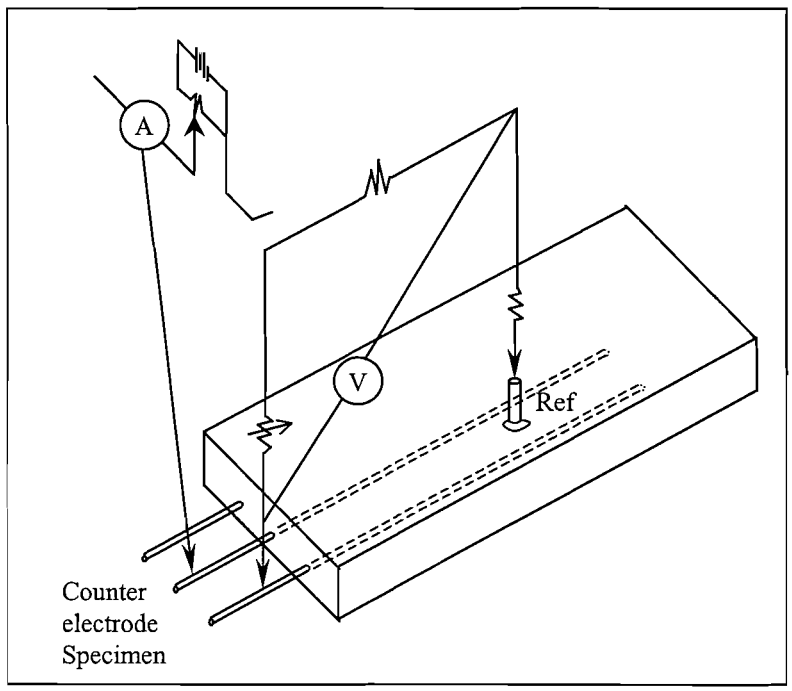

Figure 2.3. Setup for the polarization resistance method (Malhotra and Carino 1991).

measured after a chosen period. A potential of the same magnitude is then applied in the opposite direction from the rest potential and the current is again measured, after the same time interval. The polarization resistance (R_p) is given by the difference between the two potentials (ΔE) divided by the difference between the two currents (ΔI), as stated by:

$$R_p = \Delta E/\Delta I \tag{2.3}$$

The galvanostatic method is similar to the potentiostatic method, except that a small increment of current (ΔI) is applied, and the change in potential (ΔE) is monitored (Srinivasan et. al. 1994).

In the potentiodynamic method, the polarization is carried out with a linear potential sweep between the two limits of potential. The resulting current is recorded and R_p is determined from the gradient of a plot of potential against current.

The polarization resistance (R_p), is related to the corrosion current (I_{corr}) through the equation (Hassanein et al. 1998):

$$I_{corr} = B / R_p \tag{2.4}$$

where B is known as the Stern-Geary constant and can be computed from the following equation:

$$B = \beta_a\beta_c / \{2.3*(\beta_a + \beta_c)\} \tag{2.5}$$

where β_a and β_c are Tafel constants (Ahmad and Bhattacharjee 1995). In practice, B has been taken as approximately 25 mV for actively corroding steel in concrete, and 50 mV for passive steel in concrete.

It is important to note that the corrosion current, I_{corr}, is integrated over the surface area of steel bar being polarized. Therefore, the unit corrosion rate is:

$$i_{corr} = I_{corr} / A \quad (2.6)$$

where A is the effective surface area of the steel bar during the test.

The polarization resistance method is a quantitative method of testing that provides a direct measurement of corrosion rate, as opposed to indicating the probability of corrosion occurring. Moreover, the test is rapid and inexpensive to perform. However, the accuracy of the corrosion rate is severely limited by the difficulty in defining the area (A) of reinforcement polarized. If the area is overestimated, the corrosion density will be smaller than the actual amount. This leads to an underestimation of the actual corrosion rate.

2.4.3 Resistivity measurements

Concrete resistivity is the electrical resistance to current flow within the concrete. Values of concrete resistivity vary over a broad range; from 10^9 Ω-m for oven-dried concrete, to less than 100 Ω-m for very wet concrete (Lopez and Gonzalez 1993).

The resistivity of concrete can be measured using either a two-electrode system or a four-electrode system. The two-electrode method is performed by inserting two electrodes into drilled holes on the concrete surface. The potential between the electrodes is measured as an alternating current is passed between them (Bungey 1993).

For the four-electrode system, four probes are aligned with each other as shown in Figure 2.4. A small alternating current is passed through the two outer terminals, and the potential difference between the two inner electrodes is measured. The distance between

the electrodes is selected based on the depth at which the concrete is being evaluated (Srinivasan et. al. 1994). A wider spacing allows investigation of deeper material.

According to Lopez and Gonzalez (1993), concrete resistivity and corrosion rates are inversely proportional over a wide range of values. Low resistivity values are generally associated with high rates of corrosion. Table 2.2 summarizes the relationship between typical resistivity values and corrosion rates.

It is important to note that the presence of a low resistivity surface layer, which may be caused by recent rainfall, can lead to significant errors in estimating the resistivity of the material. Consequently, resistivity measurements after recent surface wetting should be avoided (Millard 1993).

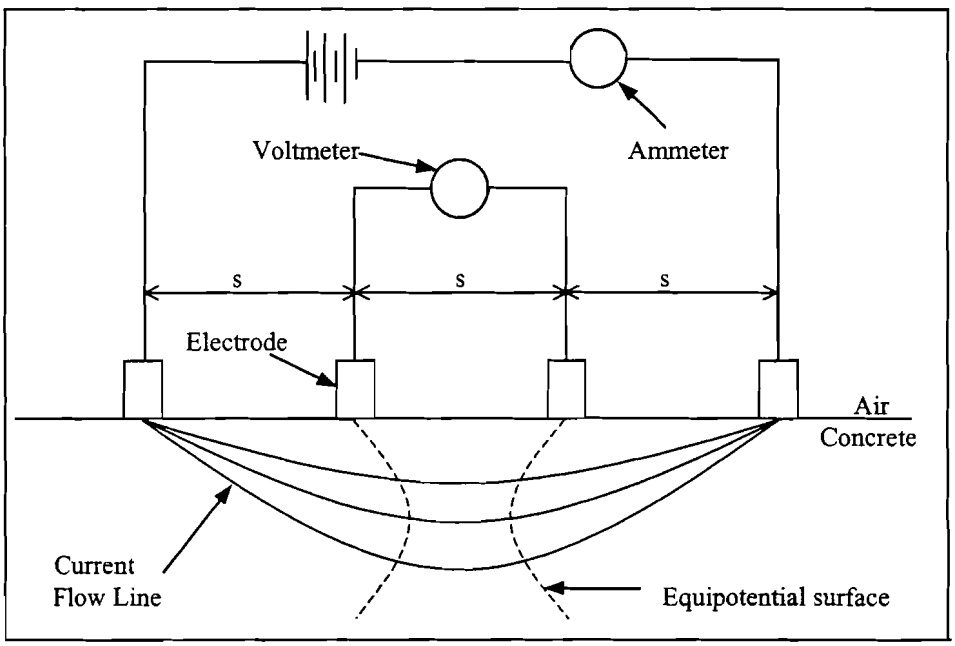

Figure 2.4. Four-probe setup for concrete resistivity tests (Malhotra and Carino 1991).

Table 2.2. Empirical resistivity thresholds (Millard 1993).

Resistivity (kohm cm)	Corrosion rate
< 5	Very high
5 – 10	High
10 – 20	Moderate / Low
> 20	Low

2.4.4 Electrical resistance probe

This technique is based on the principle that the resistance of a conductive material is a function of its cross-sectional area. During active corrosion, as a steel bar is slowly consumed and the cross-sectional area decreases, electrical resistance increases. This change in resistance enables the progress of corrosion to be measured (Dhir et. al. 1991).

The electrical resistance probe (ERP) method is performed by comparing the change in resistance between protected and exposed probes embedded in concrete. The embedded test probes should be as physically and compositionally similar as possible. Additionally, the thickness of the specimen should be thin, within the range of 50 to 500 μm to provide the probes with greater sensitivity (Malhotra and Carino 1991). Figure 2.5 shows the equipment setup for the test, which involves incorporating the probes into a Wheatstone bridge circuit.

The ERP technique provides a quantitative measure of the corrosion rate determined from resistance measurements of both the exposed and protected probes. Consequently data analysis is straightforward. However, it is not always feasible to

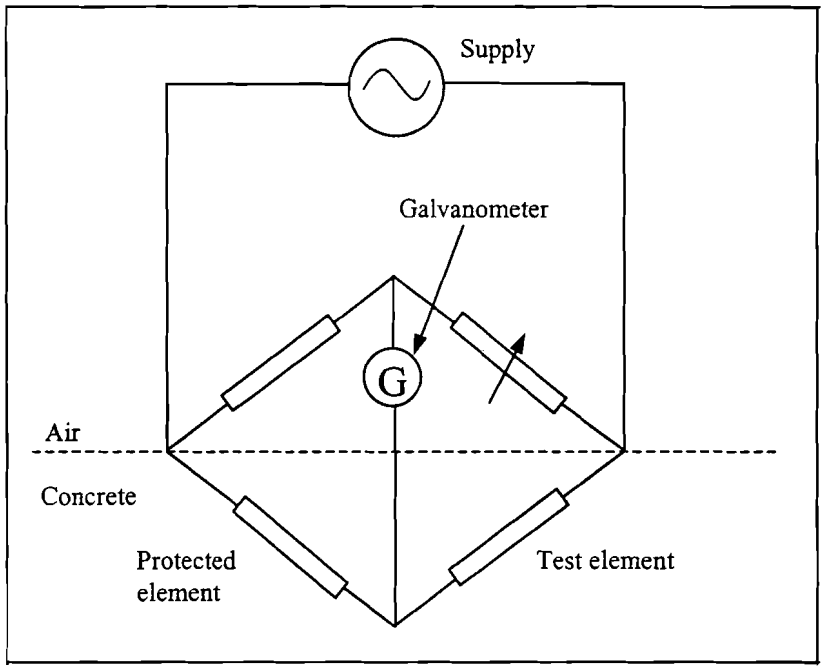

Figure 2.5. Wheatstone bridge setup for Electrical Resistance Probe Test (Dhir et. al. 1991).

install the embedded electrode during construction. As a result of this limitation, electrical resistance probe measurements are not widely used. In addition, the test is best suited to situations of uniform corrosion (such as corrosion due to carbonation), and may prove less reliable with pitting. It is suggested that the ERP method should not be performed alone, but in combination with other tests that are available (Dhir et. al. 1991).

2.4.5 Electrochemical noise

This method "listens" to the system and senses small fluctuations in corrosion potential of the steel-concrete system occurring naturally during the corrosion process (Rodriguez et. al. 1994). Electrochemical noise is seen as the spontaneous fluctuations of electrical potential and current, at the microvolt and microampere level, respectively.

The technique uses equipment similar to the half-cell potential equipment, except that a more sensitive voltmeter is used. A noise signal, or time record, is obtained between the reinforcement and the referenced electrode using the sensitive digital voltmeter. The length of the time record depends on the frequency range of testing. For example, a range of 10 Hz to 1 mHz requires a quarter of an hour to two hours of sample time (Dawson 1983).

Information relating to the corrosion process may be established from the potential versus time plots, or from an alternative form of data presentation, i.e. spectral density plots (Dhir et. al. 1991). An equipotential map, similar to the one constructed from half-cell potential tests is plotted. This equipotential map is used to analyze active and passive areas of the specimen. Dawson (1983) also reports that the standard deviation of the noise signal appears to be proportional to the corrosion penetration rate, obtained from polarization resistance measurements.

Much experience is needed to interpret the results from this test accurately. Also, this method is unreliable for field measurements, because noise from the surrounding environment may cause interference and mask the effects of corrosion (Rodriguez et. al. 1994).

2.5 Chemical tests

Because corrosion is an electrochemical process, chemical tests can also be used to assess the potential for corrosion activity. Two chemical tests, the chloride concentration test and pH test are described in this section

2.5.1 Chloride content analysis

The intrusion of chloride ions from the environment into the concrete, along with oxygen and water, contributes to the corrosion of the reinforcing steel. Exposing concrete to seawater and using deicing salts on structures such as concrete bridges and parking garages, has prompted the need for a method to determine the safe chloride ion concentration limits in hardened concrete (Berman 1972). The amount of chloride present in the powdered concrete samples is calculated as a percentage of the weight of the cement in the material analyzed. Safe limits on the chloride content of a concrete member have been determined from previous studies, and are listed in Table 2.3.

Most of the chloride ions in hardened concrete are chemically combined, while a smaller number are soluble in water and free to contribute to corrosion. Consequently, there are two types of tests for chlorides. The first is a water-soluble test to determine the concentration of chloride ions available for corrosion, while the second is an acid

Table 2.3. Limits for water-soluble chloride-ion content in concrete (ACI 318-99).

Type of member	Maximum water-soluble chloride ion content, percent by weight of cement
Prestressed concrete	0.06
Reinforced concrete exposed to chloride	0.15
Reinforced concrete that will be dry or protected from moisture in service	1.00
Other reinforced concrete construction	0.30

solubility test, which determines the total chloride concentration in the concrete. For both methods, a sample of ground concrete is obtained by drilling a small hole at the surface of the concrete. The water-soluble test involves boiling the ground concrete sample for 5 minutes and soaking it for 24 hours, and then testing the water for dissolved chloride. For the total chloride test, the ground sample is dissolved in an extraction liquid such as nitric acid, before testing for the chloride concentration (Gaynor 1987).

2.5.2 pH tests

The pH test for concrete is performed using the same methods used for determining the pH of an aqueous solution. A sample of concrete dust collected from the area surrounding the reinforcing steel is mixed with distilled water, to form an aqueous solution. A pH meter or litmus paper is then used to measure the pH of the solution.

2.6 Summary

This chapter presented a literature review of the factors that influence corrosion. The factors included permeability, pH, chloride concentrations, and corrosion inhibiting admixtures. Descriptions of electrical and chemical tests commonly used to evaluate the likelihood of corrosion were also provided.

CHAPTER 3
EXPERIMENTAL PROCEDURES

3.1 Introduction

The purpose of this research was to evaluate the corrosion resistance of existing concrete pier structures in marine environments on the island of Oahu. The field evaluation methods involved nondestructive electrical tests, developing chloride profiles, performing permeability tests, performing pH tests, and cutting cores for visual inspection of the reinforcing bars. This chapter introduces the eight test sites evaluated and discusses the experimental procedures that were carried out for the field evaluation.

3.2 Test Sites

A total of eight sites were selected for testing. Some measure to inhibit corrosion was incorporated into the design of each site. The mixture proportions for Sites 1 through 8 are provided in Appendix A. This section provides a description, including the mix design for each site. Sites that are similar in terms of structure, mix design, or location are discussed collectively.

3.2.1 Sites 1and 2

The locations of Sites 1 and 2 were on the State of Hawaii's Piers 39 and 40 on the island of Oahu. Site 1 was located on the Diamond Head side of Pier 39 (Phase 1), and Site 2 was on the Diamond Head side of Pier 40. The locations of these sites are identified in Figure 3.1. The sites had comparable exposure to the neighboring marine

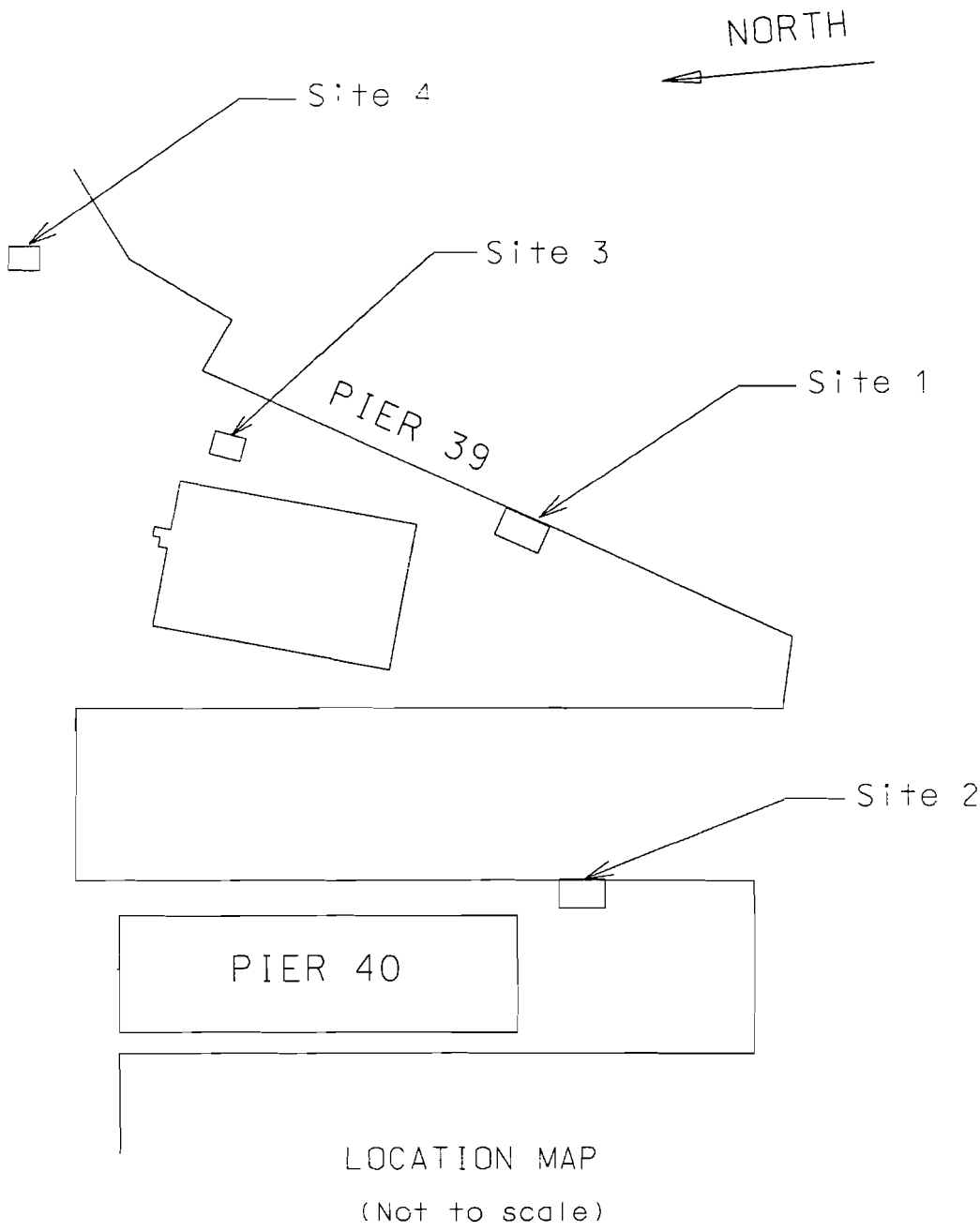

Figure 3.1. Locations of Sites 1 through 4.

environment, and experienced similar levels of traffic.

The size of the test area on each site was also similar. For Site 1, the test area was 78 x 46 ft in size, while the area for Site 2 was slightly smaller, 60 x 48 ft. Each site was divided into 2 parts; a loading zone and an approach slab. The loading zone and the approach slab were approximately equal in size for both sites.

Although Sites 1 and 2 were not constructed at the same time, the same mix design was used for both sites. Site 1 was constructed in 1994, while Site 2 was constructed three years later, in 1997. The corrosion inhibiting admixture dosage in the mix design was 2.5 gal/yd^3 of DCI (DAREX Corrosion Inhibitor). DCI is a calcium nitrite based corrosion inhibiting admixture.

3.2.2 Sites 3 and 4

The third and fourth sites each consisted of two reinforced pavement slabs located on Pier 39. Each pavement slab was approximately 12.5 x 12.5 ft in size. Site 3 was located along the Diamond Head side of Phase 1, while Site 4 was located on the Diamond Head side of Phase 2, as shown in Figure 3.1.

Sites 3 and 4 were both constructed in 1994, at the same time Site 1 was built. Consequently, the mix design used for Sites 1 and 2 was also used in constructing these pavement slabs. Sites 3 and 4 were located several yards from the edge of the pier. These pavement slabs both experienced less traffic and less exposure to the marine environment than Sites 1 and 2.

3.2.3 Sites 5 and 6

The fifth and sixth sites were both located on Pier 34, which was constructed in 1995. Site 5 was the area marked C, shown in Figure 3.2, and was approximately 72 x 42 ft in size. Site 6 was much larger in size, measuring approximately 7200 sq ft, and is marked A in Figure 3.2. Even though Sites 5 and 6 were not high traffic areas like Sites 1 and 2, their exposure to the marine environment was similar to the first two sites. As a means of combating corrosion, 4.0 gal/yd^3 of DCI was used in the mix.

3.2.4 Site 7

Site 7 was constructed in 1992 and located on the ferry terminal pier at Barbers Point Harbor on Oahu. It consisted of a 60 ft long segment at the end of the ferry terminal pier. The mix design for this site included 4.5 gal/yd^3 of DCI. This is the highest dosage of DCI used in any of the test sites. Site 7 was exposed to the ocean on three sides. Traffic on the site was light, and limited primarily to pedestrian traffic.

3.2.5 Site 8

Site 8 was constructed in 1988 and located on Pier 6 at Barbers Point Harbor. The test area was a 120 ft long strip at the northeast end of the pier. There was no corrosion inhibitor included in the mix design. However, the reinforcing bars were coated with epoxy. Site 8 had exposure conditions similar to Sites 1, 2, 5, 6, and 7. Traffic on Site 8 was comparable to the traffic on Sites 5 and 6.

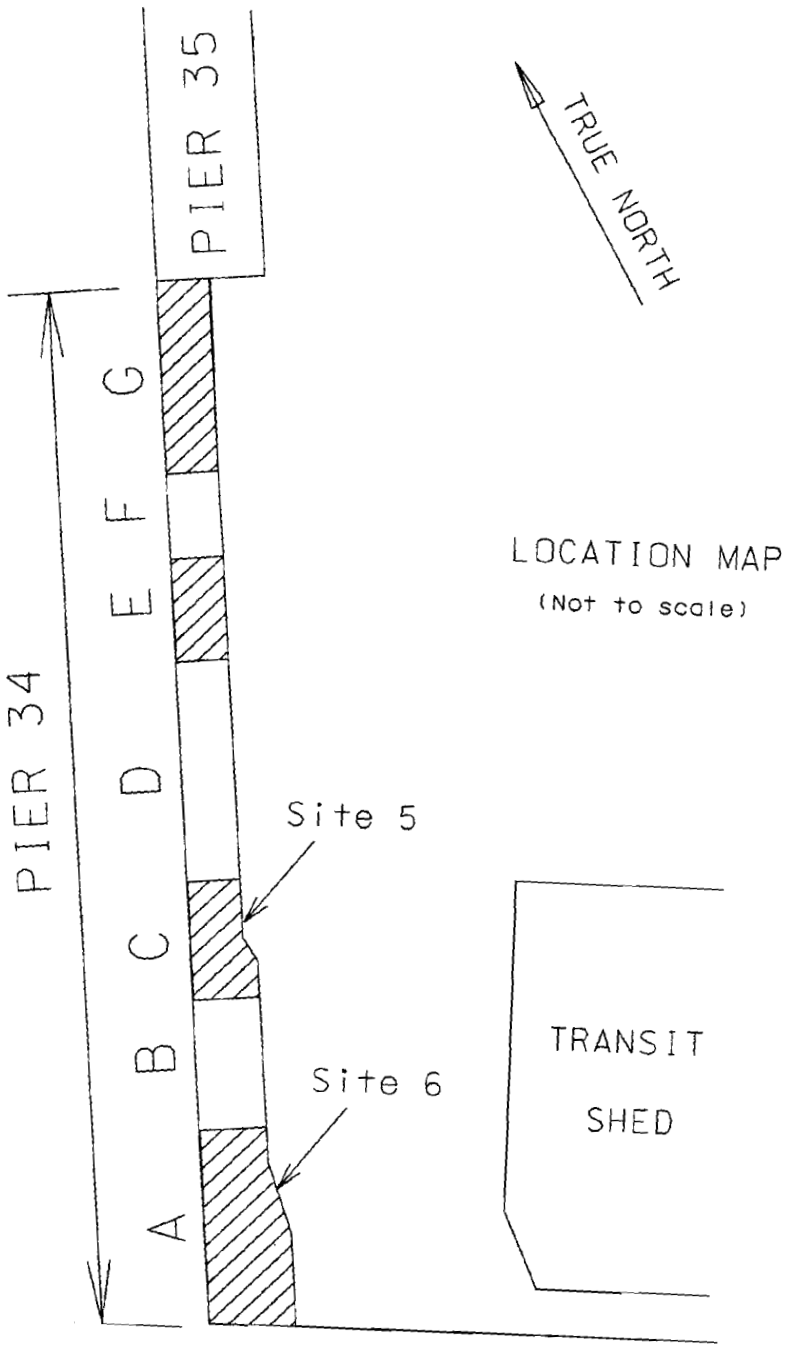

Figure 3.2. Locations of Sites 5 and 6.

3.3 Field Evaluation

The testing procedures conducted at each site are described in this section. The procedures were the same for all sites.

3.3.1 Marking out the grid

Before carrying out any tests, the location of the reinforcing steel within the structural element being tested was identified and marked out. Reinforcing bars were located with a Datascan (C-4974, James Instruments, Inc.) instrument, and then marked out with chalk lines on the surface of the concrete.

3.3.2 Performing electrical tests

Once the grid was established, testing points were chosen for half-cell potential, polarization resistance, and resistivity tests. The number of points tested depended largely on the size of the structure.

The instrument used to conduct the electrical tests was the GECOR6, manufactured by James Instruments, Inc. The GECOR6 consists of a corrosion rate meter and two separate sensors; sensor A and sensor B. The meter and sensor A were used to measure the corrosion potential, relative to a copper/copper sulfate half-cell, the electrical resistance of the concrete as required for calculating I_{corr}, and the corrosion rate (in $\mu A/cm^2$) over a defined area of reinforcing steel. The meter and sensor B were used to measure the resistivity of the concrete, ambient relative humidity, and ambient temperature.

Even though the tests performed were nondestructive, they required an electrical connection to the reinforcing steel. An access hole was drilled so that this connection could be made. Measurements were taken by placing the sensors on a wetted concrete surface with the electrical connection made to the reinforcing steel. Sponge pads were placed directly over the wet concrete, and the appropriate sensor was then placed on the sponge. The sensor was placed flat against the surface with the half-cells in full contact with the surface throughout the measurement. At each test point, the corrosion rate meter required 5-7 minutes to gather and process all the information it measured. Readings were recorded with the corrosion rate meter, and were later downloaded to a computer for analysis.

3.3.3 Performing air and water permeability tests

Six test holes, 10 mm in diameter and 40 mm deep, were drilled for permeability tests on each site. The Poroscope Plus (P-6050, James Instruments, Inc.) was used to measure the permeability of the selected locations. Each hole was drilled to a depth of 40 mm and the loose dust from the holes was blown out. A molded silicon rubber plug was then inserted into the hole. Once the plug was seated securely, a needle was inserted through the plug, into the cavity below. Then, the cavity was pressurized by forcing air through the needle. For the air permeability test, the time recorded was the time for a pressure change of 5 kPa within the cavity.

The water permeability test was conducted after the completion of the air permeability test. The Poroscope Plus was also used for this test. A tube of distilled water was connected to the needle. The distilled water was then injected into the test

hole until the hole was filled with water. The reading from the water permeability test was the time required for 0.01 ml of water to be absorbed by the concrete.

3.3.4 Making chloride profiles

A total of six chloride profiles were produced for each site. Three locations were chosen in the field, and the other three were taken from core samples. At each of these six locations, samples from 4 different depths were obtained by collecting dust as a 19 mm diameter hole was drilled. The chloride concentration was determined in the laboratory using the Chloride Test System (CL-200, James Instruments, Inc.). Three-gram samples of dust were dissolved in 20 ml of extraction liquid (acid). Sufficient time was allowed for the chloride ions to react with the acid in the liquid. Then, the chloride concentration was measured using the electronic meter from the chloride test system. This test was conducted on dust samples from at least four different depths to establish the chloride profile for each location.

3.3.5 Coring

Finally, 102 mm diameter cores were cut from each site and taken back to the laboratory. There were a total of six cores per site. Three of the cores from each site contained reinforcing steel. These cores were used for compressive strength testing and allowed the reinforcing steel to be assessed visually. The three remaining cores were used to collect more samples for making chloride profiles. Cores were also used to identify the actual concrete cover over the reinforcing steel and the actual size of the bars. Values were then compared to those determined by the rebar datascan.

3.3.6 Taking pH tests

Dust samples for the pH test were taken from the concrete area surrounding the reinforcing steel. After removing the embedded steel from the cores, a drill was used to collect dust samples. A carefully measured amount of dust was mixed with 10 drops/g distilled water. A pH probe was then used to measure the pH of the solution. Three pH tests were conducted for each site.

3.4 Summary

The eight test sites evaluated during this work were described in this chapter. Descriptions of the measures incorporated into the design of these sites to inhibit corrosion were also provided. The experimental procedures for half-cell potential, polarization resistance, resistivity, permeability, chloride concentration, and pH tests performed in the field and in the laboratory were also discussed.

CHAPTER 4
RESULTS AND DISCUSSIONS

4.1 Introduction

The test sites described in Chapter 3 were tested for half-cell potentials, corrosion rates, water and air permeabilities, concrete resistivities, chloride concentrations, and pH. The results of these tests and their interpretation are presented in this chapter. Raw data for the permeability tests, chloride concentration tests, and electrical tests are provided in Appendixes B, C, and D, respectively.

4.2 Permeability test

Average results from air and water permeability tests conducted on all 8 sites are provided in Tables 4.1 and 4.2, respectively. The permeability tests were used to rate the protective quality of the concrete tested from each site. As shown in Table 4.1, the concrete category from the air permeability test ranged from a low value of 1, indicating

Table 4.1. Air permeability for all sites

Site	Air permeability (sec)	Standard deviation	Variation (%)	Concrete category	Protective quality
1	1442	690	47.8	4	Excellent
2	292	430	147	2	Fair
3	321	285	88.8	3	Good
4	454	272	59.9	3	Good
5	92	16	17.4	1	Not very good
6	187	323	173	2	Fair
7	181	125	69.1	2	Fair
8	178	146	82.0	2	Fair

Table 4.2. Water permeability for all sites

Site	Water permeability (sec)	Standard deviation	Variation (%)	Concrete category	Protective quality
1	155	69	44.5	2	Good
2	71	44.4	62.5	1	Not very good
3	45	18.2	40.4	2	Good
4	29	37.9	131	2	Good
5	41	19	46.3	1	Not very good
6	171	126.4	73.9	2	Good
7	151	90	59.6	2	Good
8	114	72.4	63.5	2	Good

concrete that provides poor protection, to a high value of 4, symbolizing concrete that provides excellent protection.

The standard deviation values for some of the sites were quite high, compared to the average values measured. This is explained by the fact that in a given site, there may be different types or amounts of aggregate encountered. Porous aggregates will result in low air penetration times, while denser aggregates may cause the permeability to be very low and the penetration times very high. Six tests were performed on each site to account for the large variation in recorded times. For instance, on Site 2, five of the air permeability times were less than 180 seconds, whereas the last point recorded a time of 1166 seconds. The last point was probably influenced by more or denser aggregate, which caused the air permeability to be dramatically lower than the other measurements on the same site. Raw data for all of the permeability tests conducted on each site are provided in Appendix B.

Table 4.2 rates the protective quality of the concrete based on the results from the water permeability test. According to the tabulated results, concrete from six of the eight sites belonged to category 2, indicating that the concrete provides marginal protection,

sites belonged to category 2, indicating that the concrete provides marginal protection, while results for Sites 2 and 5 showed that the concrete provided poor protection for the reinforcing steel.

4.3 Chloride concentrations

Chloride profiles for each of the eight sites are presented in Figures 4.1 to 4.8. The profiles are presented as average values from 6 locations on each site. Raw data from the six tests on all eight sites are provided in Appendix C. Each profile shows the expected trend of a decreasing chloride concentration with an increasing depth. The profiles show that all of the chloride concentrations at the cover depth were lower than the 0.15% threshold identified by American Concrete Institute (ACI 318-99), for corrosion of reinforcing steel in concrete. However, results for Site 7, presented in Figure 4.7 showed that the 0.15% limit was exceeded at a depth of 0.75 inch. While the chloride concentration for Site 7 was high at the initial depth, the concentration decreased to 0.07% at the depth of the steel.

4.4 pH tests

The pH values of concrete for Sites 1 through 8 are tabulated in Table 4.3. These results are the average of three tests performed for each site. All of these values are greater than 12.0, which is expected for good quality concrete (Mindess and Young 1981).

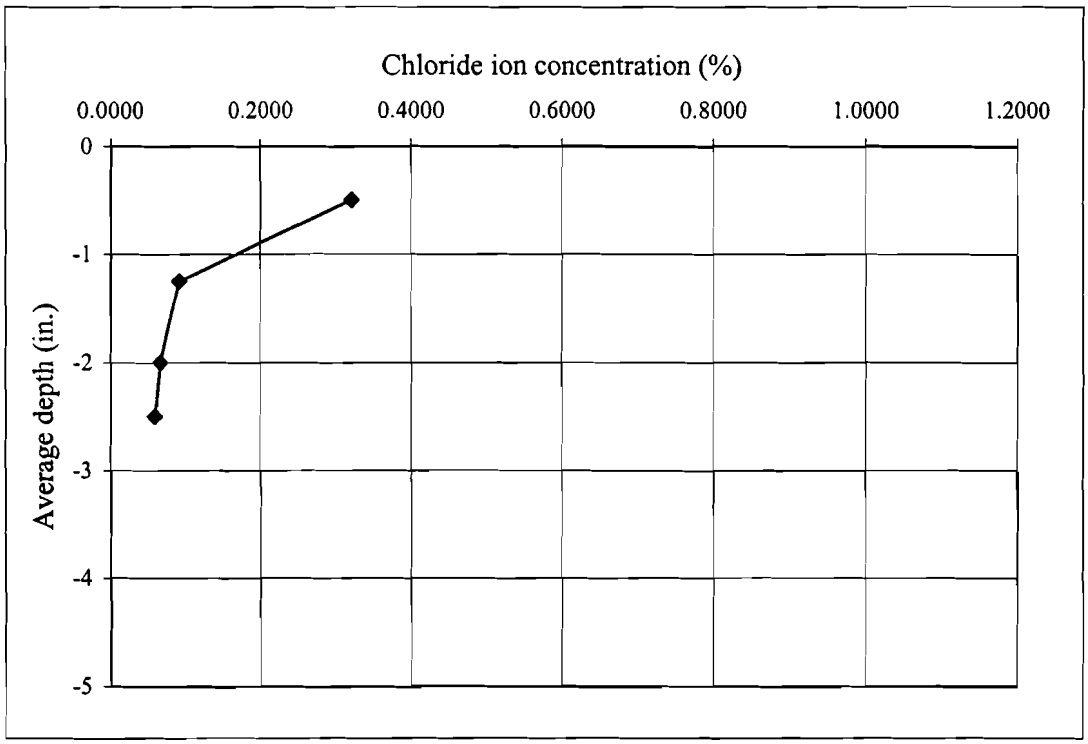

Figure 4.1. Chloride profile for Site 1.

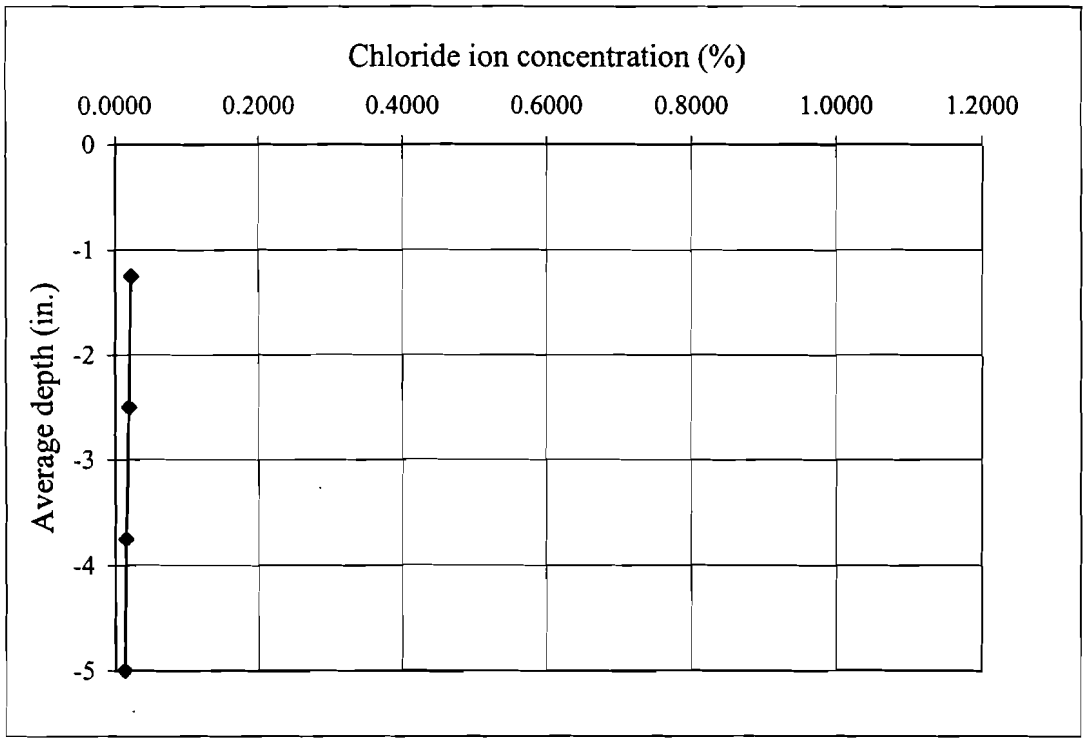

Figure 4.2. Chloride profile for Site 2.

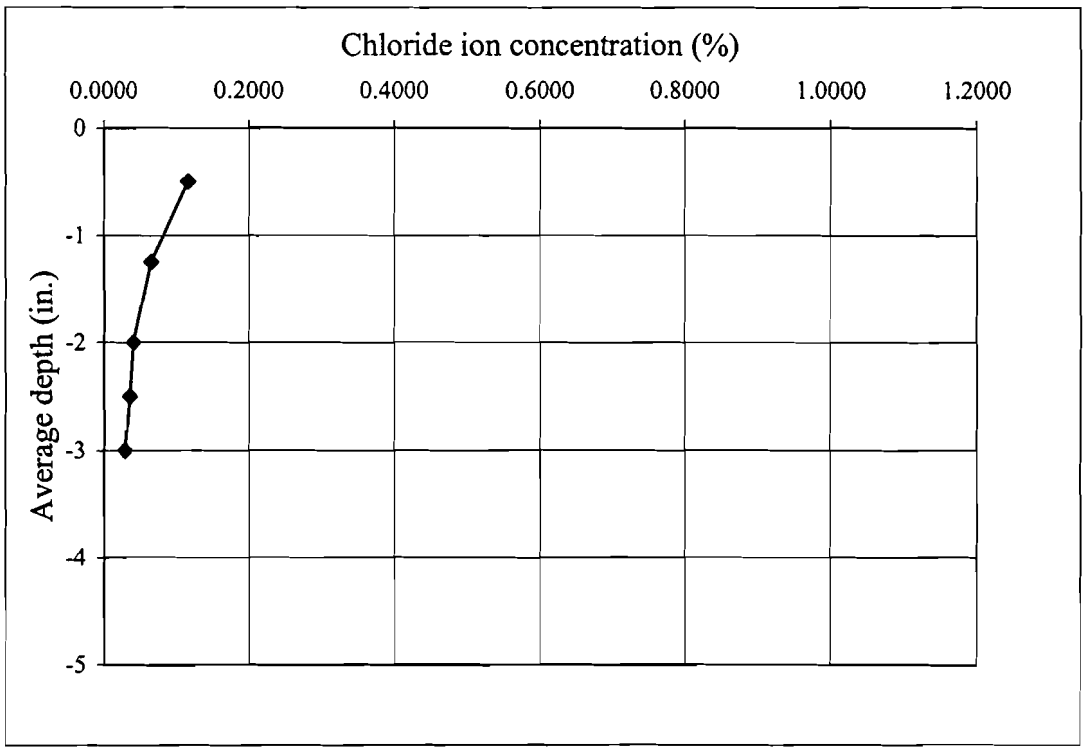

Figure 4.3. Chloride profile for Site 3.

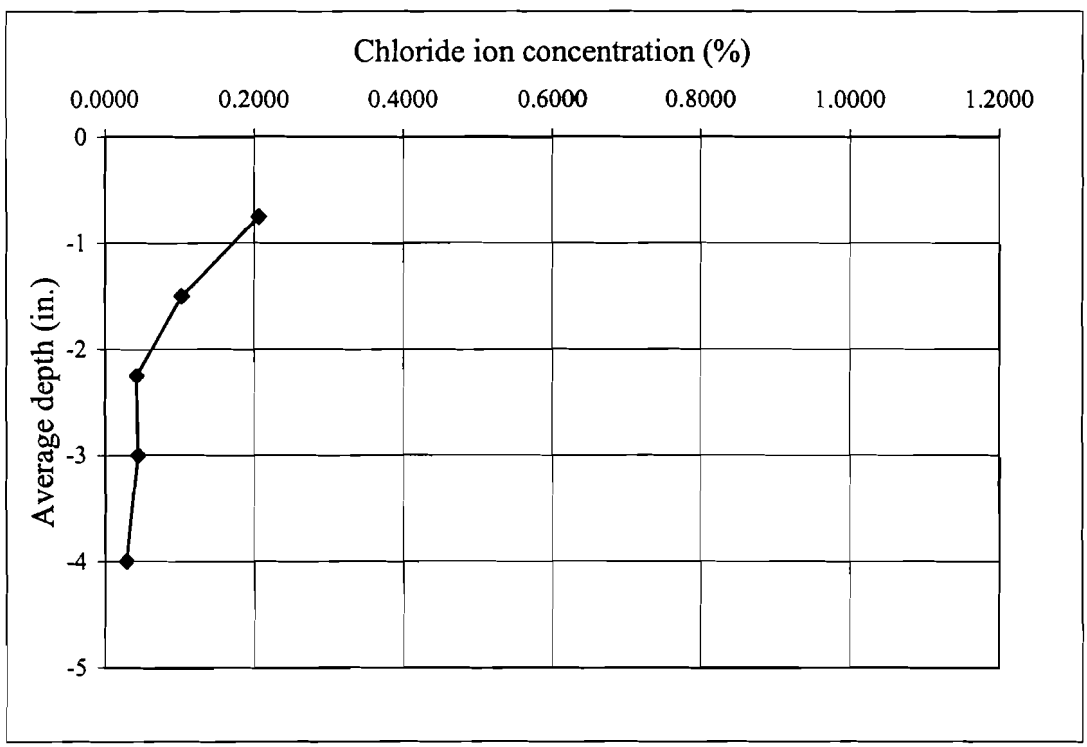

Figure 4.4. Chloride profile for Site 4.

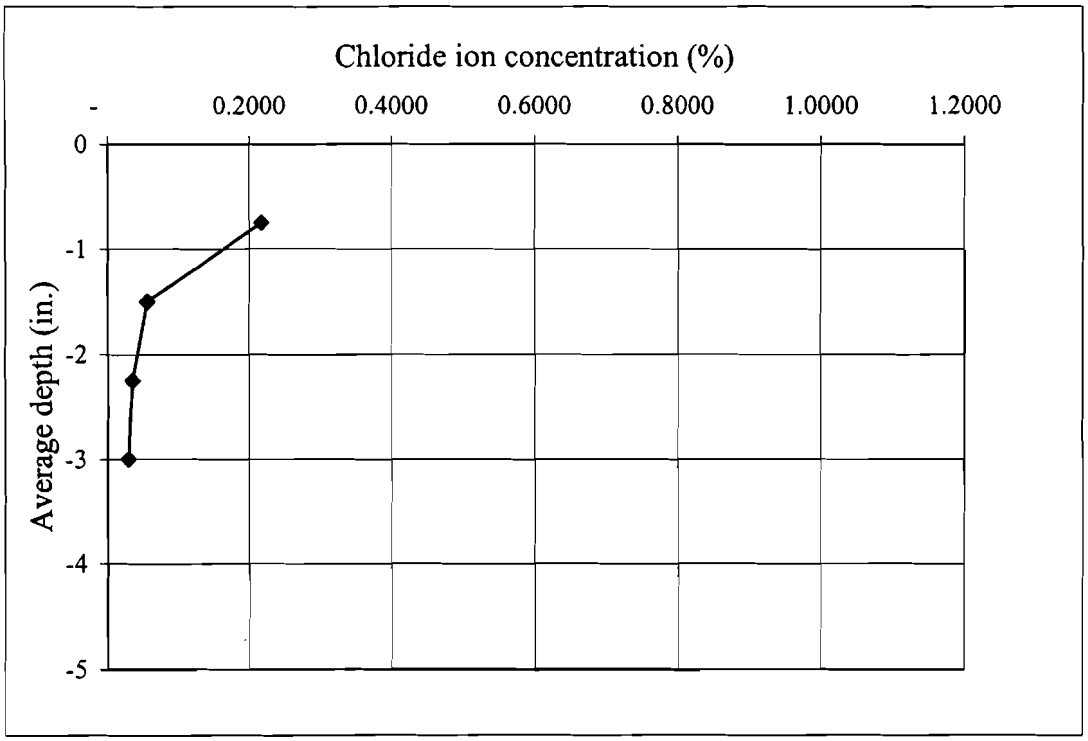

Figure 4.5. Chloride profile for Site 5.

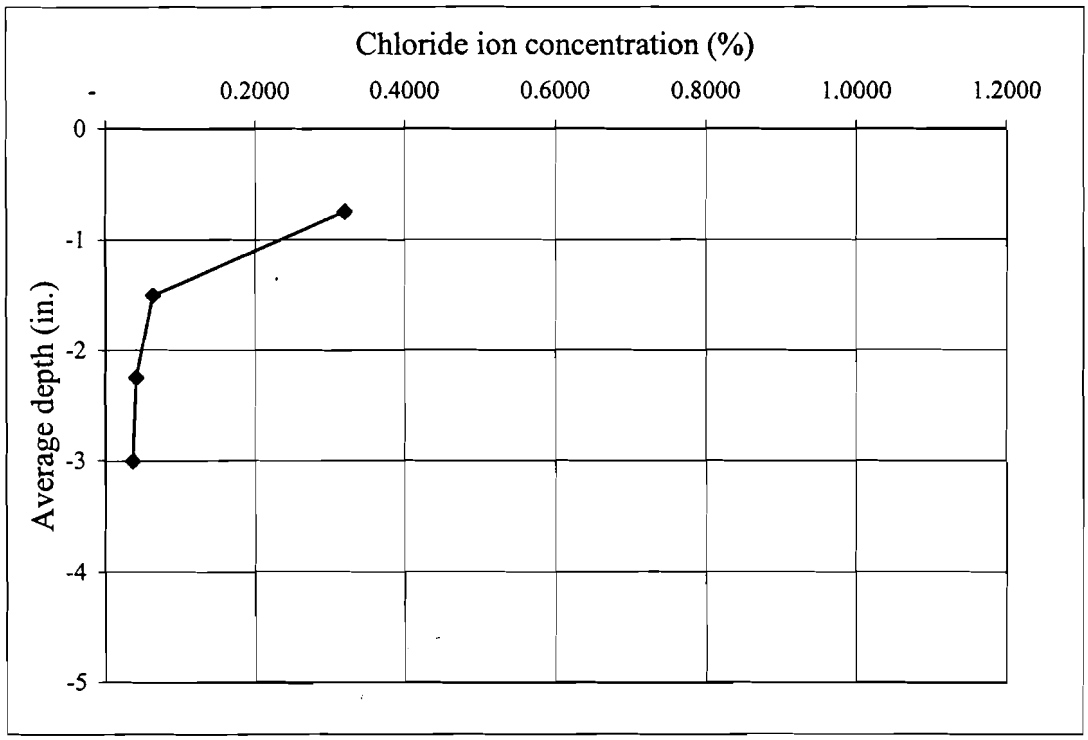

Figure 4.6. Chloride profile for Site 6.

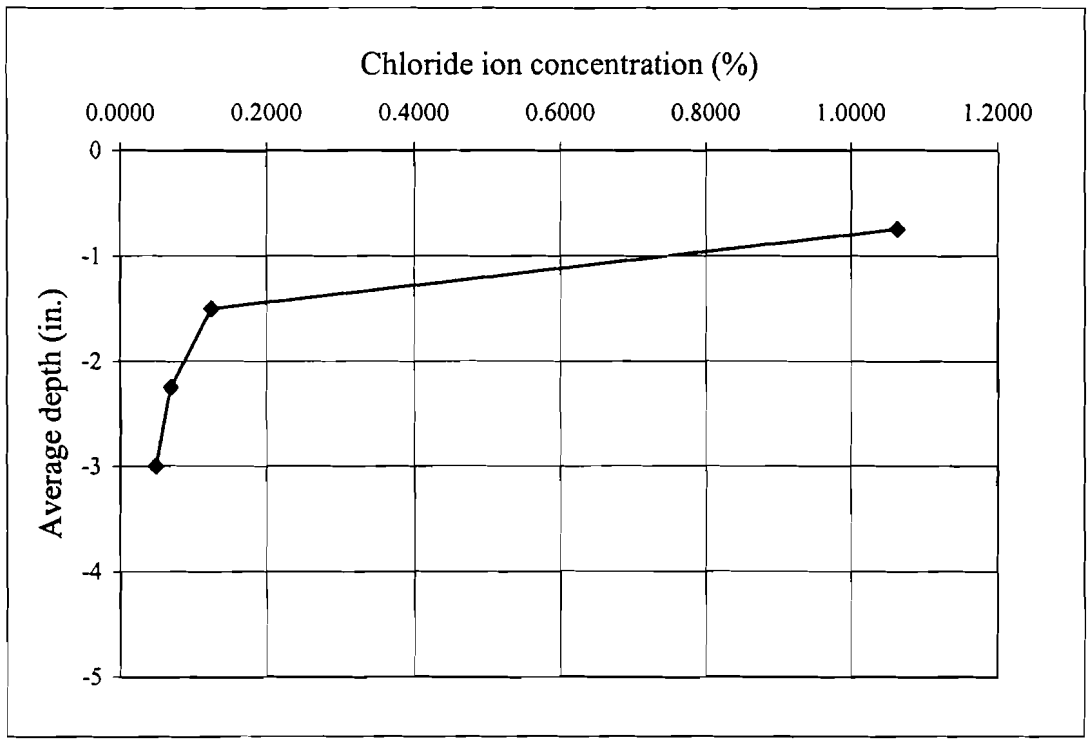

Figure 4.7. Chloride profile for Site 7.

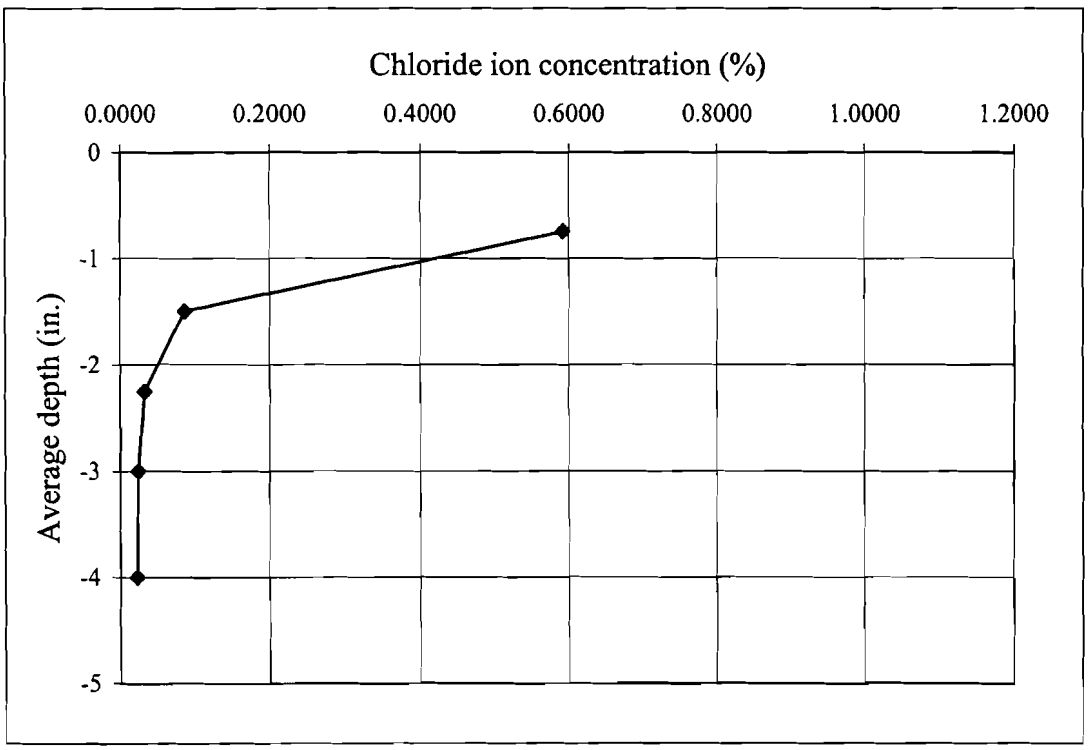

Figure 4.8. Chloride profile for Site 8.

Table 4.3. pH values for all sites.

Site	pH
1	12.48
2	12.46
3	12.49
4	12.51
5	12.44
6	12.40
7	12.59
8	12.55

4.5 Half-cell potential tests

Results from the half-cell potential tests are presented in the form of contour plots. This section describes and interprets the contour plots for each of the eight sites described in Chapter 3. As in Chapter 3, similar sites will be discussed together.

4.5.1 Sites 1 and 2

Figure 4.9 presents the half-cell potential measurements for Site 1. These results indicate a low or uncertain probability of corrosion occurring (> -350 mV), over the majority of the site. However, approximately 10% of the site, mostly along the edge of the approach slab, had half-cell potentials that were more negative than –350 mV. This indicates a high probability of corrosion occurring along the west side of the site.

Half-cell measurements for Site 2 are presented in Figure 4.10. The contour plot shows a high probability of corrosion occurring in approximately 80% of the approach slab, while the majority of the loading zone only showed a low probability of corrosion occurring (> -200 mV).

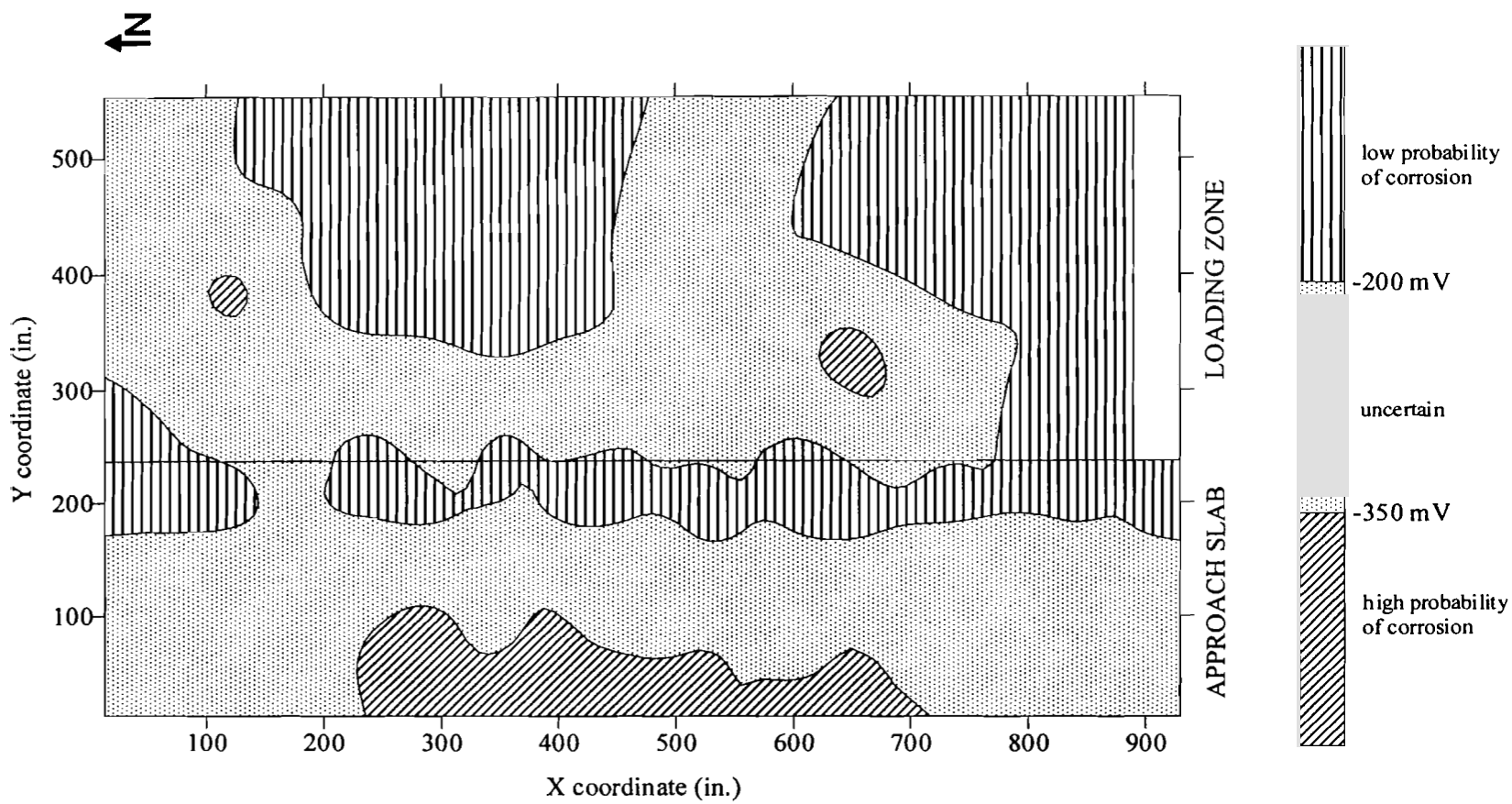

Figure 4.9. Equipotential contours for Site 1 on Pier 39 [Phase 1].

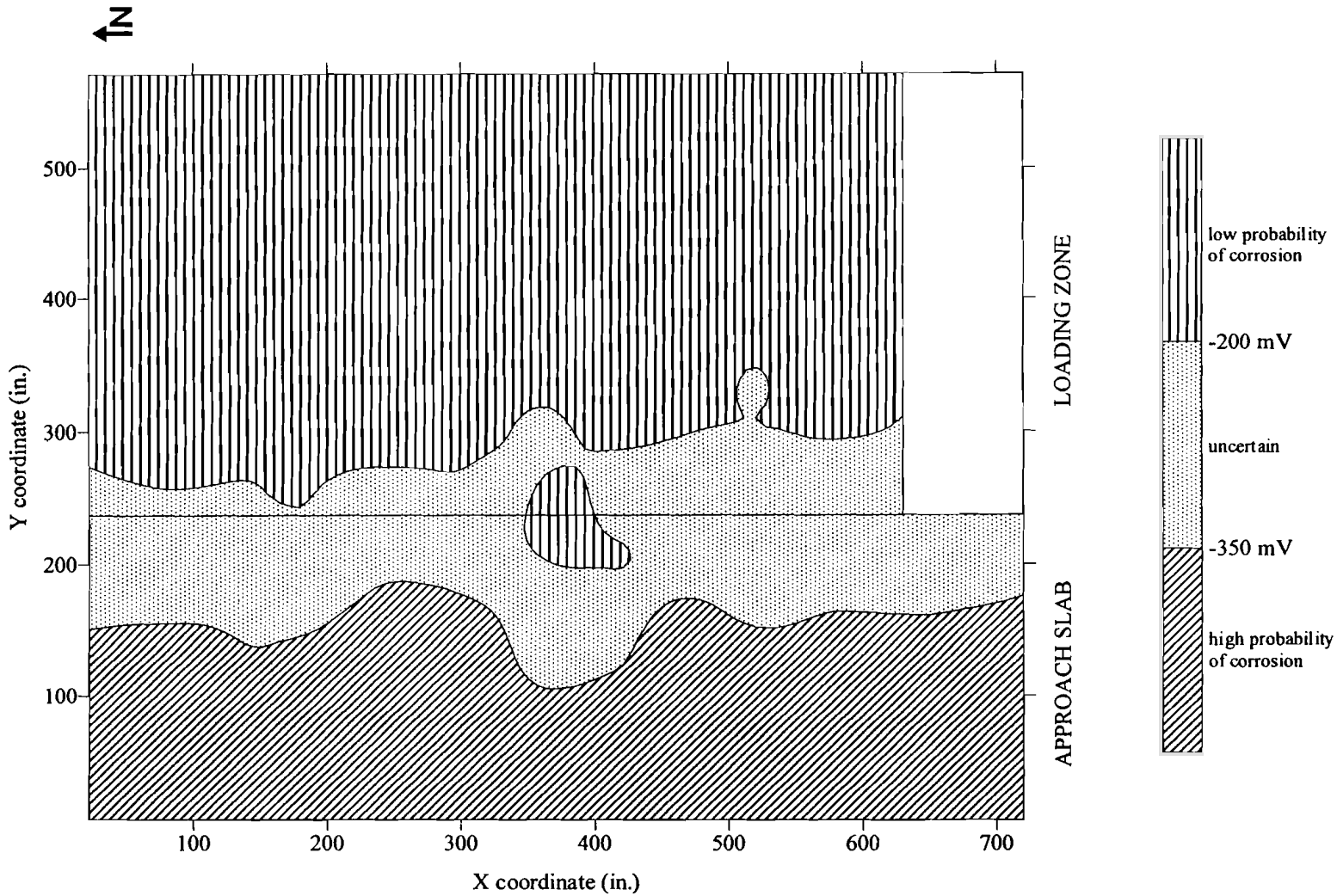

Figure 4.10. Equipotential contours for Site 2 on Pier 40.

For both sites, one would expect that high half-cell potentials would first occur on the loading zone because it is located closer to the seawater, and has more exposure to salt spray. However, the results showed that the active areas for both sites were found on the approach slab of the pier. When a ship is loaded or unloaded, a ramp is laid over the loading zone. This shelters the loading zone, reducing traffic and cycles of wetting and drying.

Although Site 2 was much younger than Site 1 (2 years versus 5 years), Site 2 had a high probability of corrosion over more than 30% of its area while Site 1 had less than 10% of its area identified as having a high probability of corrosion. One would expect Site 2 to have less corrosion activity since it is newer, had lower chloride concentrations, and has more concrete cover (2.5 inches for Site 1 versus 3.0 inches for Site 2).

There are at least two possible reasons for the larger active corrosion area for Site 2. First, the concrete for Site 2 had a much higher permeability. This would provide water and air easier access to the steel to promote corrosion. Another possibility is that the bars used in the approach slab were corroding before construction, and the concrete was unable to stop the process.

Visual inspections of bars taken from cores on Sites 1 and 2 indicate that Site 2 did have more corrosion than Site 1. However, both sites appeared to have more corrosion on the loading zones than on the approach slabs.

4.5.2 Sites 3 and 4

All of the half-cell readings for Site 3, shown in Figure 4.11, indicated low or uncertain probabilities of corrosion over the entire site. The majority of the

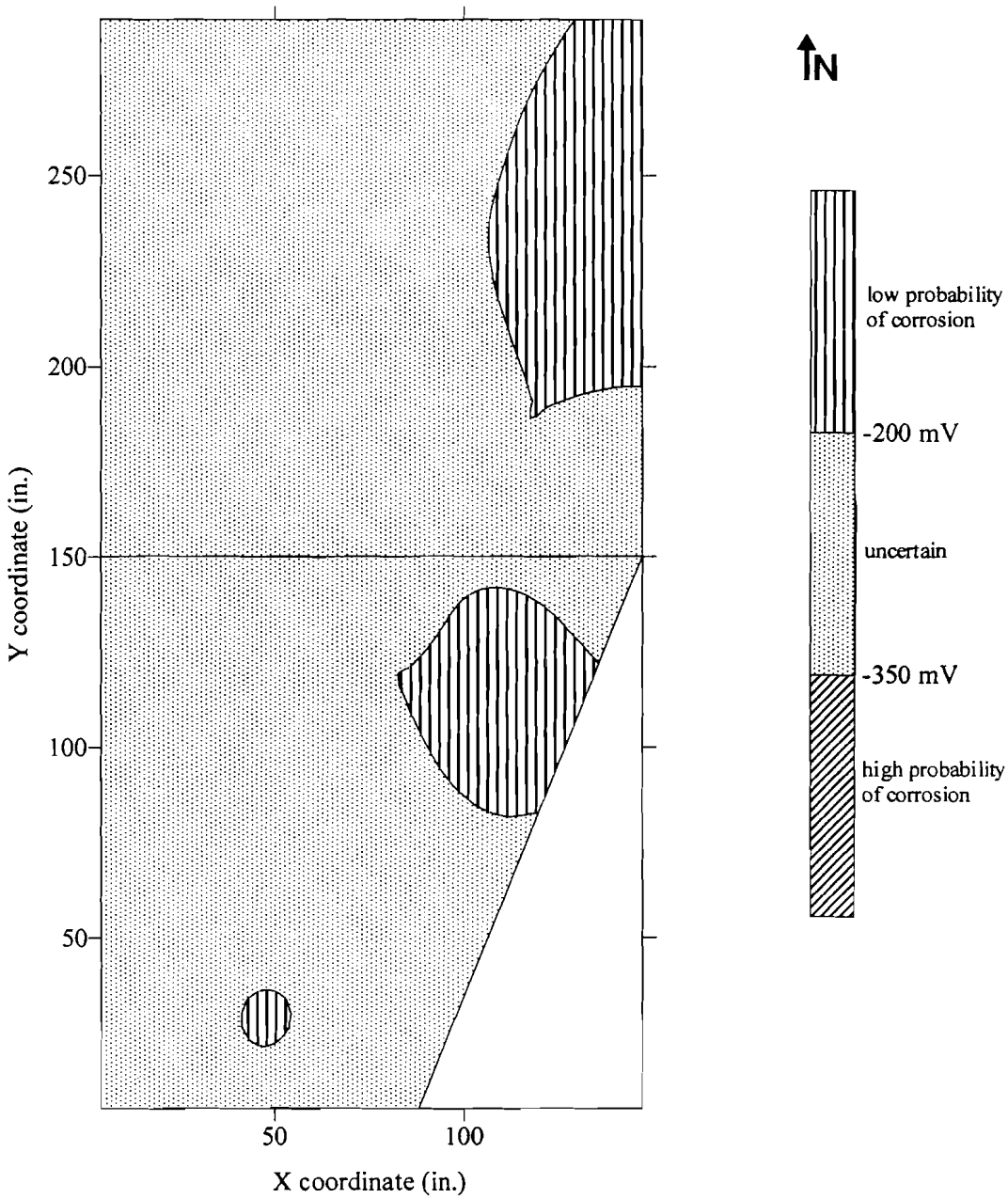

Figure 4.11. Equipotential contours for Site 3 on Pier 39 [Phase 1].

measurements were within the region of uncertainty, where the half-cell potentials measured between –200 mV and –350 mV. High half-cell potentials (> -350 mV) indicating a high probability of corrosion occurring, did not occur anywhere on Site 3.

The half-cell potential measurements for Site 4 are presented in Figure 4.12. High corrosion potentials were only recorded over a small area near the south end of the pavement. The rest of the site recorded potentials within the uncertain region.

Half-cell potential measurements for Sites 3 and 4 indicate a high probability of corrosion activity only at the south end of Site 4. However, as a percentage of the total area, Site 4 had much less corrosion activity than either Site 1 or Site 2. This was expected since Sites 3 and 4 had less exposure to the marine environment, less traffic, and comparable cover depths (3.75 inches for Site 3 and 2.5 inches for Site 4). The area on Site 4 that showed high half-cell potentials was probably due to bars that extended below the slab and were exposed to the ground. Such a bar was observed in one of the cores.

Bars taken from the cores cut on Site 3 showed significantly less corrosion than the bars taken from Sites 1 and 2. This appears to support the results of the nondestructive tests.

4.5.3 Sites 5 and 6

Half-cell potentials from Site 5 are presented in Figure 4.13. About 90% of the test area indicated a low probability of corrosion occurring, while the other 10% of the test area showed corrosion potentials within the uncertain region. None of the half-cell potentials measured for Site 5 were more negative than -350 mV.

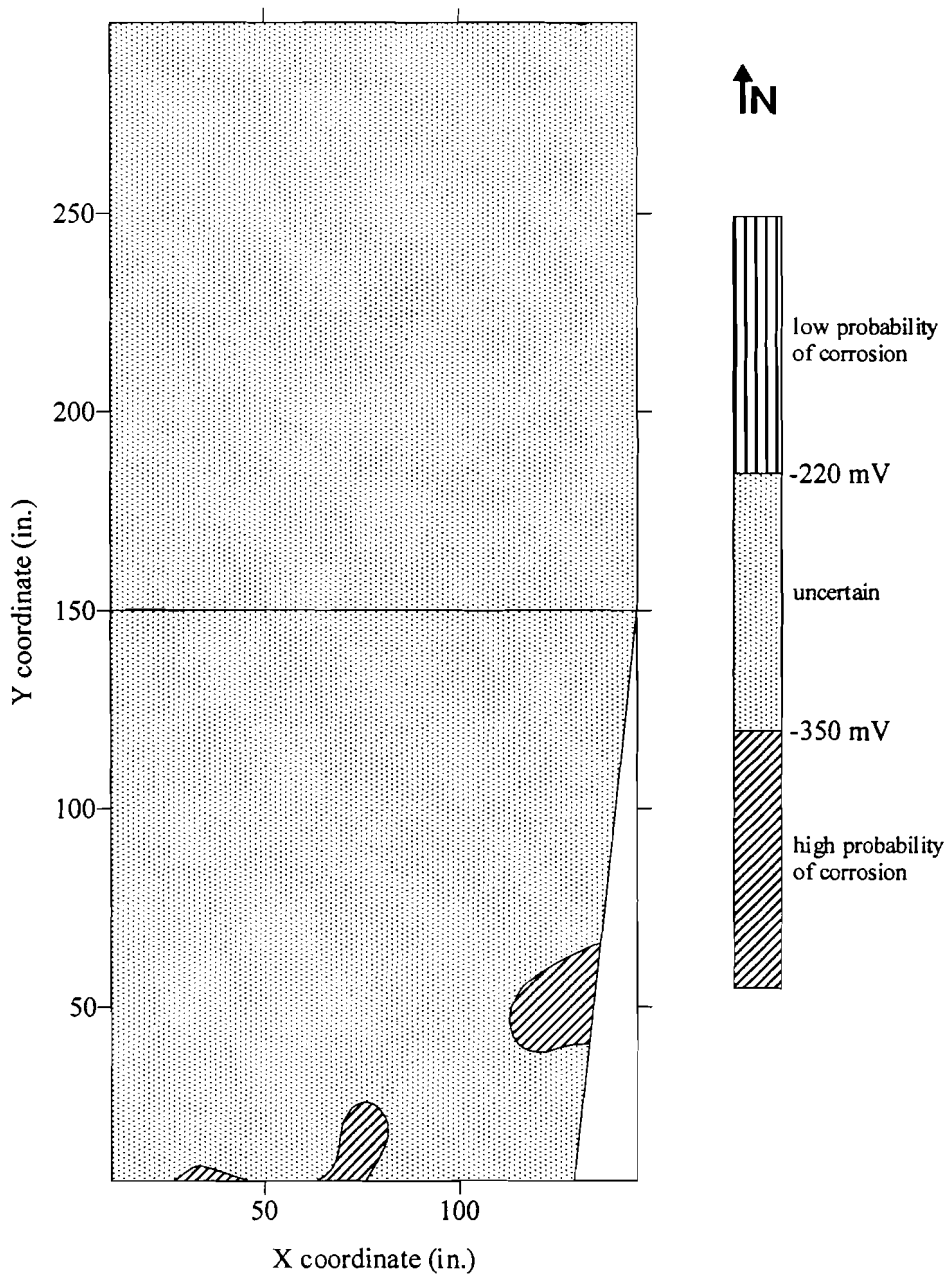

Figure 4.12. Equipotential contours for Site 4 on Pier 39 [Phase 2].

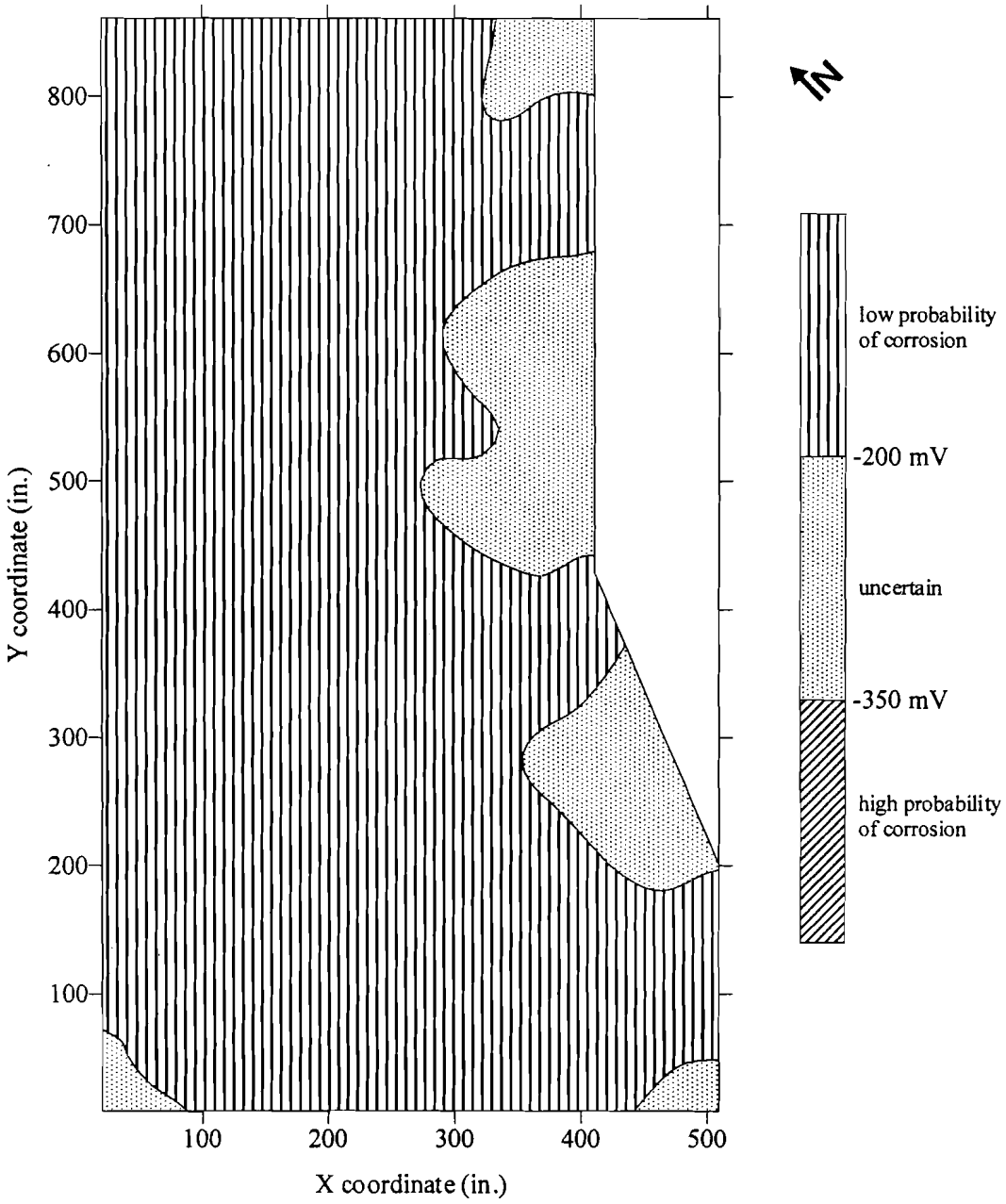

Figure 4.13. Equipotential contours for Site 5 on Pier 34.

Similarly, most of the readings for Site 6 indicated low corrosion potentials. These half-cell measurements are presented in Figure 4.14. Only about 10% of the test points had potentials within the uncertain limits, while the rest indicated a low probability of corrosion.

The exposure conditions for these sites were similar to Sites 1 and 2. A visual inspection identified extensive shrinkage cracks on both sites. The shrinkage cracks on Sites 5 and 6 should have made them more susceptible to corrosion, so the lack of corrosion activity is somewhat surprising. Additionally, Sites 5 and 6 had high permeabilities and cover depths ranging from 2.0 inches to 3.5 inches. However, the mixture design for Sites 5 and 6 specified 4.0 gal/yd^3 of DCI, which is greater than the 2.5 gal/yd^3 used for Sites 1 though 4. The increased DCI dosage appears to be responsible for the reduction in corrosion activity.

Visual inspection of bars taken from cores on Sites 5 and 6 had much less evidence of corrosion than the bars from the first four sites. This provides further support for the electrical measurements.

4.5.4 Site 7

Half-cell measurements for Site 7, as shown in Figure 4.15, mostly indicated an uncertain probability of corrosion occurring. There were no high corrosion potentials recorded.

Site 7 was exposed to seawater on three sides, but experienced lower traffic conditions (primarily pedestrian). Site 7 was also older than the first six sites, and had marginal permeability. Therefore, the lack of corrosion activity is attributed to the

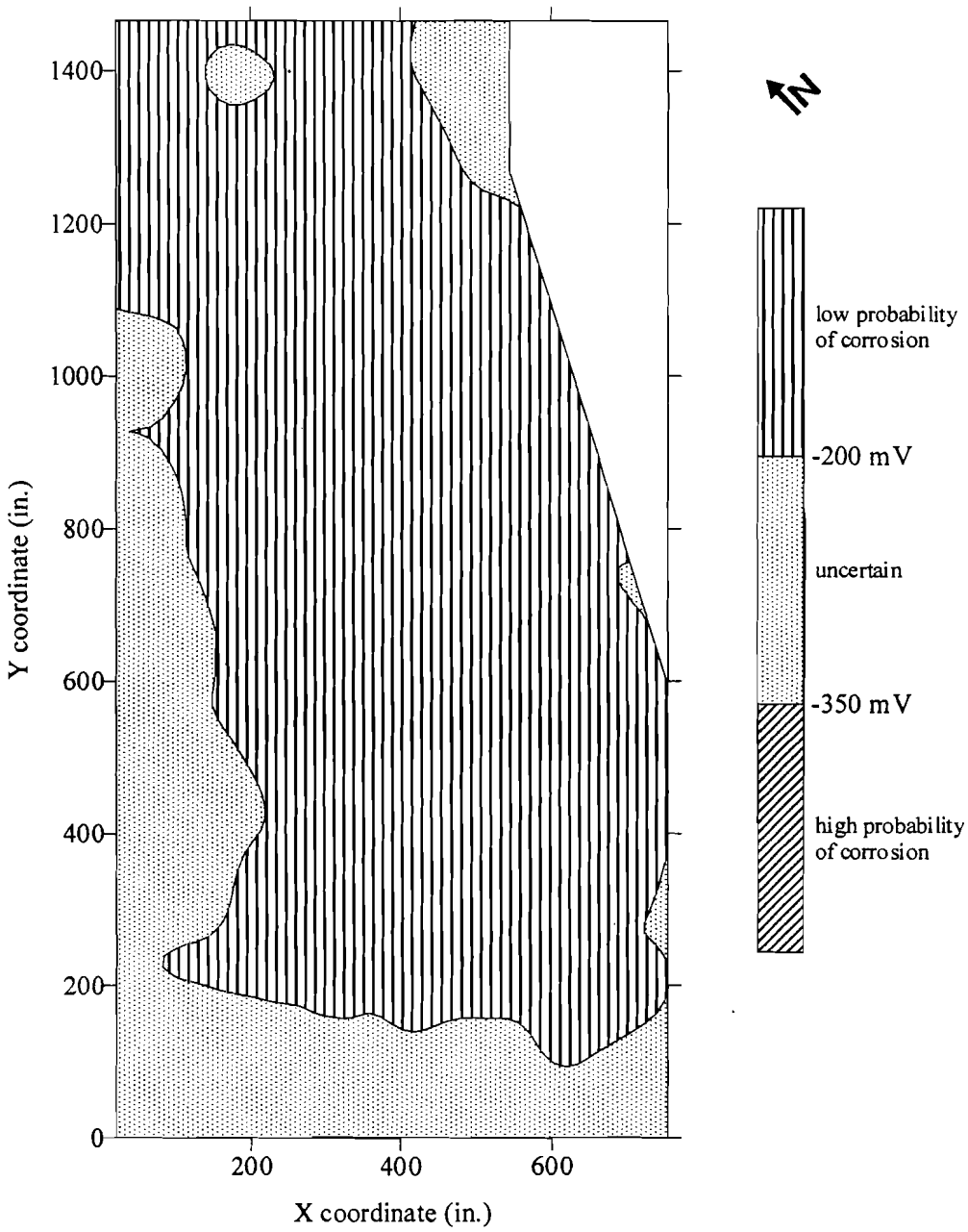

Figure 4.14. Equipotential contours for Site 6 on Pier 34.

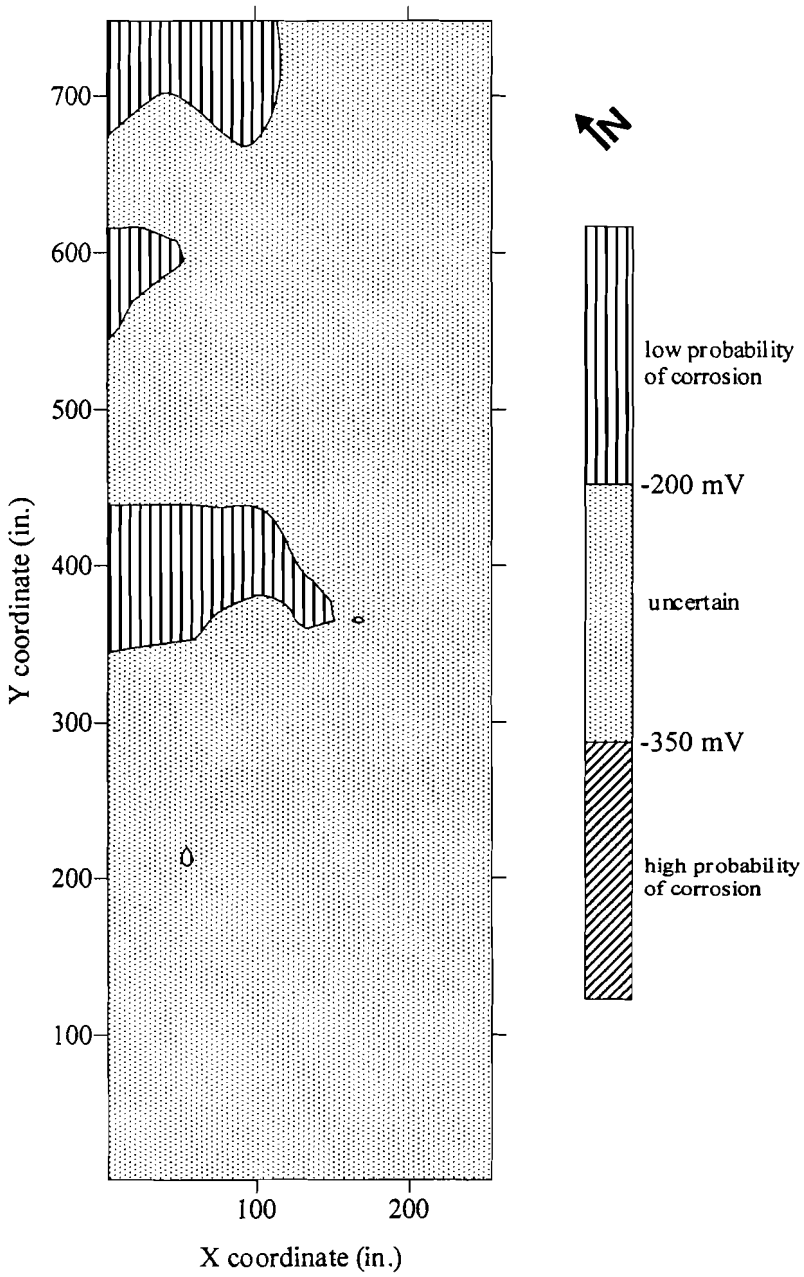

Figure 4.15. Equipotential contours for Site 7, the ferry terminal pier at Barbers Point Harbor.

4.5 gal/yd^3 of DCI that was used in the mix design. This dosage was the highest amount of DCI used in any of the sites.

Bars taken from cores on Site 7 showed virtually no evidence of corrosion. This also agrees with the electrical measurements.

4.5.5 Site 8

Figure 4.16 shows the contour plot for the corrosion potentials on Site 8. As indicated in the figure, about 70% of the test area showed an uncertain probability of corrosion occurring, while the rest of the site measured high corrosion potentials. However, the reinforcing steel in Site 8 was coated with epoxy, and half-cell measurements are not expected to provide a reliable assessment of the corrosion. Consequently, the assessment of Site 8 relies primarily on the visual inspection of bars taken from cores. No signs of corrosion were found on any of the bars from Site 8, so it appears that the epoxy coating has been effective.

4.6 Polarization resistance tests

As with the half-cell potential tests, results from the polarization resistance tests for Sites 1 through 8 are presented in the form of contour plots. Results for each of the eight sites are presented and discussed in this section, with similar sites being discussed together.

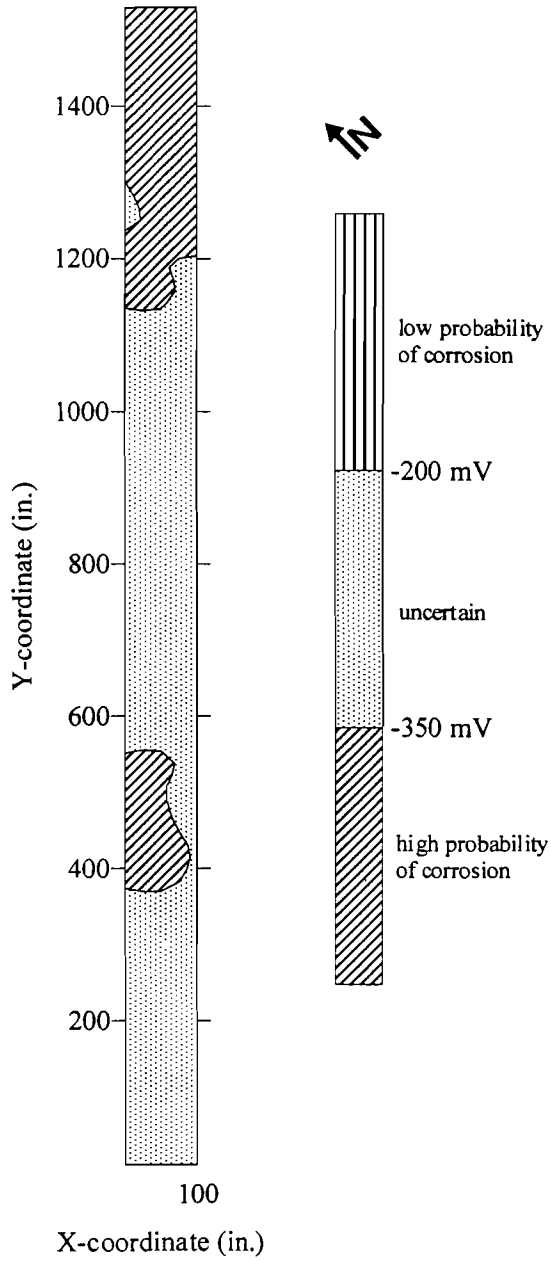

Figure 4.16. Equipotential contours for Site 8, Pier 6 at Barbers Point Harbor.

4.6.1 Sites 1 and 2

The corrosion rate measurements for Site 1 are shown in the contour plot presented in Figure 4.17. High corrosion rates (>1.0 $\mu A/cm^2$) were found on less than 5% of both the approach slab and the loading zone. The remainder of the site either had no corrosion occurring or corrosion was occurring at a low rate (< 0.5 $\mu A/cm^2$). There was only a slight overlap of the high corrosion rate regions with the region identified as having a high probability of corrosion activity.

Corrosion rates for Site 2 are presented in Figure 4.18. As with Site 1, less than 5% of the test area showed high rates of corrosion (> 1.00 $\mu A/cm^2$). Less than 15% of the area was identified as either a moderate or high corrosion rate area. All of this area was on the loading platform. There was no overlap of the high corrosion rate area and the high potential readings from the half-cell.

While the areas of corrosion identified by the half-cell potential and the polarization resistance tests show little correlation, the general trend is the same. Site 2 shows active corrosion over a larger area. As with the half-cell potential measurements, this is attributed to the higher permeability of the concrete on Site 2. The high permeability allows more water and air to reach the reinforcing steel and continue the reaction.

The polarization resistance measurements show better agreement with the visual inspection of bars taken from cores. The visual inspection found more corrosion on the

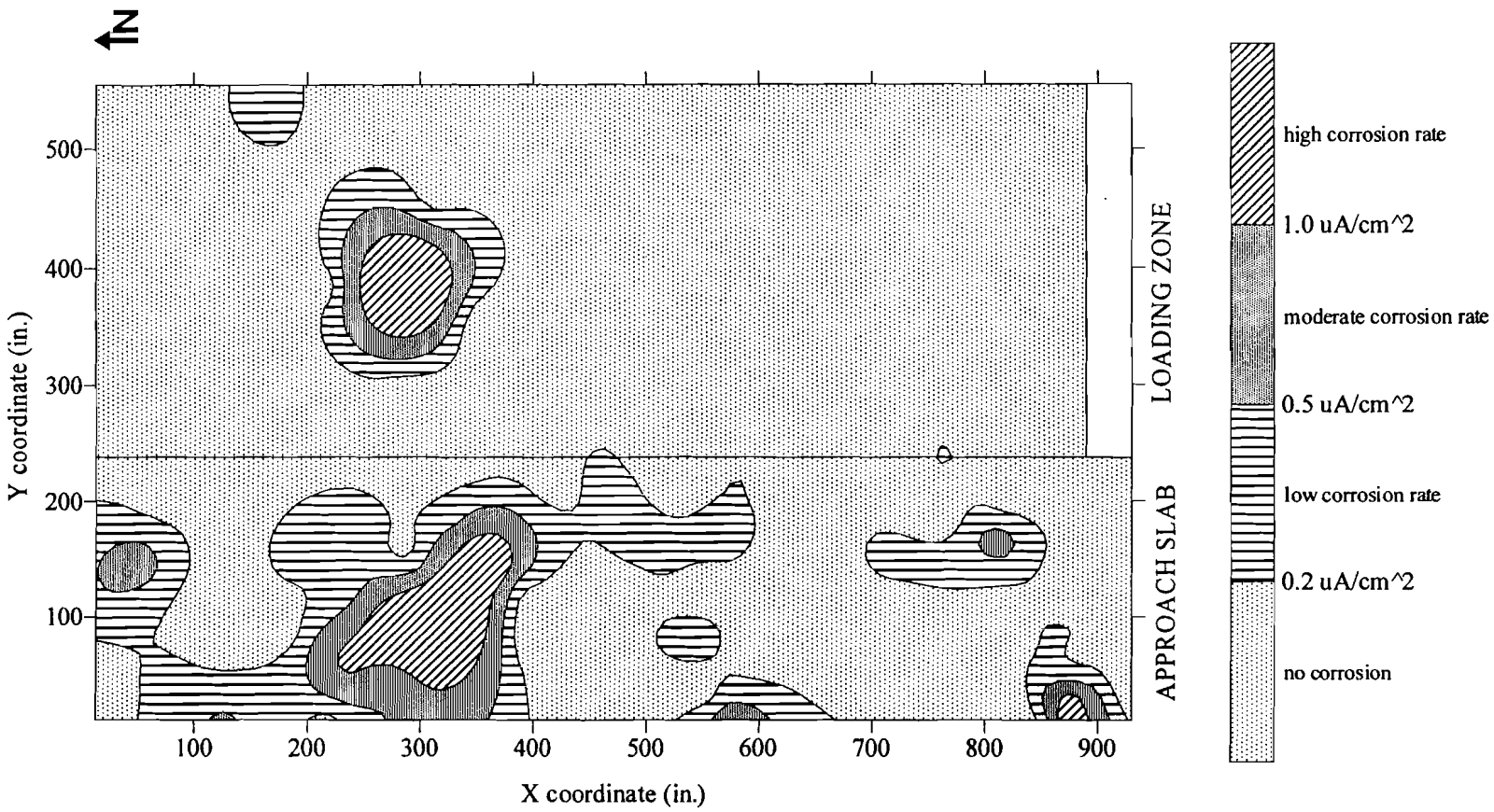

Figure 4.17. Contours of corrosion rates for Site 1 on Pier 39 [Phase 1].

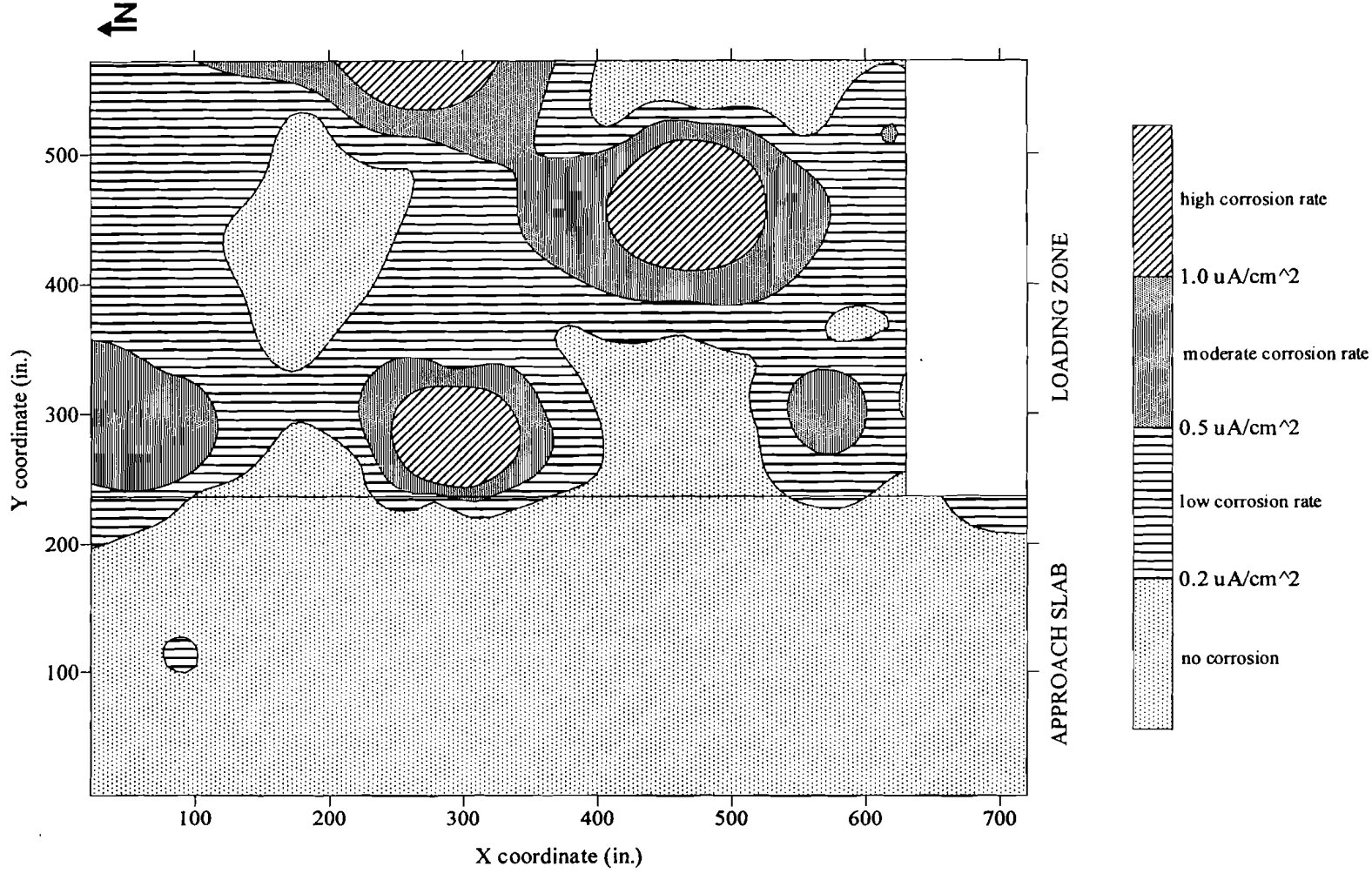

Figure 4.18. Contours of corrosion rates for Site 2 on Pier 40.

bars from Site 2, and more corrosion on the loading zones than on the approach slabs for both sites.

4.6.2 Sites 3 and 4

The corrosion rates measured on Sites 3 and 4 were mostly very low or moderate. This is shown in Figures 4.19 and 4.20. Only about 5% of Site 3 recorded high corrosion rates, while all of the area on Site 4 showed low corrosion rate measurements.

Again, Sites 3 and 4 were expected to have less corrosion activity than Sites 1 and 2 because they had less exposure to the marine environment, less traffic, and comparable cover depths.

4.6.3 Sites 5 and 6

The corrosion rate measurements for Sites 5 and 6 are presented in Figures 4.21 and 4.22, respectively. Most of the corrosion rates for Site 5 were very low. Only about 2% of the area yielded high rates of corrosion. The corrosion rates for Site 6 indicated that no part of the site had high corrosion rates, and very little area had moderate rates.

As with the half-cell measurements, the lack of corrosion activity in concrete with high permeability and extensive shrinkage cracks is attributed to the higher dosage of the calcium nitrite based admixture (4.0 gal/yd^3 vs. 2.5 gal/yd^3 for Sites 1 to 4).

4.6.4 Site 7

Figure 4.23 shows the corrosion rates recorded on Site 7. The majority of the area had corrosion rates that were mostly within the low and moderate region. The low

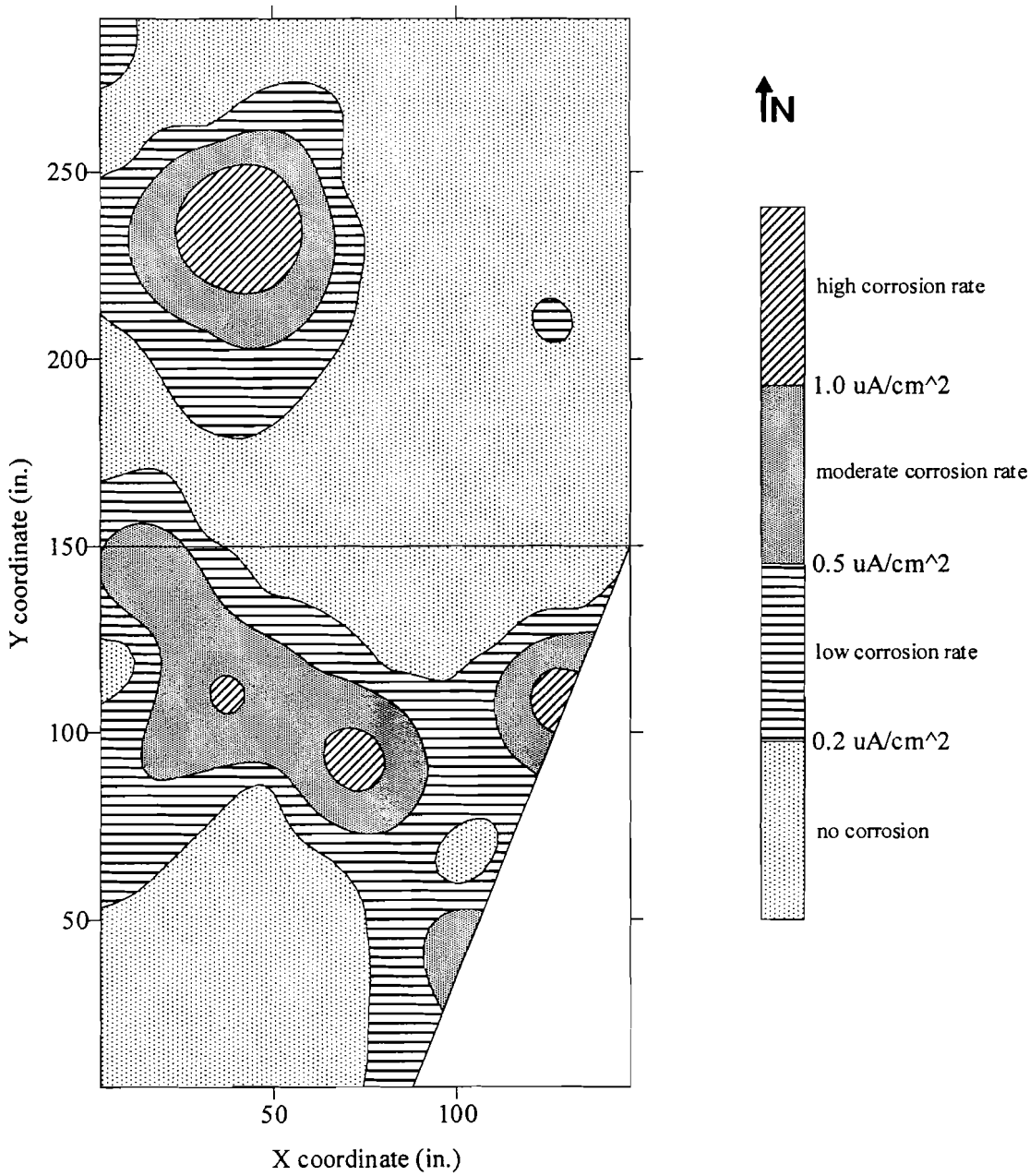

Figure 4.19. Contours of corrosion rates for Site 3 on Pier 39 [Phase 1].

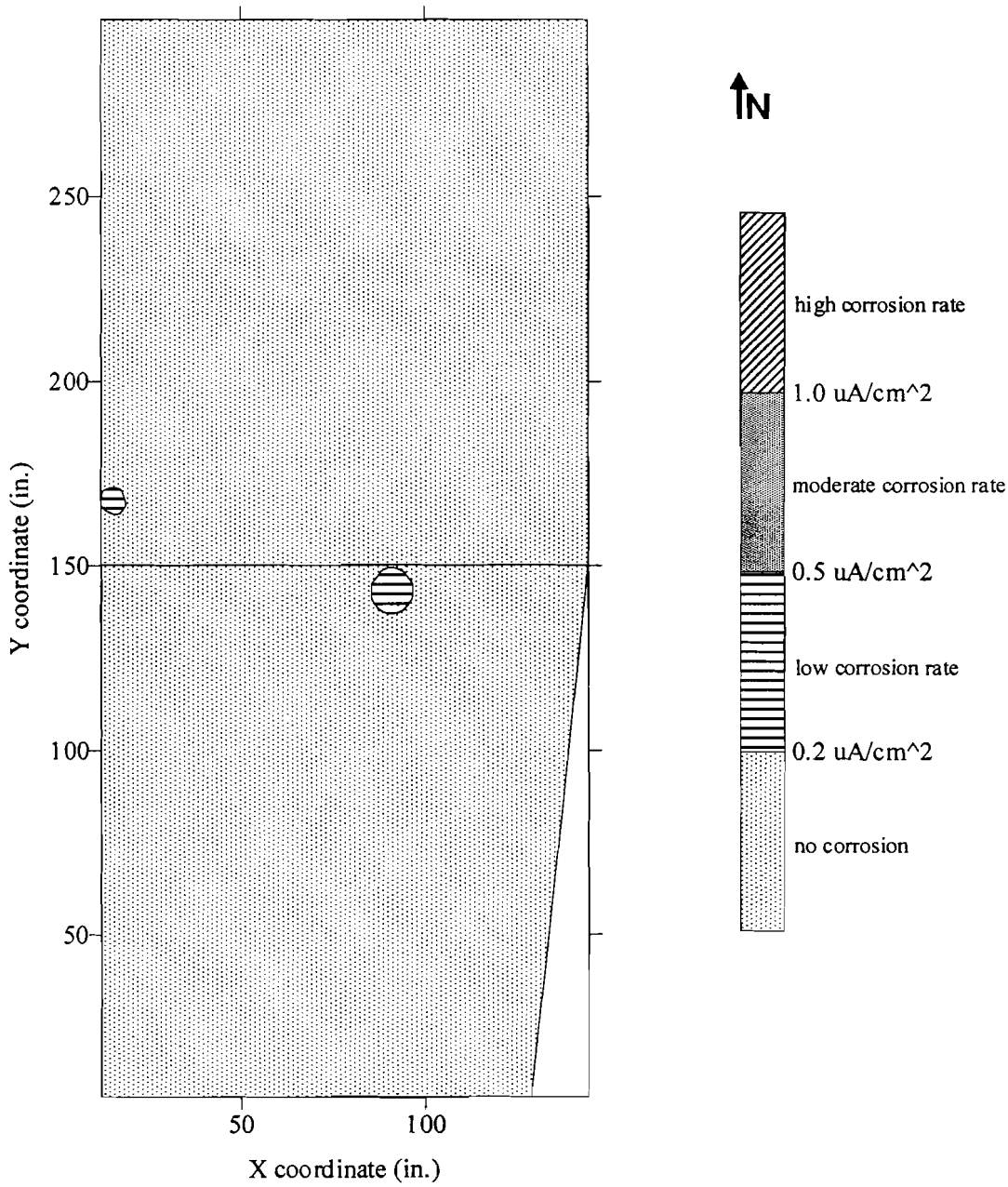

Figure 4.20: Contours of corrosion rates for Site 4 on Pier 39 [Phase 2].

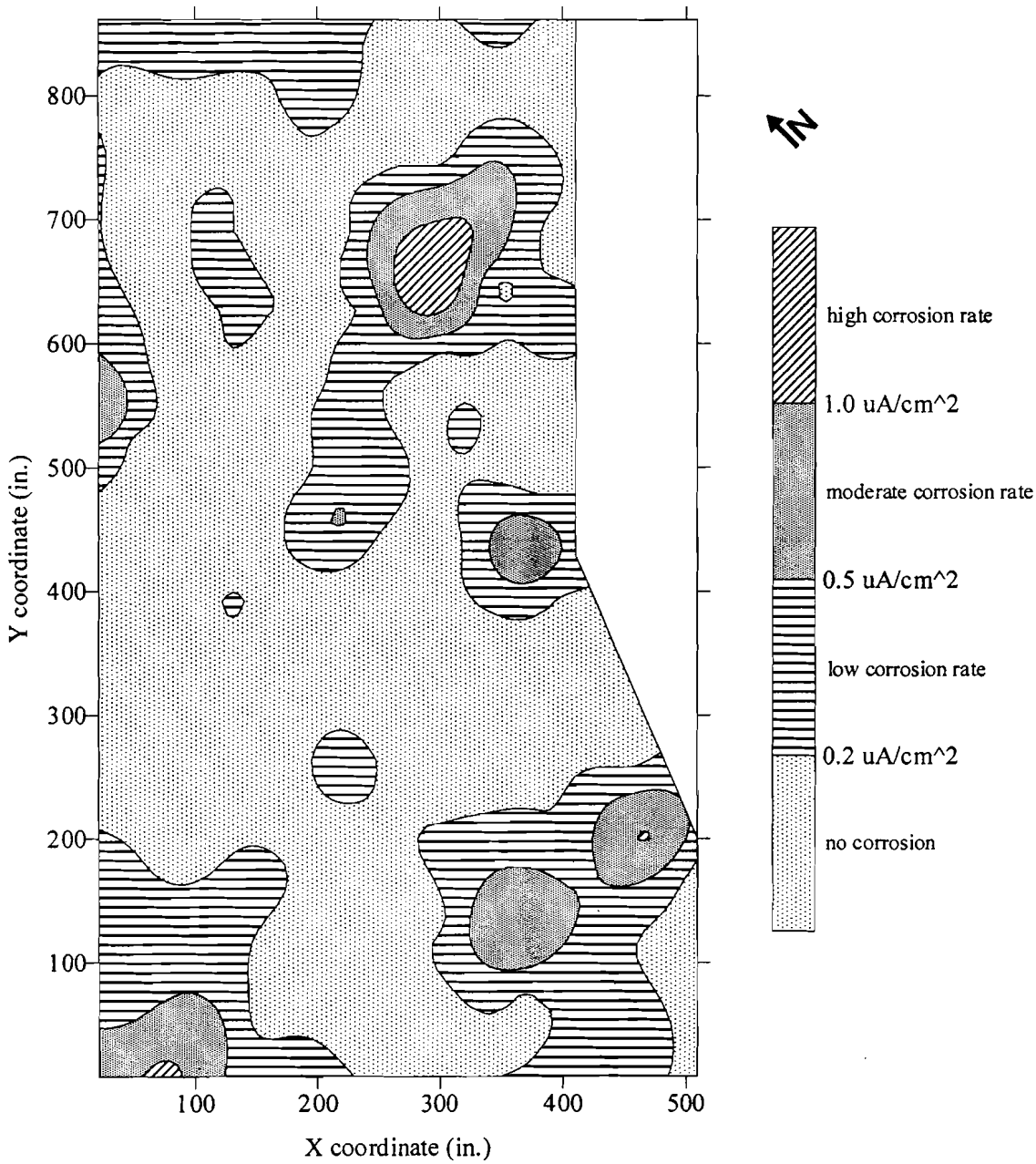

Figure 4.21. Contours of corrosion rates for Site 5 on Pier 34.

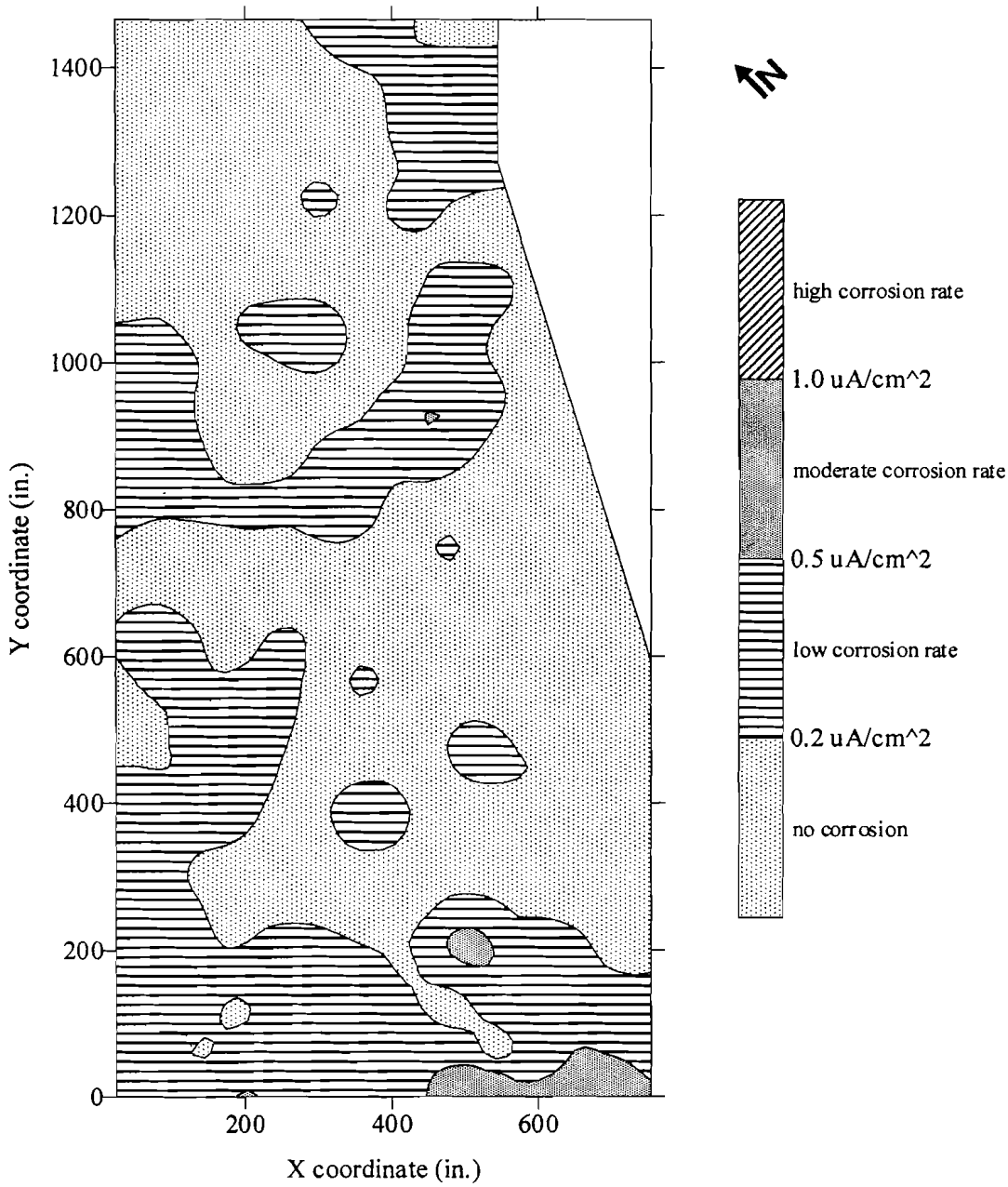

Figure 4.22. Contours of corrosion rates for Site 6 on Pier 34.

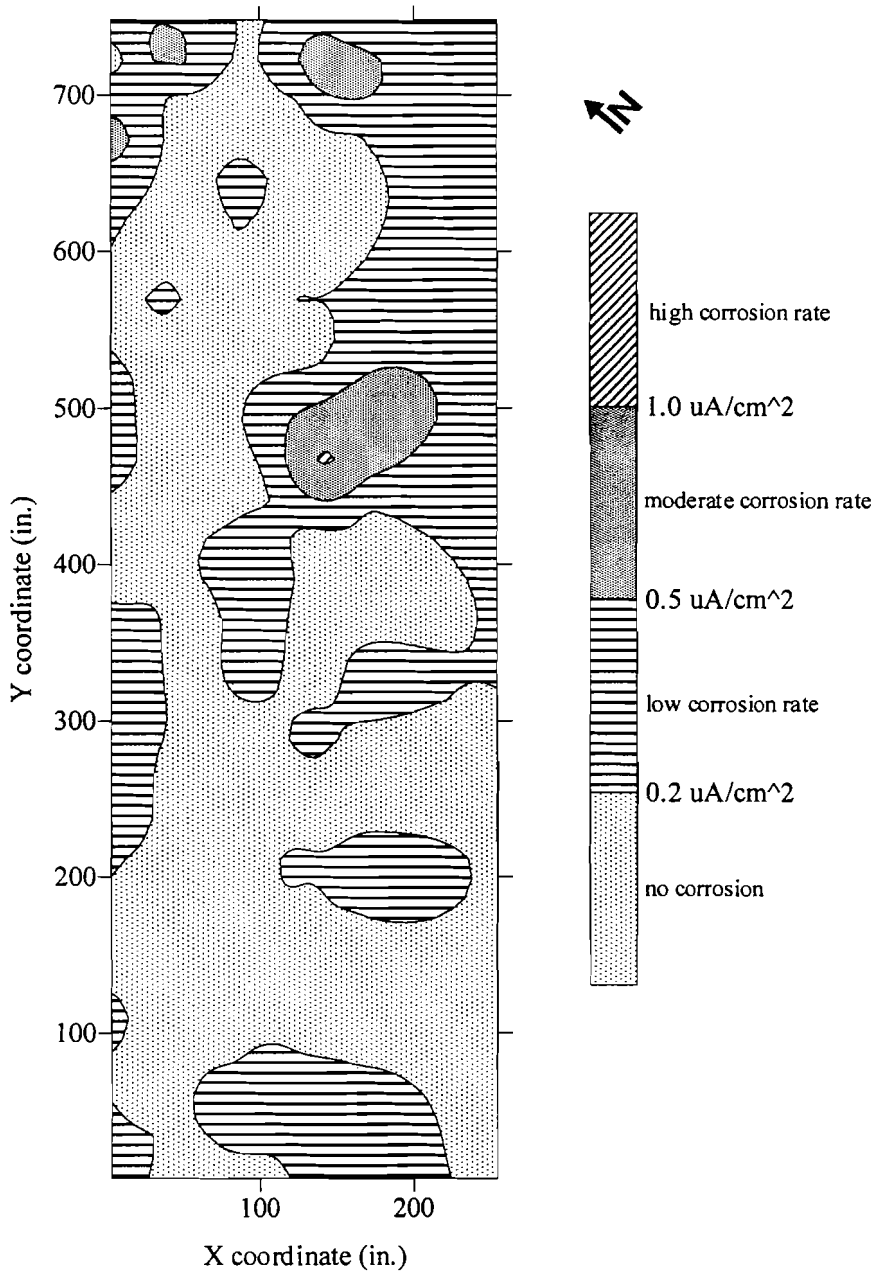

Figure 4.23. Contours of corrosion rates for Site 7, the ferry terminal pier at Barbers Point Harbor.

corrosion activity on this site is also attributed to a high dosage of the calcium nitrite admixture (4.5 gal/yd^3).

4.6.5 Site 8

Site 8 only had low corrosion rate measurements throughout the entire site. However, the corrosion meter used for testing does not provide reliable results for epoxy-coated steel. As stated earlier in the previous section, the evaluation of Site 8 relied on visual inspection of bars obtained from cores, and no evidence of corrosion was found on the bars from Site 8.

4.7 Concrete resistivity tests

Concrete reisistivity values, another measure of corrosion rate, are presented for each of the eight sites in this section. Contour plots for all eight sites are presented and discussed.

4.7.1 Sites 1 and 2

Concrete resistivity results for Sites 1 and 2 are presented in Figures 4.25 and 4.26. Site 1 showed that less than 10% of the area had high or very high corrosion rates (< 10 kΩ cm). Most of the high corrosion rate area was on the loading zone, and correlated with part of the high corrosion rate region recorded from the polarization resistance test (Figure 4.17). The resistivity plot (Figure 4.25) and the corrosion rate plot for Site 1 showed reasonable agreement.

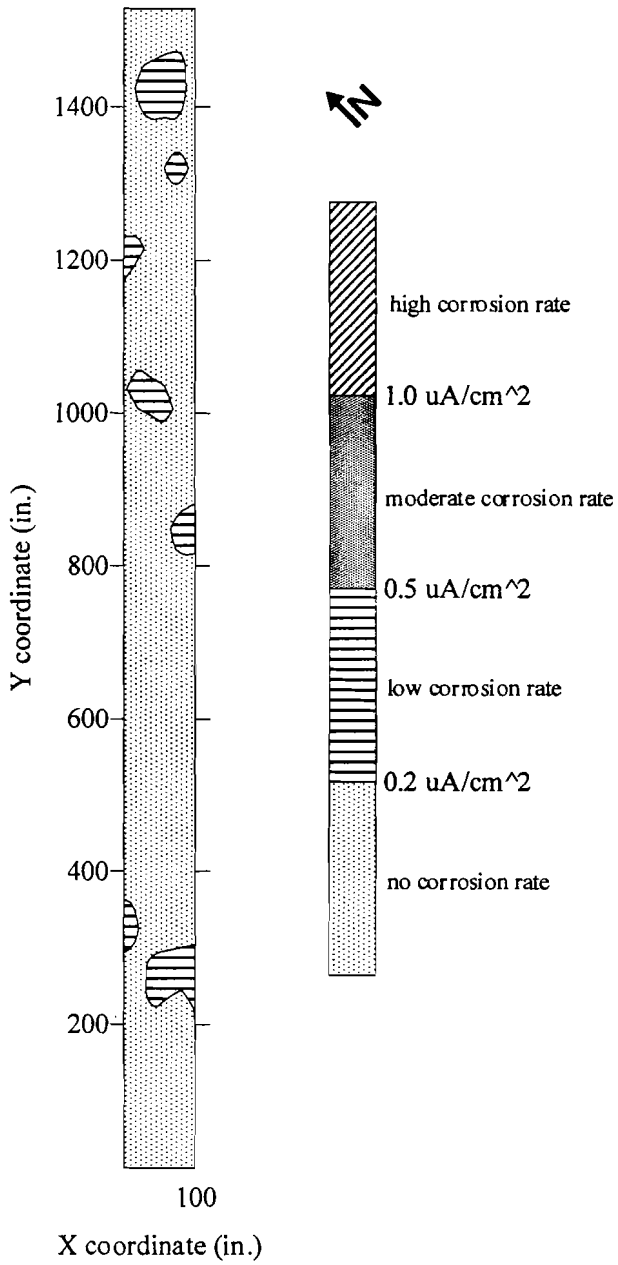

Figure 4.24. Contours of corrosion rates for Site 8, Pier 6 at Barbers Point Harbor.

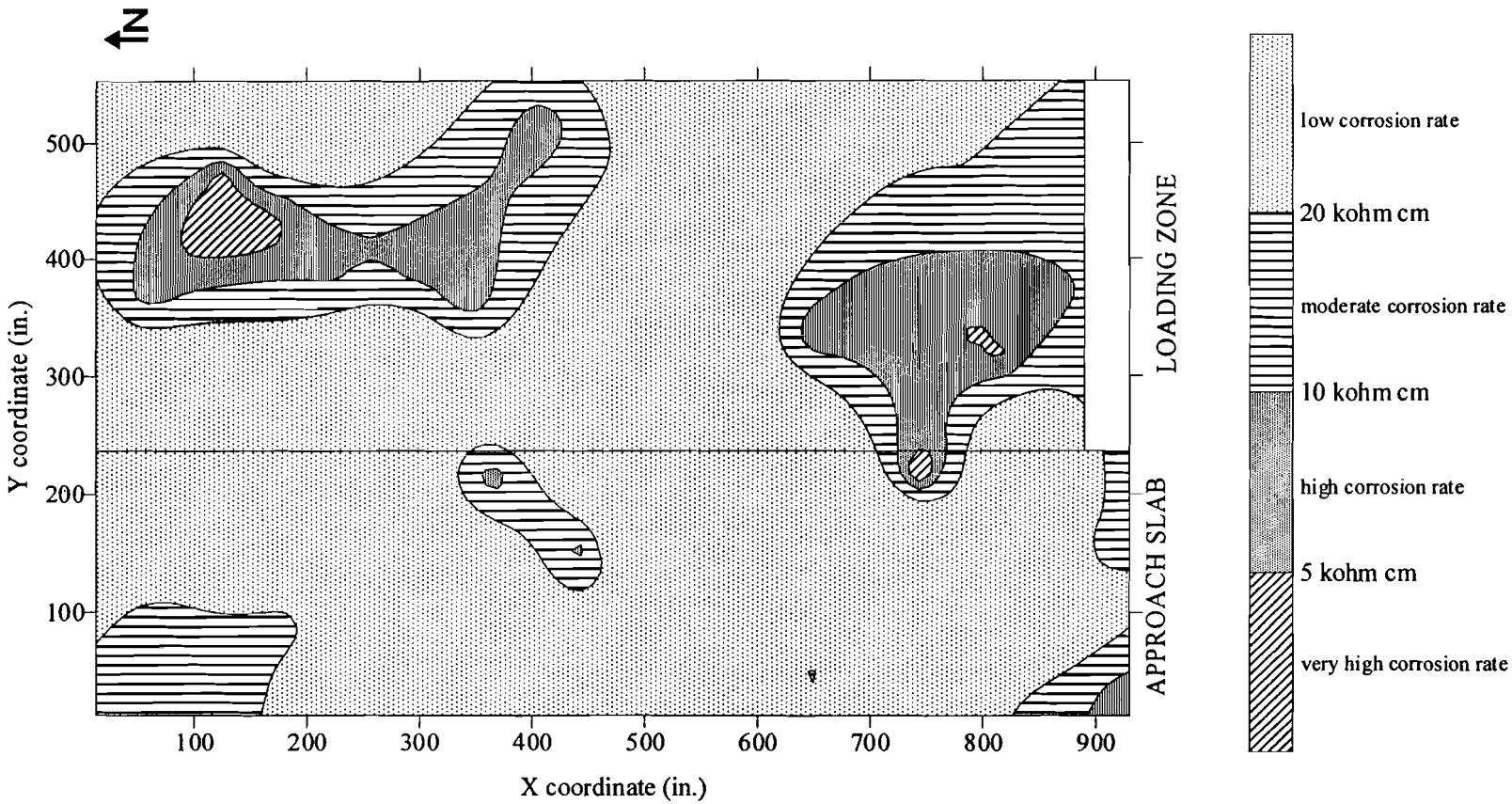

Figure 4.25. Contours of concrete resistivity for Site 1 on Pier 39 [Phase 1].

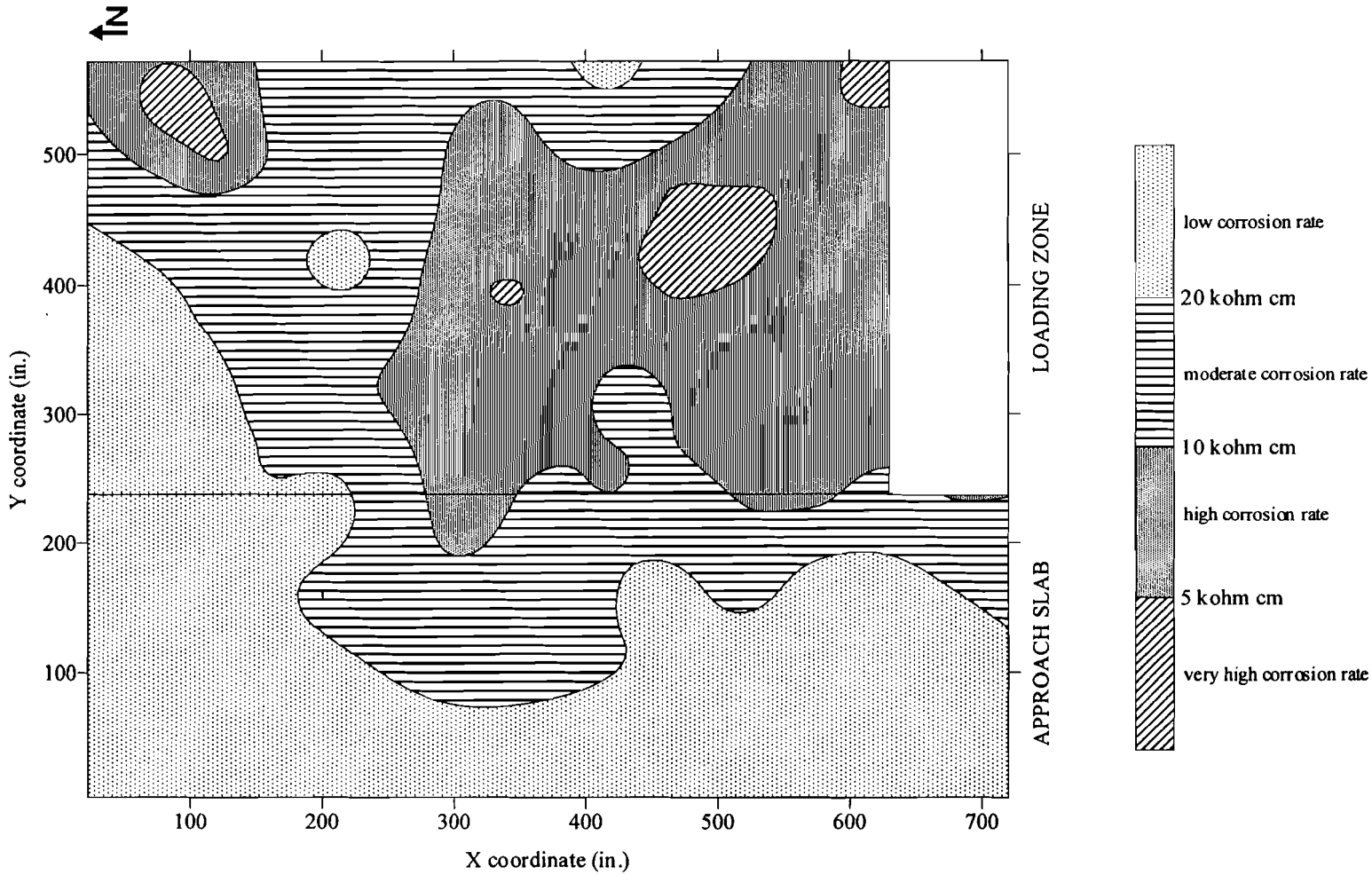

Figure 4.26. Contours of concrete resistivities for Site 2 on Pier 40.

For Site 2, the area of high corrosion rate involved about 25% of the test area, and was located mostly on the loading zone. These regions with high corrosion rates correlated well with the regions identified by the polarization resistance tests. This agreement supports the arguments presented earlier for the half-cell measurements and the polarization resistance measurements.

4.7.2 Sites 3 and 4

Resistivity results for Site 3 are presented in Figure 4.27. These results show either low or moderate corrosion rates, with the exception of about 5% of the area that had high rates of corrosion. Figure 4.28 presents the results from Site 4, and shows that the south end of the pavement had high corrosion rates. This high corrosion rate area involved a little more than 20% of Site 4.

The reduced corrosion activity of Site 3 (compared to Sites 1 and 2) follows the same trend seen for the half-cell and polarization resistance tests. For Site 4, the large region of high corrosion rate shows some agreement with the half-cell results. However, it is suspected that bars extending below the slab (described in Section 4.5.2) may be responsible for these readings.

4.7.3 Sites 5 and 6

Figures 4.29 and 4.30 present the resistivity results for Sites 5 and 6, respectively. These results show that almost half of Sites 5 and 6 had high or very high corrosion rate areas. This contradicts the trends seen for both the half-cell potential and the polarization resistance measurements.

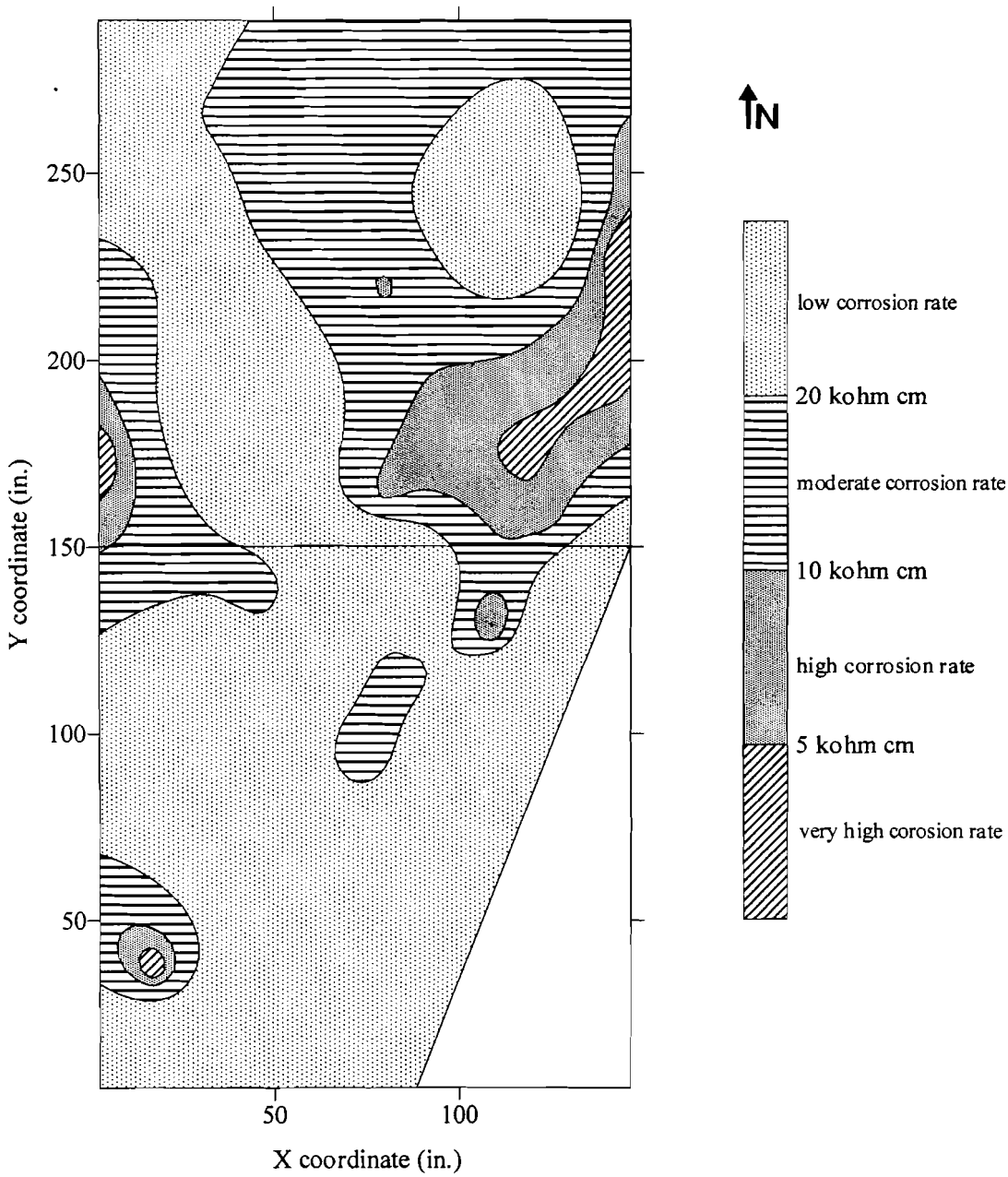

Figure 4.27. Contours of concrete resistivity for Site 3 on Pier 39 [Phase 1].

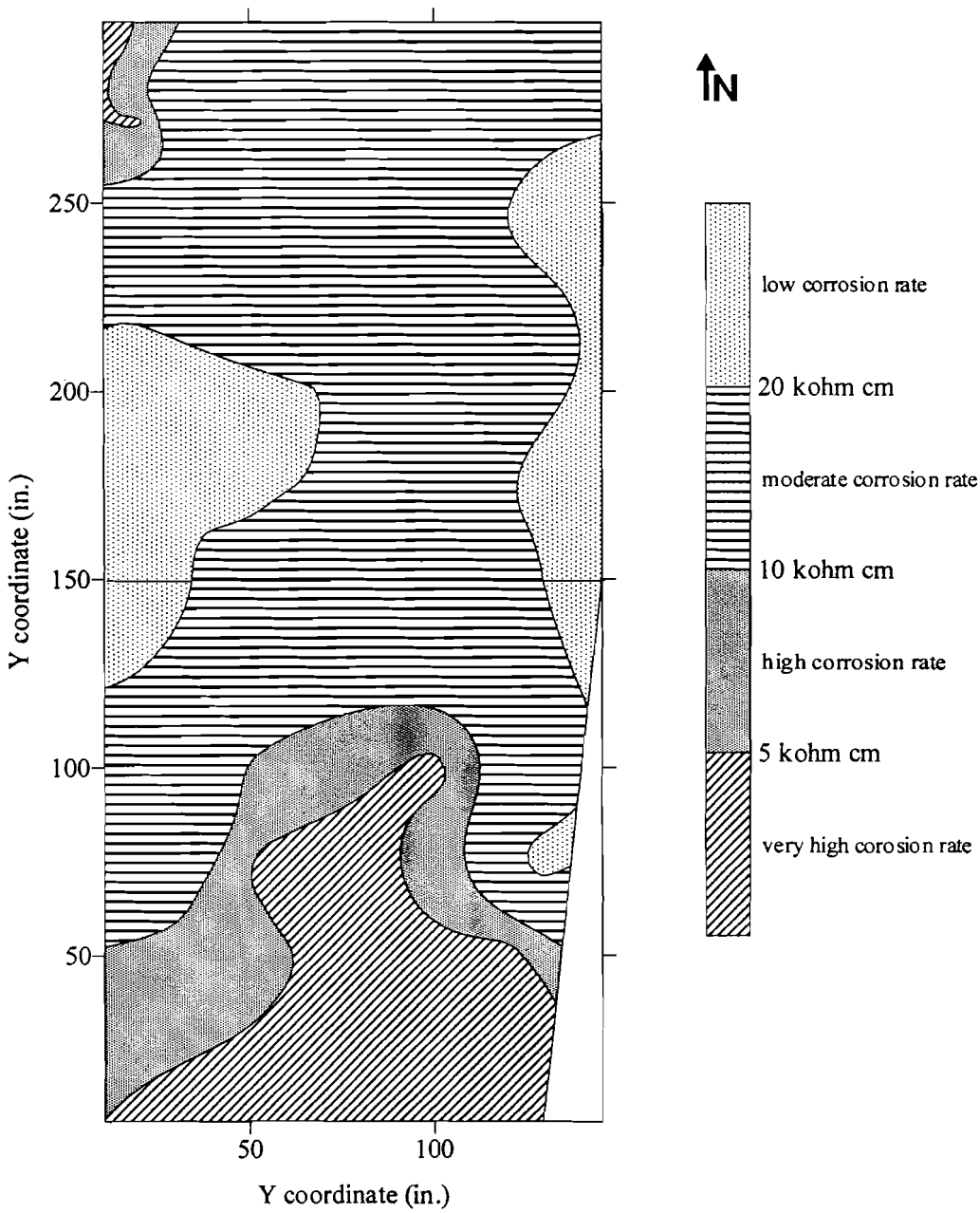

Figure 4.28. Contours of concrete resistivity for Site 4 on Pier 39 [Phase 2].

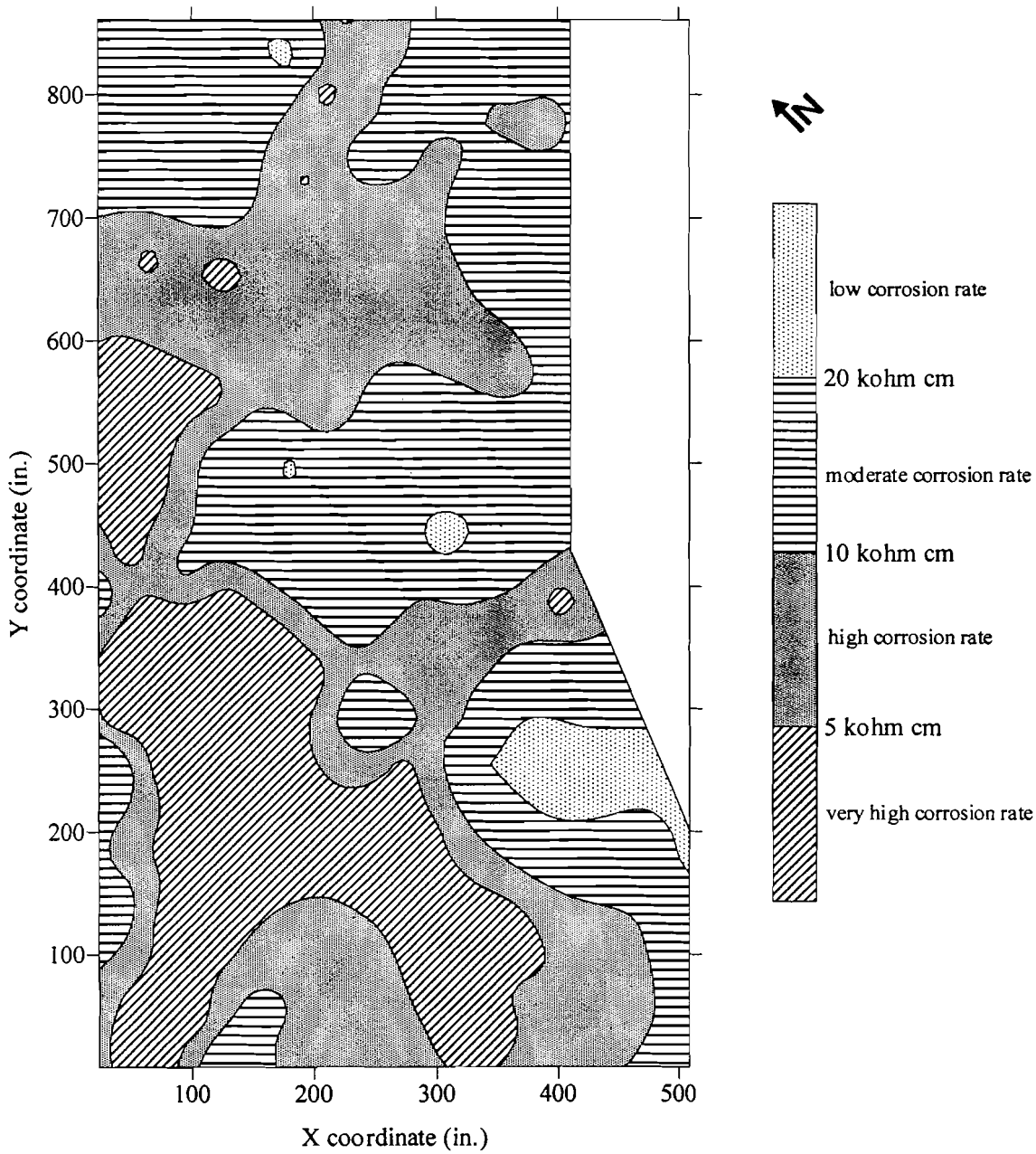

Figure 4.29. Contours of concrete resistivity for Site 5 on Pier 34.

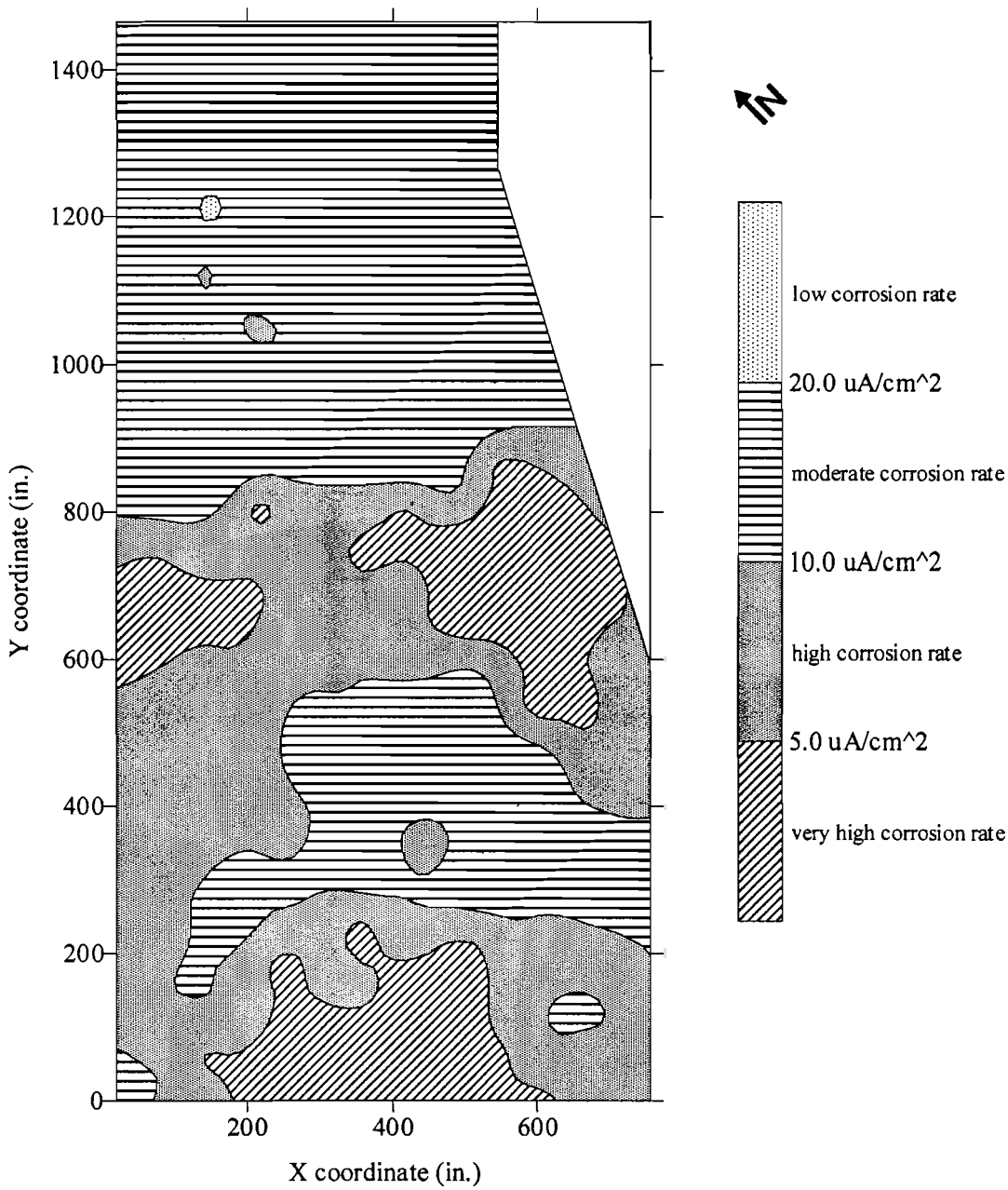

Figure 4.30. Contours of concrete resistivity for Site 6 on Pier 34

Based on the visual inspection of the bars from the cores, it appears that the half-cell potential and polarization resistance results are more accurate. Since the bars from Sites 5 and 6 showed less evidence of corrosion than the bars from Sites 1 through 4, the trend in concrete resistivity appears to be erroneous.

4.7.4 Site 7

Figure 4.31 presents the resistivity results for Site 7. On Site 7, approximately 15% of the area involved high corrosion rates, while the rest of the test site measured either moderate or low corrosion rates. This indicates that more corrosion activity was occurring on Site 7 than on Site 1. However, visual inspection showed that the bars from Site 7 were essentially free of corrosion. Therefore, the half-cell potential and polarization resistance measurements appear to be more accurate.

4.7.5 Site 8

According to the concrete resistivity results from Site 8, shown in Figure 4.32, high corrosion rates were measured on more than 50% of the site. However, results for the concrete resistivity are also unreliable for epoxy coated steel. Since no evidence of corrosion was found by visual inspection of the bars, the epoxy coating appears to have effectively protected the bars.

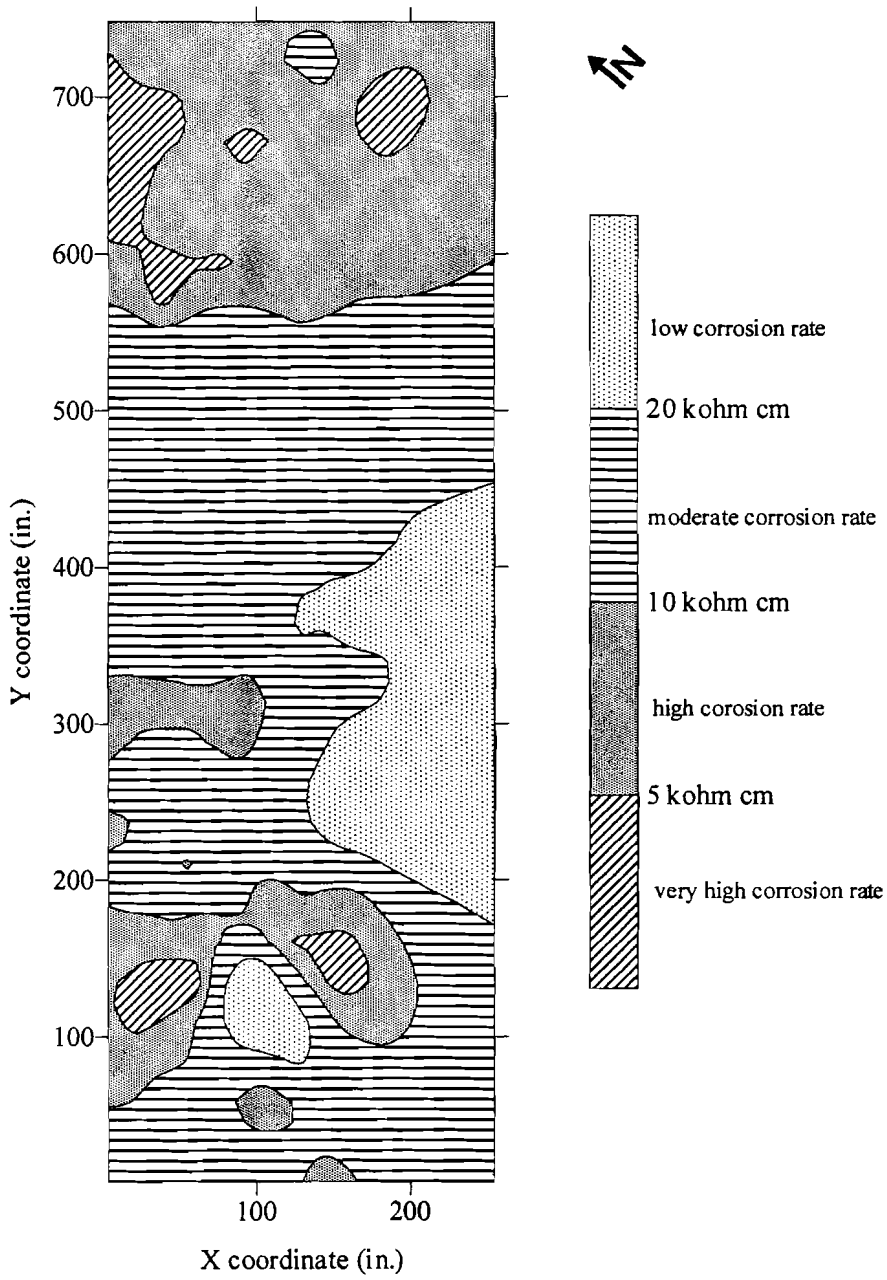

Figure 4.31. Contours of concrete resistivity for Site 7, the ferry terminal pier at Barbers Point Harbor.

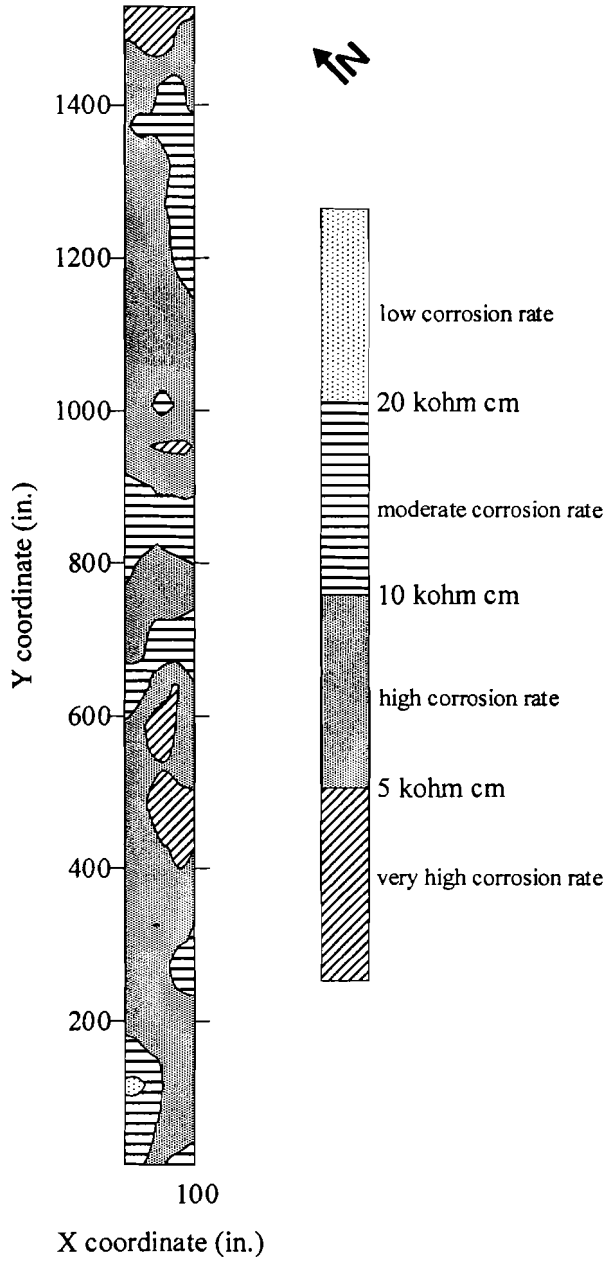

Figure 4.32. Contours of concrete resistivity for Site 8, Pier 6 at Barbers Point Harbor.

4.8 Compressive strength

Compression tests were performed on trimmed and cropped cores from each of the eight sites. Table 4.4 presents the average compressive strengths for each site, after adjustments were made for the specimen sizes according to ASTM C 39. All of the compressive strengths were greater than 5000 psi. This indicates that the condition of the concrete was good at all sites.

The cores used to measure compressive strengths contained reinforcing bars. The presence of these bars is expected to decrease the strength of the specimens because the difference in elastic modulus values for steel and concrete causes a stress concentration. Poisson's ratio of the steel is also higher than the value expected for concrete, 0.15 to 0.2 (Mindess and Young 1981). Consequently, the steel would have greater lateral expansion during the compression test. This would induce greater tension in the concrete, potentially reducing the apparent compressive strength. Since the compressive strengths were all good (> 5000 psi), the effects of the reinforcing bars have been neglected.

Table 4.4. Average compressive strengths for all sites.

Site	Average compressive strength (psi)
1	8940
2	7670
3	5440
4	7740
5	7530
6	8110
7	5360
8	8110

4.9 Summary

Results from all the tests performed to evaluate the eight sites were reported in this chapter. The results of the electrical tests were presented in the form of contour plots. Chloride profiles, permeability test results and pH values were also reported in this chapter. Visual inspection of bars taken from cores supported the results obtained from polarization resistance measurements. There was also generally good agreement with half-cell potential measurements. Results from both the half-cell potential measurements and the polarization resistance measurements indicate that higher dosages of calcium nitrite effectively reduce the rate and occurrence of corrosion. Epoxy coated bars were also effectively protected.

CHAPTER 5
SUMMARY AND CONCLUSIONS

5.1 Introduction

Reinforced concrete structures in marine environments are particularly prone to corrosion because they are constantly exposed to chloride ions in the seawater and salt-laden air. Consequently, a high level of corrosion protection is necessary to avoid premature deterioration of a structure. The use of corrosion inhibiting measures in concrete to protect reinforcing steel was investigated in this study. This chapter summarizes the findings from the non-destructive tests that were carried out to evaluate the effectiveness of calcium nitrite as an admixture in concrete and epoxy coated reinforcing steel as methods of combating the corrosion of reinforcing steel.

5.2 Summary

Eight sites were selected for field evaluation, in cooperation with the Harbors Division of the Hawaii Department of Transportation. Seven of the sites used a calcium nitrite based admixture in the concrete, while the last site used epoxy coated reinforcing steel. Each site was tested for permeability, chloride ion concentration, pH, half-cell potential to detect the likelihood of corrosion occurring, polarization resistance to determine the rate of corrosion, and concrete resistivity as another measure of corrosion rate. Results from the half-cell potential, polarization resistance, and concrete resistivity tests were presented on contour plots and then evaluated.

Contour plots for the half-cell potentials from Sites 1 and 2, showed that active areas of corrosion occurred along the edge of the approach slab. One would have expected to see the loading zone show higher potentials, due to its direct exposure to the seawater, and the high level of traffic it experiences.

Less corrosion activity was observed from the half-cell potential and polarization resistance measurements, for Sites 3 and 4. This was expected because both sites had less exposure to the marine environment and experienced less traffic than Sites 1 and 2. Site 4 experienced less traffic than Site 3, but there was a small area on Site 4 that recorded high half-cell potentials. This was most likely due to reinforcing bars that extended below the slab and were exposed to the ground.

Sites 5 and 6 had exposure conditions similar to Sites 1 and 2. Extensive shrinkage cracks were identified on both Sites 5 and 6. The shrinkage cracks would be expected to make the site more susceptible to corrosion. However, the half-cell potentials and polarization resistances identified little corrosion activity. The increased dosage of DCI from 2.5 gal/yd^3 for Sites 1 through 4, to 4.0 gal/yd^3 for Sites 5 and 6 appears to be the reason why the low corrosion activity was observed for these sites.

The 4.5 gal/yd^3 dosage of DCI used on Site 7 was the highest dosage used for any of the sites. Site 7 had the highest level of exposure to a marine environment, with seawater surrounding the site on three sides. A lower level of traffic, limited primarily to pedestrian traffic, was experienced on Site 7. The contour plots showed that high half-cell potentials and high corrosion rates were not recorded on Site 7. The reduced corrosion activity on Site 7 is also attributed to the high dosage of DCI.

Site 8 was the only site tested that had epoxy coated reinforcing bars. The half-cell potential readings, polarization resistance measurements, and concrete resistivity measurements, are all unreliable for epoxy coated bars. Therefore, the evaluation of Site 8 relied heavily on the visual inspection performed on bars taken from the cores. After peeling off the epoxy coating, the reinforcing steel taken from cores on Site 8, showed no trace of corrosion. Site 8 was constructed in 1988, which makes it the oldest site tested. Since the embedded steel was still in excellent condition, the epoxy coating has effectively protected the reinforcing steel.

Water and air permeability tests were also conducted on the test sites. Six different spots on each site were chosen for the permeability tests. The results showed that the concrete at all of the sites was fairly permeable. Site 1 appeared to have the least permeable concrete. Although the permeability tests identified Sites 5 and 6 as having the most permeable concrete, the half-cell potential tests and corrosion rate tests indicated less corrosion activity than on Sites 1 and 2. This is attributed to the high dosage of DCI (4.0 gal/yd^3).

Chloride profiles were obtained for each site by analyzing the chloride concentration in the concrete at various depths. At the depth of the steel, all of the chloride concentrations were below the maximum limit stated by the 1999 American Concrete Institute Building Code (ACI 318-99). The limit for reinforced structures exposed to chloride is 0.15 percent by weight of cement.

Visual inspection of bars taken from cores on Sites 1 to 7 supported the trends seen in the half-cell and polarization resistance measurements. These trends conflicted with concrete resistivity measurements for some sites. Consequently, the polarization

resistance and half-cell potential measurements appear more reliable than resistivity measurements.

After breaking the cores and inspecting the reinforcing bars for corrosion, the alkalinity of the concrete surrounding the steel was also evaluated. All of the samples tested had pH values between 12.48 and 12.55.

5.3 Conclusions

Based on the results of the half-cell potential, linear polarization resistance, resistivity, chloride concentration, permeability, and pH tests, the following conclusions are made:

1. Corrosion was identified in portions of pier structures as young as two years old along Hawaii's shoreline. It is possible that this corrosion was initiated prior to construction and was not stopped by the high pH of the concrete. Additionally, the corrosion appears to be progressing without high concentrations of chloride ions. This is probably due to the fact that most of the structures had high permeability concrete. This allows more oxygen and water to reach the reinforcing steel and keep the reaction progressing.
2. Increasing the dosage of the calcium nitrite based admixture decreased corrosion activity. Sites with higher dosages (4.0 or 4.5 gal/yd^3) showed no regions with high probabilities of corrosion and very little area with high rates of corrosion. This occurred even though the sites with high calcium nitrite dosages were older and usually more permeable than the sites with lower dosages.

3. Epoxy coated reinforcing bars were effective in combating corrosion in the areas tested. However, other states have had problems with epoxy coated bars. Their experiences should not be ignored based on the limited testing performed for this work.

4. Visual inspections of bars taken from cores validated the results from polarization resistance tests. The visual inspections also supported the half-cell potential measurements. However, the resistivity measurements often disagreed with the visual inspections. This leads to low confidence in the resistivity results.

APPENDIX A

Table A.1. Mix designs for all sites.

Material	Sites				
	1, 3, 4	4	5, 6	7	8
Slump	4"	4"	5"	3"	3 - 5"
#3 course	---	---	---	---	896
#3 fine	1618	1618	1651	1887	896
Dune sand	404	404	567	218	615
Concrete sand	905	905	---	970	---
#4 basalt	---	---	693	---	796
Cement	7.8 sk	7.8 sk	7.75 sk	7.5 sk	6.76 sk
Water	32.5 gal	32.5 gal	30.5 gal	31 gal	33 gal
WRDA-89	---	---	---	---	---
WRDA HA	---	---	22 oz	---	24 oz
DARATARD HC	23.4 oz	23.4 oz	---		---
DARATARD BD	---	---	30 oz	---	---
DAREX AEA	11.7 oz	11.7 oz	7.3 oz	---	2 oz
Air content	4.0%	4.0%	4.0%	1.5%	5.0%
DCI	2.5 gal	2.5 gal	4.0 gal	4.5 gal	---

* All quantities are lbs per cubic yard unless specifed otherwise.
All quantities are for SSD conditions.

APPENDIX B

Table B.1. Data for air permeability test performed on all sites.

Site	Time measured (sec)					
	1	2	3	4	5	6
1	665	1420	2524	1510	1090	1442
2	103	132	107	179	1166	65
3	714	569	116	144	130	255
4	568	695	431	75	755	199
5	107	110	95	88	84	67
6	106	9	96	4	66	841
7	207	33	21	250	317	260
8	201	436	130	15	207	81

Table B.2. Data for water permeability test performed on all sites.

SITE	Time measured (sec)					
	1	2	3	4	5	6
1	98	147	231	135	146	172
2	61	36	33	120	170	7
3	46	49	57	59	48	9
4	3	3	104	21	17	26
5	45	34	76	40	33	20
6	346	32	242	36	242	130
7	252	57	24	188	205	182
8	107	203	182	23	125	42

APPENDIX C

Table C.1. Data from the chloride concentration tests on Site 1.

	chloride concentrations (%)					
Depth (in.)	1	2	3	4	5	6
-0.50	0.3484	0.4342	0.1822	0.2341	0.4562	0.2745
-1.25	0.1018	0.0911	0.0804	0.0849	0.0928	0.0956
-2.00	0.0536	0.0590	0.0858	0.0864	0.0637	0.0482
-2.50	0.0590	0.0482	0.0697	0.0514	0.0685	0.0571

Table C.2. Data from the chloride concentration tests on Site 2.

	chloride concentrations (%)					
Depth (in.)	1	2	3	4	5	6
-1.25	0.0252	0.0166	0.0252	0.0184	0.0205	0.028
-2.50	0.0209	0.0150	0.0220	0.0185	0.0237	0.0157
-3.75	0.0150	0.0134	0.0182	0.0173	0.0155	0.0137
-5.00	0.0145	0.0107	0.0145	0.0126	0.0113	0.0157

Table C.3. Data from the chloride concentration tests on Site 3.

	chloride concentrations (%)					
Depth (in.)	1	2	3	4	5	6
-0.50	0.1983	0.0188	0.1340	0.1275	0.1131	0.1104
-1.25	0.0643	0.0858	0.0488	0.0583	0.0753	0.0653
-2.00	0.0397	0.0520	0.0332	0.0428	0.0474	0.0346
-2.50	0.0407	0.0413	0.0273	0.0342	0.0402	0.0348
-3.00	0.0359	0.0300	0.0241	0.0325	0.0283	0.0292

Table C.4. Data from the chloride concentration tests on Site 4.

	chloride concentrations (%)					
Depth (in.)	1	2	3	4	5	6
-0.75	0.1286	0.3591	0.1313	0.2517	0.1538	0.2137
-1.50	0.0536	0.2251	0.0332	0.1273	0.0875	0.0972
-2.25	0.0338	0.0750	0.0230	0.0593	0.0385	0.0342
-3.00	0.0289	0.0858	0.0214	0.0428	0.0531	0.0403
-4.00	0.0247	0.0477	0.0161	0.0352	0.0216	0.0317

Table C.5. Data from the chloride concentration tests on Site 5.

	chloride concentrations (%)					
Depth (in.)	1	2	3	4	5	6
-0.75	0.2563	0.1762	0.2189	0.2374	0.1953	0.2189
-1.50	0.0587	0.0518	0.0587	0.0602	0.0572	0.0518
-2.25	0.0374	0.0331	0.0374	0.0352	0.0342	0.0386
-3.00	0.0278	0.0304	0.0331	0.0317	0.0248	0.0357

Table C.6. Data from the chloride concentration tests on Site 6.

	chloride concentrations (%)					
Depth (in.)	1	2	3	4	5	6
-0.75	0.2029	0.4699	0.2884	0.3486	0.4081	0.2045
-1.50	0.0481	0.0908	0.0534	0.0684	0.0738	0.0501
-2.25	0.0320	0.0486	0.0454	0.0475	0.0382	0.0403
-3.00	0.0304	0.0358	0.0449	0.0413	0.0324	0.0373

Table C.7. Data from the chloride concentration tests on Site 7.

	chloride concentrations (%)					
Depth (in.)	1	2	3	4	5	6
-0.75	0.9317	1.1970	1.0612	1.1728	0.9843	1.0328
-1.50	0.1296	0.1172	0.1296	0.1312	0.1286	0.1167
-2.25	0.1111	0.0457	0.0512	0.0713	0.0878	0.0488
-3.00	0.0611	0.0420	0.0426	0.0563	0.0428	0.0464

Table C.8. Data from the chloride concentration tests on Site 8.

	chloride concentrations (%)					
Depth (in.)	1	2	3	4	5	6
-0.75	0.5940	0.4158	0.7668	0.6573	0.4846	0.6347
-1.50	0.0491	0.0810	0.1296	0.1087	0.0907	0.0604
-2.25	0.0221	0.0275	0.0475	0.0365	0.0421	0.0186
-3.00	0.0200	0.0254	0.0265	0.0279	0.0244	0.0194
-4.00	0.0184	0.0243	0.0243	0.0197	0.0238	0.0234

APPENDIX D

Table D.1. Data recorded at Site 1.

ID #	X-coord.	Y-coord.	Corrosion Rate ($\mu A/cm^2$)	Corrosion Potential (mV)	Electrical resistance (kΩ)	Resistivity (kΩ. cm)	Area (cm^2)
1	930	234	0.011	-33.7	1.69	12.52	52.4
2	923	214	0.021	-66.4	1.00	---	52.4
3	927	172	0.100	-204.3	0.35	---	52.4
4	923	154	0.001	-210.5	32.75	---	52.4
5	923	116	0.018	-251.0	1.20	26.8	52.4
6	927	86	0.023	-265.8	1.13	---	52.4
7	923	58	0.015	-260.5	0.83	---	52.4
8	923	34	0.006	-209.6	1.11	5.89	52.4
9	927	12	0.161	-263.3	0.73	---	52.4
10	878	52	0.191	-274.5	1.2	---	52.4
11	901	148	0.023	-228.5	0.75	15.33	52.4
12	901	209	0.032	-94.8	0.84	---	52.4
13	872	190	0.105	-207.7	0.39	---	52.4
14	872	130	0.016	-269.1	1.17	44.74	52.4
15	866	86	0.267	-291.9	0.66	---	52.4
16	872	20	1.730	-272.5	1.10	---	52.4
17(1)	848	12	0.039	-304.7	0.70	15.38	52.4
17(2)	817	34	0.029	-313.3	0.79	---	52.4
18	811	111	0.030	-315.6	0.78	---	52.4
19	811	172	0.809	-246.9	0.57	31.23	52.4
20	817	190	0.067	-194.6	0.53	---	52.4
21	847	209	0.024	-111.3	0.91	---	52.4
22	830	234	0.030	-29.0	1.26	52.37	52.4
23	769	178	0.083	-220.5	0.82	---	52.4

Table D.1. Continued.

ID #	X-coord.	Y-coord.	Corrosion Rate ($\mu A/cm^2$)	Corrosion Potential (mV)	Electrical resistance (kΩ)	Resistivity (kΩ. cm)	Area (cm^2)
24	757	148	0.285	-341.3	0.48	---	52.4
25	769	70	0.098	-319.0	0.68	33.60	52.4
26	722	52	0.027	-332.4	1.78	55.96	52.4
27	710	60	0.032	-307.5	0.77	---	52.4
28	704	111	0.088	-295.7	1.99	---	52.4
29	710	154	0.287	-238.6	1.86	93.28	52.4
30	739	209	0.052	-132.8	1.91	---	52.4
33	649	86	0.024	-342.3	1.08	---	52.4
34	631	148	0.017	-243.5	1.75	---	52.4
34	710	154	0.018	-108.6	1.62	20.25	52.4
35	631	209	0.023	-99.0	2.24	68.51	52.4
37	576	12	0.845	-406.2	1.90	---	52.4
38	552	34	0.042	-347.6	4.16	---	52.4
39	523	52	0.116	-369.6	2.29	---	52.4
40	541	86	0.425	-336.5	2.62	---	52.4
41	541	111	0.020	-298.2	2.06	---	52.4
43	600	58	0.050	-326.2	1.38	---	52.4
44	757	86	0.030	-325.7	0.74	---	52.4
45	775	12	0.036	-323.2	0.77	---	52.4
46	523	148	0.256	-237.2	1.61	31.00	52.4
47	523	209	0.081	-29.1	2.06	---	52.4
48	576	234	0.230	-81.4	1.25	---	52.4
49(1)	576	172	0.310	-243.6	1.22	30.81	52.4
49(2)	757	209	0.083	-136.4	1.97	---	52.4

Table D.1. Continued.

ID #	X-coord.	Y-coord.	Corrosion Rate ($\mu A/cm^2$)	Corrosion Potential (mV)	Electrical resistance (kΩ)	Resistivity (kΩ. cm)	Area (cm^2)
50	541	86	0.027	-84.2	1.82	---	52.4
51	661	46	0.057	-369.1	1.19	18.40	52.4
60	487	12	0.035	-402.5	1.63	55.85	52.4
61	492.5	70	0.167	-341.1	1.46		52.4
62	487	172	0.305	-289.0	0.51	56.84	52.4
63	469	234	0.350	-79.1	0.54	---	52.4
64	469	52	0.017	-360.1	1.17	---	52.4
65	469	111	0.021	-312.8	1.53	---	52.4
65	661	172	0.130	-317.2	0.65	---	52.4
66	445.5	154	0.161	-262.2	0.45	5.02	52.4
68	415	52	0.013	-362.3	0.75	26.21	52.4
69	415	209	0.067	-130.3	0.55	---	52.4
70	397	12	0.188	-416.5	0.54	---	52.4
72	385	81	0.093	-368.0	0.71	---	52.4
73	385	118	0.157	-346.1	0.75	38.52	52.4
74	361	215	0.252	-214.7	0.33	4.27	52.4
76	361	148	1.779	-292.0	0.51	---	52.4
77	337	93	1.806	-310.2	0.93	42.94	52.4
78	337	178	0.569	-224.7	0.97	28.97	52.4
79	343	234	0.028	-35.1	0.99	---	52.4
80	323	52	1.220	-364.9	0.62	---	52.4
81	302	12	0.754	-435.1	0.35	---	52.4
82	289	86	2.148	-401.2	0.33	---	52.4
83	289	148	0.067	-283.1	0.55	50.73	52.4

Table D.1. Continued.

ID #	X-coord.	Y-coord.	Corrosion Rate ($\mu A/cm^2$)	Corrosion Potential (mV)	Electrical resistance ($k\Omega$)	Resistivity ($k\Omega$. cm)	Area (cm^2)
84	289	209	0.129	-141.7	0.49	---	52.4
85	277	46	0.568	-464.1	0.34	---	52.4
86	235	172	0.566	-252.5	0.60	---	52.4
87	229	58	1.201	-348.7	0.69	---	52.4
88	229	118	0.212	-296.5	0.92	---	52.4
89	217	12	0.091	-307.7	0.90	42.08	52.4
90	217	234	0.043	-26.1	1.06	27.36	52.4
91	180	148	0.290	-285.7	0.86	---	52.4
94	143	111	0.028	-312.1	0.9		52.4
95	127	12	0.569	-279.3	0.77	10.39	52.4
96	121	70	0.067	-283.1	1.14	---	52.4
97	121	154	0.057	-260.7	0.78	38.28	52.4
98	121	203	0.034	-134.8	0.93	---	52.4
99	91	111	0.093	-262.5	1.09	21.31	52.4
101	72	52	0.271	-268.7	1.18	---	52.4
102	60	93	0.217	-245.2	1.50	14.95	52.4
103	60	191	0.129	-160.8	1.00	14.88	52.4
104	55	148	0.703	-265.6	0.77	32.86	52.4
105	37	234	0.032	-93.5	2.01	---	52.4
106	19	12	0.068	-307.0	2.12	13.48	52.4
107	13	58	0.036	-268.4	1.29	---	52.4
108	19	111	0.467	-285.8	0.68	---	52.4
109	19	172	0.410	-198.6	1.21	---	52.4
110	13	228	0.046	-121.6	1.28	78.24	52.4

Table D.1. Continued.

ID #	X-coord.	Y-coord.	Corrosion Rate ($\mu A/cm^2$)	Corrosion Potential (mV)	Electrical resistance (kΩ)	Resistivity (kΩ. cm)	Area (cm^2)
111	182	86	0.045	-306.5	0.98	16.44	52.4
1	70	239	0.003	-184.2	0.94	79.21	83.8
2	250	358	0.007	-220.4	1.70	---	83.8
3	320	239	0.004	-353.0	1.80	---	83.8
4	84	298	0.014	-266.9	1.65	---	52.4
5	201	239	0.011	-342.1	1.58	41.61	83.8
6	215	298	0.006	-317.8	1.77	---	52.4
7	405	274	0.006	-333.6	0.39	43.89	52.4
8	284	298	0.004	-331.4	1.44	58.03	52.4
9	344	358	0.007	-113.5	0.25	5.73	52.4
10	431	364	0.002	-179.6	1.32	---	83.8
11	171	364	0.030	-282.0	1.72	---	83.8
12	55.5	358	0.005	-253.5	1.61	8.21	52.4
13	120	385	0.002	-379.5	0.79	---	83.8
14	289	385	2.732	-114.8	1.03	9.16	83.8
15	344	287	0.004	-270.2	1.23	---	52.4
17	309	450	0.109	-85.8	1.03	---	83.8
18	220	385	0.095	-92.7	1.02	8.48	83.8
20	191	450	0.051	-107.4	0.6	---	83.8
21	181	450	0.001	-234.8	1.18	7.65	83.8
22	130	484	0.004	-197.5	1.28	6.30	83.8
23	289	498	0.128	-61.0	1.26	---	83.8
24	220	520	0.038	-105.9	0.63	---	83.8
25	410	520	0.029	-79.6	1.32	6.02	83.8

Table D.1. Continued.

ID #	X-coord.	Y-coord.	Corrosion Rate ($\mu A/cm^2$)	Corrosion Potential (mV)	Electrical resistance ($k\Omega$)	Resistivity ($k\Omega$. cm)	Area (cm^2)
26	350	554	0.102	-92.9	0.90	---	83.8
27	165	529	0.394	-115.9	0.67	81.53	52.4
28	80	554	0.006	-297.3	1.03	---	83.8
30	499	554	0.007	-225.6	1.37	---	83.8
31	701	554	0.002	-195.4	1.70	30.53	83.8
32	590	520	0.011	-228.5	1.33	62.25	83.8
33	498	484	0.020	-279.5	1.29	25.70	83.8
34	473	418	0.003	-242.2	1.21	---	52.4
35	539	364	0.003	-230.1	1.63	58.08	83.8
36	479	246	0.006	-354.8	2.04	---	83.8
37	564	239	0.005	-374.8	2.44	---	83.8
38	670	261	0.003	-332.4	2.53	---	83.8
39	762	239	0.232	-225.7	1.40	7.19	83.8
40	857	261	0.067	-195.2	1.26	---	83.8
41	484	310	0.013	-289.3	1.81	---	52.4
42	574	310	0.011	-255.5	1.85	---	52.4
43	584	418	0.003	-202.0	1.48	---	52.4
44	691	484	0.139	-68.1	1.27	25.63	83.8
45	782	484	0.068	-52.9	1.42	20.52	83.8
46	584	310	0.056	-94.7	1.52	---	83.8
47	670	239	0.060	-75.6	1.62	15.04	83.8
48	643	335	0.003	-401.5	1.86	5.49	52.4
49	736	309	0.003	-284.3	1.29	7.38	52.4
50	664	407	0.004	-204.5	1.25	---	52.4

Table D.1. Continued.

ID #	X-coord.	Y-coord.	Corrosion Rate ($\mu A/cm^2$)	Corrosion Potential (mV)	Electrical resistance ($k\Omega$)	Resistivity ($k\Omega$. cm)	Area (cm^2)
51	762	413	0.077	-73.7	1.01	---	83.8
52	787	346	0.001	-213.4	1.37	---	52.4
53	817	309	0.159	-133.5	1.18	5.31	52.4
54	826	407	0.064	-93.2	1.67	---	52.4
55	884	335	0.056	-143.9	1.34	11.64	52.4

Table D.2. Data recorded on Site 2.

ID #	X-coord.	Y-coord.	Corrosion Rate ($\mu A/cm^2$)	Corrosion Potential (mV)	Electrical resistance (kΩ)	Resistivity (kΩ. cm)	Area (cm^2)
1	22	42	0.050	-425.2	1.73	---	52.4
2	31	102	0.035	-442.6	1.39	---	52.4
3	22	161	0.077	-330.9	1.47	---	52.4
4	64	190	0.055	-283.7	1.18	86.92	52.4
5	84	113	0.241	-422.2	1.15	---	52.4
6	68	54	0.052	-438.0	1.02	---	52.4
7	58	5	0.177	-433.4	0.97	---	52.4
8	121	17	0.044	-443.1	1.94	---	52.4
9	126	59	0.179	-504.7	0.85	---	52.4
10	144	132	0.062	-352.6	1.41	77.46	52.4
11	108	155	0.160	-348.5	0.81	---	52.4
12	105	232	0.051	-225.7	1.31	93.43	52.4
13	135	190	0.058	-307.8	1.01	63.38	52.4
14	188	222	0.048	-206.7	1.28	36.80	52.4
15	188	155	0.106	-336.2	1.58	8.52	52.4
17	178	37	0.034	-466.3	1.32	---	52.4
18	241	5	0.183	-517.9	1.28	---	52.4
19	233	80	0.052	-469.9	1.35	---	52.4
20	241	139	0.036	-414.4	0.77	---	52.4
21	241	185	0.055	-352.9	0.83	---	52.4
22	283	232	0.120	-274.6	0.63	---	52.4
23	316	155	0.045	-377.8	1.11	11.77	52.4
24	288	94	0.027	-375.9	1.06	---	52.4
25	296	34	0.041	-394.8	0.84	10.45	52.4

Table D.2. Continued.

ID #	X-coord.	Y-coord.	Corrosion Rate ($\mu A/cm^2$)	Corrosion Potential (mV)	Electrical resistance (kΩ)	Resistivity (kΩ. cm)	Area (cm^2)
26	363	12	0.019	-349.5	1.31	27.00	52.4
27	357	87	0.071	-358.3	1.02	---	52.4
28	363	226	0.091	-138.7	0.99	14.03	52.4
29	380	162	0.041	-267.7	0.61	12.46	52.4
30	428	115	0.051	-361.6	0.80	19.26	52.4
31	423	202	0.066	-186.2	0.88	17.49	52.4
32	423	48	0.067	-443.9	0.74	---	52.4
34	480	80	0.038	-420.7	0.69	---	52.4
35	460	156	0.070	-407.0	1.14	27.28	52.4
36	496	234	0.061	-274.9	0.96	---	52.4
37	522	174	0.045	-300.3	1.02	10.98	52.4
38	535	115	0.033	-405.4	1.02	---	52.4
39	540	41	0.207	-456.9	0.88	---	52.4
41	590	87	0.040	-441.9	0.69	---	52.4
42	577	156	0.034	-366.3	1.68	30.25	52.4
43	568	211	0.090	-260.1	0.78	---	52.4
44	642	234	0.026	-225.7	1.21	14.64	52.4
45	651	156	0.025	-358.0	1.13	---	52.4
46	628	41	0.023	-536.7	0.85	---	52.4
47	700	5	0.057	-470.3	1.11	---	52.4
48	651	80	0.175	-531.7	0.96	---	52.4
49	720	61	0.097	-542.5	1.52	---	52.4
50	713	135	0.028	-406.1	1.16	---	52.4
51	700	185	0.087	-327.8	0.93	---	52.4

Table D.2. Continued.

ID #	X-coord.	Y-coord.	Corrosion Rate ($\mu A/cm^2$)	Corrosion Potential (mV)	Electrical resistance (kΩ)	Resistivity (kΩ. cm)	Area (cm^2)
61	80	339	0.439	-136.9	0.88	32.41	52.4
62	107	375	0.382	-136.8	0.70	19.36	83.8
63	80	474	0.276	-129.7	0.65	---	52.4
64	121	500	0.449	-105.3	0.32	3.93	52.4
65	80	542	0.347	-90.6	0.33	2.86	52.4
67	186	528	0.105	-117.7	0.73	15.60	83.8
68	142	431	0.118	-107.6	0.76	17.25	52.4
69	169	362	0.092	-146.0	0.69	11.03	52.4
70	151	299	0.263	-201.6	0.58	15.04	52.4
71	80	274	1.007	-182.4	0.73	---	52.4
72	157	240	0.090	-203.9	0.86	---	83.8
73	217	262	0.068	-208.2	0.97	17.76	83.8
73	169	375	0.292	-135.8	1.14	15.82	52.4
75	217	416	0.126	-87.2	1.05	25.33	83.8
76	186	479	0.082	-129.9	0.64	12.37	83.8
77	260	572	2.057	-144.6	0.66	18.80	83.8
78	265	500	0.227	-102.4	0.81	---	52.4
79	295	407	0.487	-175.3	0.67	5.72	52.4
80	295	339	0.294	-131.8	0.63	6.56	52.4
81	295	274	3.193	-189.4	0.56	---	52.4
82	327	240	0.443	-269.8	0.66	6.25	83.8
83	332	524	0.624	-145.0	0.83	6.05	52.4
84	265	473	0.118	-106.9	0.60	5.65	52.4
85	412	520	0.141	-142.8	0.65	16.05	52.4

Table D.2. Continued.

ID #	X-coord.	Y-coord.	Corrosion Rate ($\mu A/cm^2$)	Corrosion Potential (mV)	Electrical resistance (kΩ)	Resistivity (kΩ. cm)	Area (cm^2)
86	417	572	0.059	-122.9	0.94	23.73	83.8
87	480	536	0.082	-124.9	1.08	---	52.4
88	469	473	2.635	-201.9	0.42	4.42	52.4
89	378	362	0.150	-153.4	0.65	5.82	52.4
90	463	375	0.278	-173.2	0.71	5.40	83.8
91	358	307	0.465	-216.8	0.54	---	52.4
92	417	239	0.161	-237.4	1.00	9.22	83.8
93	431	321	0.097	-169.3	1.04	12.25	52.4
94	515	285	0.145	-202.3	0.64	---	83.8
95	576	239	0.300	-268.5	0.64	7.68	83.8
96	522	339	0.190	-207.2	0.71	7.11	52.4
97	532	457	0.877	-159.5	0.58	4.78	52.4
98	552	520	0.095	-139.3	0.62	5.28	52.4
99	627	572	0.193	-160.1	0.58	3.07	83.8
100	622	520	0.568	-152.9	0.65	5.80	52.4
101	647	528	0.108	-144.6	0.79	5.67	83.8
102	641	457	0.295	-150.8	0.93	8.54	52.4
103	580	362	0.122	-156.2	0.84	6.37	52.4
104	632	307	0.104	-202.0	0.60	6.53	52.4
105	674	251	0.521	-253.7	0.55	6.44	52.4
106	674	362	0.266	-222.7	0.61	5.32	52.4
107	571	307	0.973	-186.8	0.84	---	52.4

Table D.3. Data recorded on Site 3.

ID #	X-coord.	Y-coord.	Corrosion Rate ($\mu A/cm^2$)	Corrosion Potential (mV)	Electrical resistance (kΩ)	Resistivity (kΩ. cm)	Area (cm^2)
1	18	144	0.989	-274.6	1.06	14.41	41.9
2	9	119	0.034	-225.8	1.72	---	41.9
3	18	92	0.575	-241.9	0.70	36.57	41.9
4	9	64	0.259	-254.0	0.76	18.97	41.9
5	18	37	0.104	-237.4	1.10	---	41.9
6	9	12	0.179	-269.7	0.76	56.23	41.9
7	37	5	0.125	-230.4	0.59	60.95	41.9
8	47	28	0.031	-186.1	1.20	48.59	41.9
9	37	55	0.042	-230.6	0.75	---	41.9
10	47	83	0.041	-214.1	0.94	46.20	41.9
11	37	110	1.173	-266.6	0.83	52.83	41.9
12	47	136	0.212	-232.4	1.38	14.45	41.9
13	64	119	0.410	-240.9	0.78	35.11	41.9
14	73	92	1.433	-228.1	0.76	9.65	41.9
15	64	64	0.116	-227.0	0.92	57.26	41.9
16	73	37	0.133	-221.2	0.97	---	41.9
17	64	12	0.080	-231.8	0.71	---	41.9
18	101	46	0.769	-218.1	0.83	33.86	41.9
19	101	64	0.034	-207.4	0.95	---	41.9
20	119	83	0.283	-200.1	0.69	100.28	41.9
21	101	101	0.175	-188.1	0.74	---	41.9
22	82	119	0.130	-199.9	0.84	12.55	41.9
23	82	136	0.089	-233.4	0.66	70.26	41.9
24	126	110	1.409	-190.7	1.02	99.12	41.9

Table D.3. Continued.

ID #	X-coord.	Y-coord.	Corrosion Rate ($\mu A/cm^2$)	Corrosion Potential (mV)	Electrical resistance (kΩ)	Resistivity (kΩ. cm)	Area (cm^2)
25	110	128	0.032	-167.1	1.16	---	41.9
26	133	136	0.083	-213.0	1.18	48.48	41.9
30	3	174	0.089	-315.9	0.70	---	41.9
31	10	202	0.115	-284.5	0.69	14.01	41.9
32	3	229	0.304	-301.5	0.62	16.80	41.9
33	10	256	0.094	-301.0	0.68	42.53	41.9
34	3	283	0.336	-292.0	0.63	---	41.9
35	42	291	0.034	-293.6	1.04	20.53	41.9
36	33	265	0.060	-300.3	0.72	17.91	41.9
37	42	237	2.181	-274.9	0.68	---	41.9
38	33	211	0.574	-263.2	0.75	---	41.9
39	42	184	0.271	-241.3	1.21	47.69	41.9
40	33	157	0.043	-268.8	1.22	---	41.9
41	80	164	0.028	-216.5	0.87	7.76	41.9
42	72	193	0.042	-259.5	1.34	---	41.9
43	80	220	0.015	-236.9	1.35	8.66	41.9
44	72	247	0.049	-259.3	1.14	---	41.9
45	80	274	0.165	-270.1	1.34	9.60	41.9
47	125	265	0.063	-184.0	0.73	---	41.9
48	118	237	0.025	-180.2	1.09	---	41.9
49	125	211	0.255	-188.7	1.09	11.19	41.9
50	118	184	0.039	-200.0	1.25	---	41.9
51	125	157	0.043	-236.6	0.84	7.53	41.9
52	147	184	0.126	-212.9	0.93	6.33	41.9

Table D.3. Continued.

ID #	X-coord.	Y-coord.	Corrosion Rate ($\mu A/cm^2$)	Corrosion Potential (mV)	Electrical resistance ($k\Omega$)	Resistivity ($k\Omega$. cm)	Area (cm^2)
53	170	220	0.020	176.4	1.56	22.61	41.9
54	143.5	229	0.021	-167.0	1.21	---	41.9
55	147	256	0.027	-165.7	1.38	5.57	41.9
56	143.5	283	0.039	-182.8	1.12	16.58	41.9
57	170	291	0.087	-184.9	1.03	---	41.9
58	179	265	0.103	-191.9	1.00	5.64	41.9
60	125	220	0.018	-186.8	1.89	8.79	41.9

Table D.4. Data recorded on Site 4.

ID #	X-coord.	Y-coord.	Corrosion Rate ($\mu A/cm^2$)	Corrosion Potential (mV)	Electrical resistance (kΩ)	Resistivity (kΩ. cm)	Area (cm^2)
1	145	131	0.018	-312.6	2.08	21.81	41.9
2	119	139	0.070	-303.7	1.62	---	41.9
3	91	145	0.254	-308.7	1.23	19.70	41.9
4	53	131	0.052	-271.9	1.27	16.22	41.9
5	33	139	0.028	-286.9	1.31	---	41.9
6	11	131	0.020	-307.4	1.95	24.83	41.9
7	19	100	0.184	-300.3	1.23	9.58	41.9
8	38	107	0.113	-247.2	1.16	10.96	41.9
10	101	100	0.014	-278.4	1.56	3.57	41.9
11	127	107	0.069	-336.4	1.25	---	41.9
12	127	74	0.038	-337.8	1.32	21.87	41.9
13	101	61	0.013	-274.5	1.51	---	41.9
14	61	86	0.022	-298.8	1.37	---	41.9
15	53	74	0.119	-327.6	1.11	3.59	41.9
16	33	86	0.072	-328.1	1.21	16.70	41.9
17	11	74	0.130	-340.2	1.00	---	41.9
18	19	49	0.035	-295.2	1.23	---	41.9
19	38	55	0.086	-330.6	1.15	8.82	41.9
20	61	49	0.039	-336.3	1.27	5.18	41.9
22	119	49	0.121	-377.2	0.87	2.41	41.9
23	127	34	0.076	-336.0	1.27	3.19	41.9
24	101	28	0.044	-328.9	1.11	2.88	41.9
25	76	22	0.014	-356.9	1.47	3.28	41.9
26	46	28	0.020	-300.2	1.63	---	41.9

Table D.4. Continued.

ID #	X-coord.	Y-coord.	Corrosion Rate ($\mu A/cm^2$)	Corrosion Potential (mV)	Electrical resistance (kΩ)	Resistivity (kΩ. cm)	Area (cm^2)
27	27	34	0.024	-295.6	1.23	---	41.9
28	11	22	0.054	-299.4	1.19	---	41.9
29	33	6	0.007	-362.2	1.30	3.14	41.9
30	84	6	0.044	-345.6	1.41	---	41.9
31	16	167	0.221	-298.8	0.83	---	41.9
32	39	159	0.022	-255.9	1.57	19.33	41.9
33	60	167	0.065	-273.1	1.2	19.33	41.9
34	78	159	0.047	-292.6	1.47	19.27	41.9
35	96	167	0.032	-292.7	1.16	---	41.9
36	120	159	0.030	-304.0	1.11	18.78	41.9
37	39	190	0.028	-269.3	1.50	24.29	41.9
38	16	213	0.062	-289.8	1.11	21.05	41.9
39	50	227	0.025	-310.6	0.89	14.37	41.9
40	68	199	0.049	-277.0	0.83	20.24	41.9
41	87	227	0.039	-309.6	1.14	18.34	41.9
42	96	199	0.053	-288.3	1.08	14.65	41.9
44	134	175	0.023	-314.4	1.14	22.40	41.9
45	138	213	0.043	-324.2	1.13	---	41.9
46	134	247	0.075	-281.6	1.32	22.96	41.9
47	144	271	0.071	-299.8	1.16	19.57	41.9
48	110	264	0.059	-331.8	0.92	17.20	41.9
49	92	257	0.073	-294.4	1.18	19.83	41.9
50	64	247	0.148	-299.2	0.94	16.55	41.9
51	120	219	0.045	-266.4	1.01	16.49	41.9

Table D.4. Continued.

ID #	X-coord.	Y-coord.	Corrosion Rate ($\mu A/cm^2$)	Corrosion Potential (mV)	Electrical resistance ($k\Omega$)	Resistivity ($k\Omega$. cm)	Area (cm^2)
52	16	241	0.044	-289.8	1.04	15.80	41.9
53	16	296	0.099	-281.6	1.26	3.43	41.9
54	22	271	0.043	-320.0	0.95	4.24	41.9
55	28	276	0.045	-344.5	0.99	15.98	41.9
56	64	296	0.107	-341.3	1.07	17.12	41.9
57	87	284	0.010	-344.9	1.01	---	41.9
58	110	284	0.049	-328.9	0.97	16.68	41.9
59	130	298	0.002	-215.6	3.73	17.29	41.9

Table D.5. Data recorded on Site 5.

ID #	X-coord.	Y-coord.	Corrosion Rate ($\mu A/cm^2$)	Corrosion Potential (mV)	Electrical resistance (kΩ)	Resistivity (kΩ. cm)	Area (cm^2)
1	76.5	8	1.161	-209.3	0.20	2.45	83.8
2	104.5	47	0.798	-146.2	0.23	2.91	41.9
3	133	8	0.369	-182.3	0.97	19.45	83.8
4	155.5	54.75	0.070	-151.9	0.64	12.64	83.8
5	183	16	0.425	-107.4	0.39	5.40	41.9
6	222.5	54.75	0.048	-131.8	0.65	8.54	83.8
7	42	70.25	0.221	-197.6	0.54	5.22	83.8
8	271.5	21.75	0.024	-121.3	0.60	6.33	83.8
9	297.5	70.25	0.112	-153.2	0.45	3.84	83.8
10	331	21.75	0.195	-117.7	0.49	3.71	83.8
11	356	127	1.103	-124.8	0.37	2.44	83.8
12	303	140.75	0.142	-118.9	0.48	2.86	83.8
13	247	111.75	0.171	-112.0	0.73	5.65	83.8
14	187	127	0.033	-128.2	0.70	5.65	83.8
15	129	105.5	0.260	-152.3	0.48	4.07	41.9
16	76.5	127	0.278	-144.4	0.40	2.89	83.8
17	42	184.5	0.245	-123.8	0.55	5.96	83.8
18	149	170	0.392	-161.9	0.55	3.97	83.8
19	101	200	0.011	-145.7	0.44	3.43	83.8
20	226.25	193	0.059	-146.4	0.74	4.63	41.9
21	289.5	200	0.228	-115.7	0.46	2.80	83.8
21	149	127	0.908	-125.1	0.53	0.00	83.8
23	368.5	70.25	0.150	-136.6	0.65	5.50	83.8
24	411	8	0.265	-183.6	0.57	7.57	83.8

Table D.5. Continued.

ID #	X-coord.	Y-coord.	Corrosion Rate ($\mu A/cm^2$)	Corrosion Potential (mV)	Electrical resistance (kΩ)	Resistivity (kΩ. cm)	Area (cm^2)
25	457.5	42.5	0.459	-185.9	0.42	5.62	83.8
26	411	82.75	0.234	-150.3	0.55	5.45	83.8
27	486.25	16	0.193	-233.9	0.86	14.56	41.9
28	509	70.25	0.007	-180.6	1.04	14.29	83.8
29	457.5	127	0.217	-190.7	0.60	8.80	83.8
31	411	184.5	0.364	-187.5	0.81	16.68	83.8
32	466.25	207	1.180	-214.5	1.02	18.56	41.9
33	457.5	252.25	0.187	-235.6	0.84	23.28	83.8
34	430	309.25	0.043	-225.4	0.94	15.91	83.8
35	393	228.75	0.163	-198.2	0.86	22.65	83.8
36	372	283	0.209	-209.3	0.89	21.62	41.9
37	339	252.25	0.085	-187.5	0.76	19.68	83.8
38	393	338.5	0.077	-188.0	0.82	13.97	83.8
39	401.5	387	0.096	-184.9	1.04	3.04	41.9
40	344	382	0.183	-187.5	0.82	8.78	83.8
41	339	338.5	0.074	-181.1	0.83	8.65	83.8
42	315	291.75	0.070	-188.1	0.89	8.72	83.8
43	271.5	252.25	0.064	-171.3	0.83	3.26	83.8
44	271.5	338.5	0.064	-168.3	0.85	4.49	83.8
45	289.5	382	0.089	-154.2	0.72	8.00	83.8
46	172.5	216.5	0.042	-134.6	0.89	2.73	83.8
47	222.5	264.25	0.440	-153.8	1.18	7.77	83.8
49	76.5	252.25	0.051	-134.2	1.04	2.52	83.8
49	217	216.5	0.069	-146.4	0.93	2.37	83.8

Table D.5. Continued.

ID #	X-coord.	Y-coord.	Corrosion Rate ($\mu A/cm^2$)	Corrosion Potential (mV)	Electrical resistance ($k\Omega$)	Resistivity ($k\Omega$. cm)	Area (cm^2)
50	35	291.75	0.047	-178.3	0.85	2.14	83.8
51	82.5	309.25	0.061	-182.8	0.88	2.38	83.8
52	172.5	277	0.029	-156.0	1.02	2.13	83.8
53	247	291.75	0.047	-173.4	1.10	19.90	83.8
54	199.5	324.5	0.027	-157.0	1.08	2.32	83.8
54	58.5	291.75	0.060	-157.8	0.87	9.98	83.8
55	137.5	309.25	0.098	-171.4	1.09	2.43	83.8
56	236	382	0.034	-141.9	1.09	16.78	83.8
57	167	353.5	0.064	-130.6	0.80	1.77	83.8
58	108	353.5	0.104	-129.7	0.77	1.88	83.8
59	129	387	0.240	-135.2	0.81	2.09	41.9
60	35	338.5	0.079	-191.4	0.85	2.19	83.8
61	58.5	372.75	0.081	-113.6	0.91	1.45	83.8
62	367.5	435.25	0.980	-203.5	0.78	16.24	83.8
63	307	435.25	0.062	-192.5	0.77	22.87	83.8
64	259.5	435.25	0.056	-170.0	0.78	15.73	83.8
65	183	412.75	0.156	-159.1	0.85	13.93	83.8
66	93	412.75	0.055	-155.8	0.79	11.67	83.8
67	156	446.25	0.119	-176.8	0.81	15.75	83.8
68	217	460.5	0.589	-175.3	0.98	16.02	83.8
69	289.5	500.25	0.159	-213.6	0.76	15.90	83.8
70	344	500.25	0.143	-224.2	0.82	14.40	83.8
71	379.25	490.5	0.018	-201.8	1.12	14.12	41.9
72	390.5	536.75	0.044	-206.1	0.92	11.13	83.8

Table D.5. Continued.

ID #	X-coord.	Y-coord.	Corrosion Rate ($\mu A/cm^2$)	Corrosion Potential (mV)	Electrical resistance (kΩ)	Resistivity (kΩ. cm)	Area (cm^2)
73	319	536.75	0.286	-182.9	0.63	12.74	83.8
74	241	519.25	0.338	-177.1	0.83	13.31	83.8
75	183	500.25	0.069	-182.4	0.88	20.85	83.8
76	123.5	500.25	0.063	-176.3	0.80	13.99	83.8
77	156	536.75	0.010	-161.1	0.88	11.48	83.8
78	278	546.75	0.053	-184.4	0.89	15.77	83.8
79	354.75	585	0.130	-241.5	0.79	7.32	41.9
80	300.5	588.25	0.089	-200.2	0.70	7.89	83.8
81	223.5	576.75	0.273	-181.5	0.74	7.93	83.8
82	183	576.75	0.056	-179.2	0.66	6.54	83.8
83	206.5	536.75	0.297	-173.5	0.76	6.10	83.8
84	123.5	546.75	0.133	-166.0	0.63	4.56	83.8
85	74	474.75	0.066	-185.8	0.81	3.85	83.8
86	45	426.25	0.092	-169.4	0.83	3.18	83.8
87	22	474.75	0.174	-147.7	0.61	3.91	83.8
88	53	519.25	0.102	-189.8	0.66	1.43	83.8
89	27	546.75	0.877	-160.2	0.80	3.41	83.8
90	74	576.75	0.084	-187.7	0.81	3.30	83.8
91	93	618.75	0.046	-149.6	0.70	9.29	83.8
92	130.5	602	0.230	-170.3	0.74	6.45	41.9
93	183	633.5	0.199	-177.0	0.81	7.66	83.8
94	241	633.5	0.234	-190.1	0.84	8.29	83.8
95	289.5	646	1.847	-192.2	0.76	7.76	83.8
96	344	646	0.167	-220.6	0.66	11.37	83.8

Table D.5. Continued.

ID #	X-coord.	Y-coord.	Corrosion Rate ($\mu A/cm^2$)	Corrosion Potential (mV)	Electrical resistance ($k\Omega$)	Resistivity ($k\Omega$. cm)	Area (cm^2)
97	390.5	618.75	0.367	-228.1	0.82	13.72	83.8
98	390.5	689	0.119	-192.2	0.70	10.81	83.8
99	319	689	1.158	-167.0	0.72	11.02	83.8
100	344	736.5	0.659	-179.8	0.55	10.81	83.8
101	259.5	689	0.818	-152.8	0.81	5.68	83.8
102	217	689	0.061	-139.9	0.83	7.94	83.8
103	156	689	0.058	-152.7	0.89	7.48	83.8
104	123.5	659.75	0.342	-209.4	0.65	3.34	83.8
105	64.5	670	0.075	-186.7	0.79	4.33	83.8
106	22	702.75	0.204	-144.6	0.73	10.24	83.8
107	70	702.75	0.164	-185.0	0.52	9.93	83.8
108	123.5	713.75	0.237	-156.6	0.72	15.31	83.8
109	194	736.5	0.197	-160.1	0.72	3.84	83.8
110	241	748.25	0.088	-120.6	0.73	13.06	83.8
111	300.5	748.25	0.081	-196.1	0.59	9.38	83.8
112	390.5	785.5	0.101	-160.6	0.78	9.39	83.8
113	344	804.75	0.116	-219.7	0.58	10.23	83.8
114	264.5	804.75	0.099	-182.7	0.58	11.01	83.8
115	206.5	804.75	0.323	-135.2	0.74	3.50	83.8
116	143	763	0.104	-150.3	0.83	12.98	83.8
117	87	763	0.132	-181.9	0.92	15.84	83.8
118	22	763	0.213	-139.3	0.66	14.51	83.8
119	41.5	804.75	0.135	-162.7	0.78	13.85	83.8
120	123.5	804.75	0.158	-172.7	0.81	12.94	83.8

Table D.5. Continued.

ID #	X-coord.	Y-coord.	Corrosion Rate ($\mu A/cm^2$)	Corrosion Potential (mV)	Electrical resistance ($k\Omega$)	Resistivity ($k\Omega$. cm)	Area (cm^2)
121	93	861	0.393	-164.1	0.77	18.39	83.8
122	183	830	0.205	-147.5	0.78	23.07	83.8
123	223.5	861	0.230	-194.1	0.80	4.11	83.8
124	300.5	830	0.019	-171.4	0.73	11.64	83.8
125	344	861	0.340	-204.8	0.67	16.50	83.8
126	390.5	830	0.073	-255.4	0.68	11.97	83.8
127	22	394.75	0.182	-130.8	0.77	14.46	83.8
128	22	252.25	0.116	-169.7	0.97	21.31	83.8
129	27	140.75	0.280	-175.2	0.71	19.11	83.8

Table D.6. Data recorded on Site 6.

ID #	X-coord.	Y-coord.	Corrosion Rate ($\mu A/cm^2$)	Corrosion Potential (mV)	Electrical resistance (kΩ)	Resistivity (kΩ. cm)	Area (cm^2)
1	494	5.5	0.077	-249.4	0.76	14.52	83.8
2	426.5	47.5	0.201	-210.9	0.78	10.97	83.8
3	494	106	0.421	-218.6	1.06	14.30	83.8
4	426.5	160.5	0.288	-187.0	0.79	14.95	83.8
5	500	216	0.249	-203.4	0.85	16.31	83.8
6	426.5	263	0.303	-167.9	0.79	14.61	83.8
7	377.5	212	0.102	-179.5	0.90	16.22	83.8
8	353	5.5	0.381	-142.2	0.68	11.98	83.8
9	353	121.5	0.111	-166.5	0.77	13.24	83.8
10	282	70	0.107	-198.4	0.71	14.36	83.8
11	227.5	24	0.115	-187.9	0.85	14.90	83.8
12	169	80	0.093	-217.7	0.76	14.38	83.8
13	100.5	24	0.047	-178.9	1.00	18.16	83.8
14	169	192.5	0.142	-176.8	0.97	16.95	83.8
15	227.5	136	0.149	-187.3	0.77	12.65	83.8
16	289.5	192.5	0.123	-167.1	0.85	15.60	83.8
17	300.5	253	0.271	-150.1	0.78	16.85	83.8
18	227.5	244.5	0.080	-155.2	0.85	12.26	83.8
19	152	263	0.115	-168.7	0.82	22.95	83.8
20	95.5	192.5	0.131	-138.2	0.69	11.28	83.8
21	33	244.5	0.087	-165.4	0.66	11.10	83.8
22	70.5	312.5	0.079	-157.0	0.69	15.41	83.8
23	27	387.5	0.096	-202.2	0.68	13.90	83.8
24	215	338	0.063	-160.3	0.74	13.44	83.8

Table D.6. Continued.

ID #	X-coord.	Y-coord.	Corrosion Rate ($\mu A/cm^2$)	Corrosion Potential (mV)	Electrical resistance (kΩ)	Resistivity (kΩ. cm)	Area (cm^2)
25	377.5	312.5	0.090	-158.8	0.84	11.76	83.8
26	500	309	0.051	-166.9	0.89	18.15	83.8
27	421	361.5	0.073	-157.9	0.68	11.77	83.8
28	300.5	338	0.060	-165.1	0.77	13.82	83.8
29	135	338	0.178	-197.3	0.54	8.95	83.8
30	135	428.5	0.128	-192.7	0.59	12.16	83.8
31	215	415.5	0.255	-180.4	0.67	9.37	83.8
32	300.5	428.5	0.356	-150.5	0.61	11.09	83.8
33	377.5	415.5	0.095	-150.6	0.78	14.50	83.8
34	494	387.5	0.580	-180.6	0.70	10.70	83.8
35	549.5	439.5	0.070	-193.5	0.78	12.57	83.8
36	478.5	477	0.384	-175.1	0.69	9.82	83.8
37	611	501	0.148	-187.1	0.72	14.90	83.8
38	402	477	0.115	-161.4	0.68	12.61	83.8
39	227.5	501	0.114	-159.7	0.61	10.71	83.8
40	65	477	0.472	-224.2	0.65	13.41	83.8
41	28	554	0.321	-194.8	0.69	11.66	83.8
42	132	522.25	0.181	-181.1	0.81	16.66	83.8
43	346	522.25	0.138	-188.1	0.67	16.49	83.8
44	538.5	522.25	0.243	-172.3	0.67	14.40	83.8
45	455	554	0.573	-173.5	0.90	16.08	83.8
46	40.5	642.25	0.514	-266.4	0.55	14.20	83.8
47	113	618.5	0.345	-194.7	0.74	20.59	83.8
48	186	580	0.039	-162.0	0.83	17.38	83.8

Table D.6. Continued.

ID #	X-coord.	Y-coord.	Corrosion Rate ($\mu A/cm^2$)	Corrosion Potential (mV)	Electrical resistance ($k\Omega$)	Resistivity ($k\Omega$. cm)	Area (cm^2)
49	264	601	0.123	-166.3	0.65	13.07	83.8
50	388.5	601	0.220	-180.4	0.65	14.09	83.8
51	549	601	0.076	-173.9	0.85	4.27	83.8
52	609	601	0.055	-171.5	0.74	5.68	83.8
53	652	642.25	0.143	-127.9	0.70	5.00	83.8
54	484.5	642.25	0.140	-150.2	0.61	11.00	83.8
55	328	642.25	0.476	-161.1	0.39	9.36	83.8
56	216	655.5	0.253	-146.3	0.58	3.65	83.8
57	70.5	707.25	0.070	-213.3	0.68	5.86	83.8
58	414	669.75	0.108	-151.0	0.65	4.19	83.8
59	274.5	707.25	0.172	-152.7	0.65	7.41	83.8
60	352	720	0.178	-162.3	0.62	4.48	83.8
61	555	681.75	0.021	-152.7	0.88	2.46	83.8
62	480	720	0.232	-138.0	0.97	2.82	83.8
63	150.5	720	0.170	-190.3	0.53	7.00	83.8
64	28	784.5	0.108	-259.9	0.78	3.48	83.8
65	216	784.5	0.102	-177.8	0.64	4.79	83.8
66	299	784.5	0.112	-163.1	0.68	6.33	83.8
67	424	771.25	0.130	-177.7	0.56	6.62	83.8
68	555	771.25	0.079	-159.0	0.77	2.99	83.8
69	498	824.25	0.106	-163.7	0.64	3.17	83.8
70	364.5	824.25	0.110	-174.2	0.62	5.19	83.8
71	256	854.75	0.263	-188.0	0.58	6.42	83.8
72	118.5	797.5	0.141	-216.3	0.57	4.08	83.8

Table D.6. Continued.

ID #	X-coord.	Y-coord.	Corrosion Rate ($\mu A/cm^2$)	Corrosion Potential (mV)	Electrical resistance (kΩ)	Resistivity (kΩ. cm)	Area (cm^2)
73	70.5	854.75	0.466	-270.7	0.64	2.87	83.8
74	20	900.75	0.108	-277.5	0.72	4.52	83.8
75	179	854.75	0.127	-185.5	0.56	4.72	83.8
76	328.5	888	0.117	-161.0	0.64	5.86	83.8
77	437	874.75	0.098	-170.6	0.66	6.91	83.8
78	626	734	0.044	-156.5	0.92	4.96	83.8
79	696.5	727	0.048	-206.8	1.11	4.48	41.9
80	726	811.25	0.140	-196.3	0.96	5.09	83.8
81	639	797.5	0.059	-168.4	0.80	4.08	83.8
82	679.5	874.75	0.022	-113.4	1.00	5.45	83.8
83	756	874.75	0.118	-163.4	0.67	6.72	41.9
84	579	854.75	0.081	-157.7	0.75	4.26	83.8
85	120	914.75	0.199	-210.85	0.73	9.25	83.8
86	227.5	941.5	0.284	-167.0	0.59	7.26	83.8
87	300	954	0.147	-163.1	0.756	15.28	83.8
88	358.5	900.75	0.248	-151.5	0.72	10.26	83.8
89	509.5	914.75	0.105	-158.9	0.70	14.23	83.8
90	430.5	967	0.136	-161.4	0.66	16.12	83.8
91	364.5	1005.5	0.102	-175.5	0.72	11.17	83.8
92	287	1030	0.130	-189.2	0.65	13.21	83.8
93	442.5	1043.25	0.139	-158.9	0.80	15.80	83.8
94	520	993.25	0.300	-180.7	0.66	14.66	83.8
95	520	1089.5	0.114	-169.4	0.76	13.56	83.8
96	593	1030	0.205	-151.3	0.78	16.97	83.8

Table D.6. Continued.

ID #	X-coord.	Y-coord.	Corrosion Rate ($\mu A/cm^2$)	Corrosion Potential (mV)	Electrical resistance ($k\Omega$)	Resistivity ($k\Omega$. cm)	Area (cm^2)
97	370.5	1089.5	0.375	-179.3	0.63	14.52	83.8
98	588	941.5	0.059	-135.1	0.75	3.73	83.8
99	666.5	954	0.027	-156.5	0.94	4.39	83.8
100	730	967	0.063	-130.3	0.83	7.23	83.8
101	674	1030	0.120	-186.2	0.56	6.52	83.8
102	730	1056.5	0.082	-196.8	0.75	7.24	83.8
103	166	993.25	0.337	-225.0	0.49	5.06	83.8
104	27	993.25	0.159	-301.8	0.51	8.90	83.8
105	99.5	1030	0.187	-297.1	0.49	6.95	83.8
106	77	1089.5	0.352	-284.2	0.50	8.33	83.8
107	173	1089.5	0.351	-207.52	0.51	6.73	83.8
108	246	1089.5	0.133	-192.6	0.55	5.04	83.8
109	442.5	1114.5	0.151	-170.3	0.62	5.77	83.8
110	678	1114.5	0.107	-176.4	0.56	13.30	83.8
111	588	1114.5	0.093	-166.9	0.68	10.66	83.8
112	730	1197.5	0.078	-206.2	0.68	16.59	83.8
113	636	1197.5	0.060	-128.9	0.80	11.17	83.8
114	509.5	1173	0.101	-179.7	0.55	14.07	83.8
115	377	1161	0.128	-192.5	0.54	13.34	83.8
116	300	1134	0.124	-186.1	0.51	11.61	83.8
117	203.5	1147.5	0.098	-182.3	0.57	11.59	83.8
118	130.5	1161	0.137	-231.6	0.52	9.50	83.8
119	35	1173	0.432	-267.6	0.43	9.31	83.8
120	94.5	1238	0.377	-189.3	0.70	8.87	83.8

Table D.6. Continued.

ID #	X-coord.	Y-coord.	Corrosion Rate ($\mu A/cm^2$)	Corrosion Potential (mV)	Electrical resistance ($k\Omega$)	Resistivity ($k\Omega$. cm)	Area (cm^2)
121	274.5	1211.5	0.127	-198.2	0.55	9.82	83.8
122	442.5	1211.5	0.118	-189.8	0.60	10.26	83.8
123	569	1225	0.183	-174.7	0.60	10.24	83.8
124	353	1238	0.099	-179.9	0.67	3.71	83.8
125	185	1238	0.122	-184.9	0.51	12.06	83.8
126	27	1276.5	0.176	-213.4	0.56	8.59	83.8
127	82	1355.5	0.398	-311.1	0.65	9.32	83.8
128	136.5	1324.5	0.270	-228.0	0.52	10.64	83.8
129	246	1276.5	0.353	-185.1	0.59	3.56	83.8
130	311	1297	0.435	-171.6	0.61	6.62	83.8
131	418.5	1297	0.154	-170.0	0.67	4.58	83.8
132	358.5	1324.5	0.453	-215.6	0.58	5.59	83.8
133	281.5	1355.5	0.484	-273.6	0.54	4.24	83.8
134	198	1355.5	0.161	-250.2	0.61	6.24	83.8
135	77	1451	0.225	-252.3	0.58	10.52	83.8
136	136.5	1413	0.170	-287.8	0.56	4.74	83.8
137	208.5	1471	0.573	-295.0	0.55	4.45	83.8
138	269	1451	0.153	-304.9	0.51	4.56	83.8
139	335	1413	0.429	-238.3	0.48	3.36	83.8
140	412	1413	0.424	-235.1	0.61	3.63	83.8
141	401	1471	0.320	-243.2	0.45	4.03	83.8
142	496.5	1263	0.717	-159.5	0.71	3.37	83.8
143	478	1345	0.045	-230.0	0.68	3.64	83.8
144	467	1413	0.445	-229.0	0.52	4.03	83.8

Table D.6. Continued.

ID #	X-coord.	Y-coord.	Corrosion Rate ($\mu A/cm^2$)	Corrosion Potential (mV)	Electrical resistance ($k\Omega$)	Resistivity ($k\Omega$. cm)	Area (cm^2)
145	557.5	1324.5	0.460	-205.3	0.61	6.17	83.8
146	545	1413	0.050	-229.8	0.66	4.21	83.8
147	623	1276.5	0.454	-153.6	0.65	6.86	83.8
148	528	1451	0.804	-257.5	0.46	5.11	83.8
149	606	1471	0.569	-235.5	0.49	4.53	83.8
150	623	1372	0.485	-191.2	0.61	10.94	83.8
151	704	1276.5	0.103	-162.2	0.94	5.76	83.8
152	659	1345	0.422	-188.9	0.61	12.00	83.8
153	730	1413	0.484	-268.5	0.56	9.70	83.8
154	666.5	1413	0.512	-248.6	0.56	6.18	83.8

Table D.7. Data from Site 7.

ID #	X-coord.	Y-coord.	Corrosion Rate ($\mu A/cm^2$)	Corrosion Potential (mV)	Electrical resistance ($k\Omega$)	Resistivity ($k\Omega$. cm)	Area (cm^2)
1	145	7	0.307	-235.6	0.82	8.45	41.9
2	254.5	28.5	0.145	-215.6	1.26	16.32	41.9
3	109	17.75	0.151	-245.6	1.03	12.12	52.4
4	113.5	40	0.280	-272.4	0.83	11.05	41.9
5	77	34.25	0.241	-271.4	0.88	12.88	52.4
6	49.25	7	0.031	-206.8	2.45	15.37	41.9
7	29	34.25	0.214	-241.4	0.90	13.41	52.4
8	4	7	0.372	-198.8	1.38	17.64	41.9
9	38	50.25	0.089	-245.7	0.98	17.63	52.4
10	73.5	60.5	0.354	-261.6	0.75	11.45	41.9
11	145	50.25	0.352	-285.3	0.84	12.51	41.9
12	160	81.75	0.189	-270.2	0.87	12.96	52.4
13	109	69	0.384	-275.7	0.72	4.98	52.4
14	125.5	95.5	0.122	-263.3	1.18	29.29	52.4
15	77	95.5	0.055	-205.2	0.43	14.80	52.4
16	22.5	69	0.083	-236.0	0.99	6.70	52.4
17	8	108.75	0.245	-222.3	0.91	5.27	52.4
18	45	108.75	0.075	-242.0	1.20	5.94	52.4
19	97.5	127	0.131	-241.2	0.75	42.57	41.9
20	149	121	0.114	-269.1	0.74	4.43	52.4
21	160	156.5	0.045	-253.6	0.89	3.96	52.4
22	121.75	150	0.139	-240.6	0.62	3.55	41.9
23	61.5	133.25	0.097	-232.8	0.72	2.95	52.4
24	29	144.75	0.032	-213.9	1.35	3.82	52.4

Table D.7. Continued.

ID #	X-coord.	Y-coord.	Corrosion Rate ($\mu A/cm^2$)	Corrosion Potential (mV)	Electrical resistance (kΩ)	Resistivity (kΩ. cm)	Area (cm^2)
25	8	169.25	0.146	-235.8	0.65	9.28	52.4
26	85	156.5	0.122	-213.6	0.72	11.52	52.4
27	132	181.25	0.116	-236.2	0.87	9.52	52.4
28	165	201.5	0.418	-237.1	0.84	10.38	41.9
29	45	181.25	0.067	-237.4	0.68	11.88	52.4
30	22.5	199.75	0.119	-264.3	0.72	11.72	52.4
31	85	192.5	0.105	-203.5	0.77	10.82	52.4
32	121.75	201.5	0.296	-251.6	0.80	9.64	41.9
33	53.5	212	0.026	-194.6	0.80	9.66	52.4
34	15.25	235	0.313	-297.2	0.55	9.38	41.9
35	85	228.75	0.004	-258.3	2.56	9.74	52.4
36	141	240.25	0.003	-299.8	1.40	8.48	52.4
37	170	264.25	0.003	-335.1	1.48	54.20	52.4
38	109	251.75	0.127	-265.2	0.85	11.55	52.4
39	53.5	251.75	0.068	-198.0	0.80	16.84	52.4
40	136.5	282.5	0.269	-280.3	0.68	12.89	41.9
41	77	276.5	0.135	-270.6	0.56	9.63	52.4
42	22.5	264.25	0.237	-220.0	0.74	13.55	52.4
43	8	286.25	0.231	-220.1	0.76	9.24	52.4
44	38	295.25	0.209	-268.2	0.72	9.65	52.4
45	109	295.25	0.167	-255.2	0.77	10.67	52.4
46	136.5	332.5	0.080	-244.6	1.30	13.16	52.4
47	170	333	0.329	-239.9	0.68	7.06	52.4
50	101.5	333	0.267	-264.8	0.75	9.86	52.4

Table D.7. Continued.

ID #	X-coord.	Y-coord.	Corrosion Rate ($\mu A/cm^2$)	Corrosion Potential (mV)	Electrical resistance ($k\Omega$)	Resistivity ($k\Omega$. cm)	Area (cm^2)
51	141	353.75	0.113	-212.4	0.69	13.23	52.4
52	170	364.75	0.075	-197.9	1.10	38.93	52.4
53	45	333	0.150	-225.8	0.72	10.17	52.4
54	8	353.75	0.422	-193.3	0.77	11.02	52.4
55	65.75	359	0.145	-219.7	0.94	13.38	41.9
56	101.5	364.75	0.349	-229.3	0.72	11.24	52.4
57	132	366.25	0.070	-189.2	1.27	24.37	52.4
58	29	376.75	0.205	-175.8	0.68	12.38	52.4
59	8	378.25	0.081	-181.9	1.05	14.43	52.4
60	61.5	366.25	0.093	-166.3	0.96	15.10	52.4
61	99.5	407	0.432	-167.3	0.82	8.16	41.9
62	165	407	0.106	-237.9	0.89	11.7	41.9
63	132	424.75	0.102	-224.1	1.01	13.76	52.4
64	45	412.5	0.173	-175.3	0.90	11.23	52.4
65	22.5	437	0.144	-198.4	1.07	18.92	52.4
66	77	437	0.118	-202.2	0.96	16.27	52.4
67	170	437	0.163	-248.6	1.02	19.26	52.4
68	141	460.75	1.151	-240.6	0.82	10.53	52.4
69	105.25	454.5	0.131	-214.0	0.98	18.79	41.9
70	45	460.75	0.148	-220.1	1.01	13.71	52.4
71	8	472.75	0.263	-220.3	0.90	17.78	52.4
72	77	484.25	0.136	-224.0	1.08	13.43	52.4
73	118	496.5	0.451	-244.6	0.86	15.94	52.4
74	38	496.5	0.071	-222.6	0.99	18.16	52.4

Table D.7. Continued.

ID #	X-coord.	Y-coord.	Corrosion Rate ($\mu A/cm^2$)	Corrosion Potential (mV)	Electrical resistance ($k\Omega$)	Resistivity ($k\Omega$. cm)	Area (cm^2)
75	8	509	0.292	-214.8	0.86	16.03	52.4
76	165	503	0.721	-262.9	0.67	10.17	41.9
77	141	529	0.111	-296.6	0.92	15.31	52.4
78	85	529	0.139	-253.2	0.98	20.32	52.4
79	45	529	0.083	-243.2	1.07	16.20	52.4
80	15.25	549.5	0.131	-200.0	0.9	14.95	41.9
81	73.5	555	0.070	-207.1	1.14	14.81	41.9
82	118	543.75	0.081	-268.5	0.93	15.45	52.4
83	165	560	0.315	-271.7	0.55	11.88	41.9
84	125.5	573.5	0.223	-254.6	0.94	4.17	52.4
85	38	573.5	0.260	-212.7	0.87	2.57	52.4
86	25.75	603.5	0.074	-175.8	0.99	5.43	41.9
87	77	585.5	0.217	-209.5	0.75	3.53	52.4
88	149	597.5	0.122	-241.3	0.86	5.29	52.4
89	109	609.5	0.074	-212.5	0.96	8.16	52.4
90	61.5	621.5	0.059	-205.9	1.24	8.68	52.4
91	8	633.5	0.308	-221.5	0.80	3.11	52.4
92	45	657.25	0.100	-284.4	0.72	5.83	52.4
93	89.25	639.5	0.399	-229.0	0.70	6.90	41.9
94	125.5	645.25	0.061	-248.0	0.92	9.79	52.4
95	170	633.5	0.160	-238.3	0.77	5.38	52.4
96	160	669	0.125	-247.1	0.79	5.38	52.4
97	93.5	669	0.076	-195.8	0.82	3.64	52.4
98	8	680.5	0.690	-197.1	0.58	3.87	52.4

Table D.7. Continued.

ID #	X-coord.	Y-coord.	Corrosion Rate ($\mu A/cm^2$)	Corrosion Potential (mV)	Electrical resistance ($k\Omega$)	Resistivity ($k\Omega$. cm)	Area (cm^2)
99	45	692.75	0.095	-218.9	0.86	3.82	52.4
100	125.5	692.75	0.132	-222.1	0.77	4.27	52.4
101	170	705	0.574	-271.9	0.72	4.22	52.4
102	85	705	0.103	-146.2	0.87	9.79	52.4
103	8	716.75	0.036	-122.3	0.96	4.48	52.4
104	49.25	722.5	0.550	-162.6	0.73	7.53	41.9
105	25.75	729	0.571	-179.9	0.68	6.69	41.9
106	141	716.75	0.8585	-247.7	0.77	14.03	52.4
107	154.5	748	0.232	-280.2	0.60	7.05	52.4
108	93.5	741.75	0.131	-159.5	0.78	7.73	52.4

Table D.8. Data from Site 8.

ID #	X-coord.	Y-coord.	Corrosion Rate ($\mu A/cm^2$)	Corrosion Potential (mV)	Electrical resistance (kΩ)	Resistivity (kΩ. cm)	Area (cm^2)
1	74.5	1040.75	0.081	-309.2	1.08	9.84	52.4
2	90	1077.75	0.104	-286.4	0.93	6.43	52.4
3	52	1077.75	0.106	-290.2	0.86	5.25	73.3
4	31	1040.75	0.262	-290.1	0.89	9.00	73.3
5	7	1077.75	0.142	-324.5	0.87	9.55	73.3
6	26.75	1098	0.134	-280.1	1.12	8.13	73.3
7	74.5	1103.5	0.035	-328.2	1.01	6.48	52.4
8	14.75	1126	0.097	-338.6	0.67	4.01	73.3
9	63	1121.5	0.048	-338.1	0.85	9.19	73.3
10	90	1132	0.353	-295.8	1.08	7.75	52.4
11	40.5	1143.5	0.040	-364.1	0.69	4.29	73.3
12	74.5	1154.5	0.139	-359.2	0.80	7.32	52.4
13	90	1176.25	0.030	-314.7	1.08	12.60	52.4
14	26.75	1170.5	0.038	-388.0	0.83	11.16	73.3
15	63	1176.25	0.081	-359.2	0.89	9.26	73.3
16	14.75	1197.5	0.539	-375.8	0.82	3.86	73.3
17	52	1203.75	0.069	-342.3	0.82	4.02	73.3
18	86	1210	0.099	-352.0	1.00	16.53	73.3
19	7	1224.5	0.116	-378.3	0.78	11.13	73.3
20	38.5	1234.25	0.074	-350.7	0.57	5.98	73.3
21	73	1234.25	0.272	-432.8	0.71	0.00	52.4
22	14.75	1258.5	0.055	-304.4	0.46	4.44	73.3
23	57.5	1258.5	0.085	-398.7	0.70	0.00	73.3
24	90	1264.25	0.056	-468.7	0.73	---	52.4

Table D.8. Continued.

ID #	X-coord.	Y-coord.	Corrosion Rate ($\mu A/cm^2$)	Corrosion Potential (mV)	Electrical resistance (kΩ)	Resistivity (kΩ. cm)	Area (cm^2)
25	46.25	1287.5	0.085	-390.9	0.57	10.46	73.3
26	74.5	1295.75	0.112	-458.9	0.71	---	52.4
27	52	1315.75	0.121	-427.0	0.68	---	73.3
28	90	1315.75	0.156	-449.6	0.86	10.99	52.4
29	40.5	1340	0.335	-389.3	0.69	6.21	73.3
30	74.5	1340	0.559	-442.3	0.71	10.93	52.4
31	90	1360.5	0.090	-409.8	0.94	10.06	52.4
32	57.5	1366.5	0.051	-418.2	0.86	---	73.3
33	26.75	1376	0.093	-397.3	0.78	---	73.3
34	7	2804	0.152	-402.1	0.85	---	73.3
35	46.25	1396.5	0.341	-408.6	0.71	8.88	73.3
36	82	1391.25	0.132	-371.9	0.99	11.30	52.4
37	90	1424	0.117	-366.7	1.00	9.21	52.4
38	31	1424	0.346	-388.6	0.76	7.95	73.3
39	68.75	1436	0.634	-389.8	0.73	13.42	73.3
40	90	1462	0.042	-393.0	0.82	7.13	52.4
41	22.5	1441	0.061	-417.2	0.80	---	73.3
42	57.5	1467	0.153	-399.1	0.79	3.39	73.3
43	7	1481.5	0.050	-371.2	1.03	5.14	73.3
44	46.25	1487	0.084	-395.7	0.78	2.98	73.3
45	86	1487	0.231	-377.7	0.87	7.29	73.3
46	90	1512.75	0.054	-408.9	0.87	3.93	52.4
47	68.75	1507.5	0.172	-421.8	0.79	---	73.3
48	22.5	1502	0.042	-393.8	0.89	5.38	73.3

Table D.8. Continued.

ID #	X-coord.	Y-coord.	Corrosion Rate ($\mu A/cm^2$)	Corrosion Potential (mV)	Electrical resistance (kΩ)	Resistivity (kΩ. cm)	Area (cm^2)
49	7	1523.5	0.063	-376.7	1.05	3.26	73.3
50	40.5	1523.5	0.069	-408.6	0.92	3.42	73.3
51	68.75	1529	0.034	-408.3	0.91	---	73.3
52	7	1016	0.213	-284.2	0.87	12.06	73.3
53	54.25	1010	0.288	-276.4	0.90	12.94	73.3
54	23	987.5	0.125	-264.5	0.92	3.52	73.3
55	56.5	976.75	0.051	-282.3	1.27	3.82	73.3
56	85	955	0.157	-266.6	1.14	4.36	73.3
57	68.25	930	0.061	-318.5	1.04	5.29	73.3
58	11.5	930	0.057	-289.6	1.27	9.78	73.3
59	85	899.5	0.027	-240.5	0.89	7.57	73.3
60	16	838.75	0.132	-230.2	1.34	14.14	73.3
61	74.5	871.5	0.071	-222.7	1.50	15.95	52.4
62	48.5	850.75	0.054	-236.3	1.17	11.06	73.3
63	16	838.75	0.127	-263.5	1.17	13.93	73.3
64	88.75	832	0.552	-220.6	1.47	15.41	73.3
65	97.5	805.5	0.099	-238.1	1.74	10.59	52.4
66	52.5	813	0.190	-273.5	1.68	8.98	73.3
67	30	793.5	0.029	-267.2	1.10	9.04	73.3
68	74.5	784	0.029	-250.5	0.95	7.19	73.3
69	48.5	762.5	0.014	-255.3	1.34	10.06	52.4
70	9.5	757	0.023	-261.6	1.28	10.39	73.3
71	68.25	729	0.016	-253.5	1.20	7.90	73.3
72	30	723.5	0.024	-255.9	1.21	6.65	73.3

Table D.8. Continued.

ID #	X-coord.	Y-coord.	Corrosion Rate ($\mu A/cm^2$)	Corrosion Potential (mV)	Electrical resistance ($k\Omega$)	Resistivity ($k\Omega$. cm)	Area (cm^2)
73	9.5	688	0.016	-294.7	1.05	5.15	73.3
74	48.5	692.75	0.058	-280.0	1.05	12.80	73.3
75	88.75	667.5	0.015	-232.1	0.97	16.32	73.3
76	41.5	662.5	0.033	-287.9	1.44	13.60	73.3
77	9.5	640.5	0.057	-317.5	0.99	15.99	73.3
78	74.5	635.5	0.076	-274.0	1.40	2.98	52.4
79	48.5	615.75	0.025	-291.1	1.12	3.13	73.3
80	23	599.5	0.296	-362.0	0.79	8.85	73.3
81	88.75	599.5	0.078	-264.7	1.21	8.71	73.3
82	16	575	0.072	-323.4	1.10	6.72	73.3
83	52.5	570.5	0.090	-326.9	0.88	---	73.3
84	97.5	564.75	0.032	-302.9	1.23	9.66	52.4
85	44.25	542	0.047	-375.0	1.05	5.83	73.3
86	80	536	0.085	-334.5	1.02	7.11	52.4
87	56.5	509.25	0.032	-352.2	0.61	3.12	73.3
88	97.5	495.5	0.024	-309.9	1.68	3.38	52.4
89	63	466.5	0.048	-363.6	1.09	3.13	73.3
90	39.5	475	0.044	-358.0	0.85	4.72	73.3
91	8	466.5	0.023	-384.3	1.16	8.07	73.3
92	26	435	0.020	-367.6	1.32	7.09	73.3
93	63.5	435	0.069	-361.5	1.15	5.99	73.3
94	31.5	405.5	0.231	-386.5	1.08	9.58	73.3
95	63.5	412	0.031	-417.6	0.90	---	73.3
96	96	393.5	0.028	-319.7	1.45	6.82	52.4

Table D.8. Continued.

ID #	X-coord.	Y-coord.	Corrosion Rate ($\mu A/cm^2$)	Corrosion Potential (mV)	Electrical resistance ($k\Omega$)	Resistivity ($k\Omega$. cm)	Area (cm^2)
97	56.5	376	0.098	-358.5	0.85	7.74	73.3
98	13.75	372	0.095	-359.0	1.06	8.24	73.3
99	88.25	360	0.020	-345.3	1.09	5.17	73.3
100	47	345.5	0.019	-310.8	1.73	4.97	73.3
101	88.25	327.5	0.028	-262.2	1.82	5.37	73.3
102	8	322.25	0.356	-261.9	1.47	8.62	73.3
103	47	312.5	0.019	-297.8	1.26	4.68	73.3
104	96	296	0.153	-244.7	1.39	29.98	52.4
105	51.75	281	0.321	-302.4	1.05	7.12	73.3
106	13.75	281	0.041	-283.6	1.12	6.58	73.3
107	39.75	255	0.278	-323.3	0.81	6.47	73.3
108	8	239.25	0.125	-281.9	1.15	3.46	73.3
109	98	255	0.555	-318.2	0.88	5.52	73.3
110	47	219	0.192	-282.6	1.03	9.05	73.3
111	80.5	219	0.029	-222.5	1.84	8.39	73.3
112	88.25	184.5	0.242	-212.7	1.60	11.21	73.3
113	56.5	188.5	0.043	-262.1	1.23	10.64	73.3
114	5.5	184.5	0.184	-329.5	0.91	7.23	73.3
115	39.75	164.5	0.062	-254.2	1.34	7.60	73.3
116	80.5	151.5	0.062	-303.3	0.90	7.94	73.3
117	26	133	0.037	-216.0	1.18	26.02	73.3
118	56.5	125.25	0.027	-271.2	1.08	7.02	73.3
119	88.25	89	0.029	-195.6	1.42	3.53	73.3
120	47	104	0.039	-243.1	1.03	15.27	73.3

Table D.8. Continued.

ID #	X-coord.	Y-coord.	Corrosion Rate ($\mu A/cm^2$)	Corrosion Potential (mV)	Electrical resistance ($k\Omega$)	Resistivity ($k\Omega$. cm)	Area (cm^2)
121	26	79.5	0.027	-274.5	0.84	15.28	73.3
122	42	51.25	0.071	-324.9	0.97	8.87	73.3
124	43	11.5	0.073	-349.3	1.04	9.20	73.3
125	88	19.75	0.342	-298.4	1.26	10.84	73.3
126	94	11.5	0.015	-262.7	1.48	14.40	73.3

REFERENCES

ACI 222R-96, (1996). "Corrosion of Metals in Concrete," ACI Manual of Concrete Practice – Part 1, ACI 222 Committee Report.

ACI 318-99, (1999). *Building Code Requirements for Structural Concrete (318-99) and Commentary 318R-99),* Farmington Hills, Michigan.

Ahmad, S. and Bhattacharjee, B., (1995). "A Simple Arrangement and Procedure for In-Situ Measurement of Corrosion Rate of Rebar Embedded in Concrete," *Corrosion Science,* Vol. 37, No. 5, pp. 781-791.

ASTM, (1997). *1997 Annual Book of ASTM Standards*, Easton, Maryland.

Berke, Neal S., (1991). "Corrosion Inhibitors in Concrete," *Concrete International,* Vol. 13, No. 7, pp. 24-27.

Berke, N.S. and Hicks, M.C., (1994). "Predicting Chloride Profiles in Concrete," *Corrosion,* Vol. 50, No. 3, pp. 234-239.

Berman, H.A., (1972). "Determination of Chloride in Hardened Portland Cement Paste, Mortar, and Concrete," *Journal of Materials,* Vol. 7, No. 3, pp. 330-335.

Bungey, John, (1993). "Non-destructive testing for reinforcement corrosion," *Concrete,* Vol. 27, No. 1, pp. 16-18.

Cabrera, J.G., (1996). "Deterioration of Concrete Due to Reinforcement Steel Corrosion," *Cement & Concrete Compositions,* No. 18, Elsier Science Limited, pp. 47-59.

Cornet, I., Ishikawa, T., and Bresler, B., (1968). "The Mechanism of Steel Corrosion in Concrete Structures," *Materials Protection,* Vol. 7, No. 3, pp. 44-47.

Craig, R.J. and Wood, L.E., (1970). "Effectiveness of Corrosion Inhibitors and Their Influence on the Physical Properties of Portland Cement Mortars," Highway Research Record, No. 328, Transportation Research Board, pp. 77-88.

Dawson, J.L., (1983). "Chapter 12: Corrosion Monitoring of Steel in Concrete," *Corrosion of Reinforcement in Concrete Construction*, Ellis Horwood, Chichester, pp. 173-191.

Dhir, R.K., Jones, M.R., and McCarthy, M.J., (1991). "Measurement of Reinforcement orrosion in Concrete Structures," *Concrete,* Vol. 25, No. 1, pp. 15-19.

Erlin, Bernard and George J. Verbeck, (1975). "Corrosion of Metals in Concrete - Needed Research," *Corrosion of metals in concrete,* SP 49-4, pp. 39-46.

Gaynor, R., (1987). "Understanding Chloride Percentages," *Corrosion, Concrete and Chlorides,* SP-102, American Concrete Institute, pp. 161-166.

Gonzalez, J. A., Lopez, W., and Rodriguez, P., (1993). "Effects of Moisture on Corrosion Kinetics of Steel Embedded in Concrete," *Corrosion,* Vol. 49, No. 12, pp. 1004-1010.

Gowers, K.R., Millard, S.G., Gill, J.S., and Gill, R.P., (1994). "Programmable Linear Polarization Meter for Determination of Corrosion Rate of Reinforcement in Concrete Structures," *British Corrosion Journal,* Vol. 29, No. 1, pp. 25-32.

Gu, Ping, Elliott, S., Hristova, R., Beaudoin, J.J., Brousseau, R., and Baldock, B., (1997). "A Study of Corrosion Inhibitor Performance in Chloride Contaminated Concrete by the Electrochemical Impedence Spectroscopy," *ACI Materials Journal,* Vol. 94, No. 4, pp. 385-395.

Hassanein, A.M., Glass, G.K., and Buenfeld, N.R., (1998). "The Use of Small Electrochemical Perturbations to Assess the Corrosion of Steel in Concrete," *NDT&E International,* Vol. 31, No. 4, pp. 265-272.

Hausmann, D.A., (1967). "Steel Corrosion in concrete - how does it occur?," *Materials Protection,* Vol. 6, No. 11, pp. 19-23.

Hime, W. and Erlin, B., (1987). "Some Chemical and Physical Aspects of Phenomena Associated with Chloride-Induced Corrosion," *Corrosion, Concrete and Chlorides,* SP 102-1, pp. 1-12.

Hope, Brian B. and Alan K. C. Ip, (1989). "Corrosion Inhibitors for Use in Concrete," *ACI Materials Journal,* Vol. 86, No. 6, pp. 602-608.

Hussain, Syed Ehtesham, Al-Gahtani, Ahmad S., and Rasheeduzzafar, (1996). "Chloride Threshold for Corrosion of Reinforcement in Concrete," *ACI Materials Journal,* Vol. 94, No. 6, pp. 534-538.

Kitowski, C.J. and Wheat, H.G., (1997). "Effect of Chlorides on Reinforcing Steel Exposed to Simulated Concrete Solutions," *Corrosion,* Vol. 53, No. 3, pp. 216-226.

Lewis, D. A. and W. J. Copenhagen, (1959). "Corrosion of Reinforcing Steel in Concrete in Marine Atmospheres," *Corrosion,* Vol. 15, No. 7, pp. 60-66.

Liam, K. C., S. K. Roy and D. O. Northwood, (1992). "Chloride ingress measurements and corrosion potential mapping study of a 24-year old reinforced concrete jetty structure in a tropical marine environment," *Magazine of Concrete Research,* Vol. 44, No. 160, pp. 205-215.

Lopez, W. and J. A. Gonzalez, (1993). "Influence of the degree of pore saturation on the resistivity of concrete and the corrosion rate of steel reinforcement," *Cement and Concrete Research,* Vol. 23, pp. 368-376.

Loto, C. A., (1992). "Effect of Inhibitors and Admixed Chloride on Electrochemical Corrosion Behavior of Mild Steel Reinforcement in Concrete in Seawater," *Corrosion,* Vol. 48, No. 9, pp. 759-763.

Malhotra, V. M. and Carino, N.J., (1991). *Handbook on Non-Destructive Testing of Concrete,* CRC Press, pp. 219-225.

Millard, S. G., (1993). "Corrosion Rate Measurement of In-Situ Reinforced Concrete Structures," *Proceedings of the Institution of Civil,* Vol. 99, No. 1, pp. 84-88.

Mindess, Sidney, and Young, J.Francis, (1981). *Concrte,* Prentice Hall, Inc., Englewood Cliffs, New Jersey, pp. 544-580.

Rodriguez, P., Ramirez, E., and Gonzalez, J.A., (1994). "Methods for Studying Corrosion in Reinforced Concrete," *Magazine of Concrete Research* (London), Vol. 46, No. 167, pp. 81-90.

Slater, John E., (1983). *Corrosion of Metals in Association with Concrete*, ASTM, STP-818.

Srinivasan, S., Rengaswammy, N.S., and Pranesh, M.R., (1994). "Corrosion Monitoring of Marine Concrete Structures - An Appraisal," *The Indian Concrete Journal,* Vol. 68, No. 1, pp. 13-19.

Stratfull, R. R., (1957). "The Corrosion of Steel in a Reinforced Concrete Bridge," *Corrosion,* Vol. 13, No. 3, pp. 173-178.

Suryavanshi, A. K. and Nayak, B. U., (1990). "Half-cell Potential Corrosion-Monitoring Technique: A Review," *The Indian Concrete Journal,* Vol. 164, No. 4, pp. 198-202.

Verbeck, George J., (1975). "Mechanisms of Corrosion of Steel in Concrete," Corrosion of Metals in Concrete, SP 49-3, pp. 21-38.